

**A NOVEL ALGORITHM FOR OPTIMAL OPERATION  
AND SIZING OF GENERATOR-PHOTOVOLTAIC-  
ENERGY STORAGE SYSTEM FOR MINIMIZING COST  
OF ENERGY**

**CHOK EU-TJIN**

**MASTER OF ENGINEERING SCIENCE**

**LEE KONG CHIAN FACULTY OF ENGINEERING AND  
SCIENCE  
UNIVERSITI TUNKU ABDUL RAHMAN  
SEPTEMBER 2017**

**A NOVEL ALGORITHM FOR OPTIMAL OPERATION AND SIZING  
OF GENERATOR-PHOTOVOLTAIC-ENERGY STORAGE SYSTEM  
FOR MINIMIZING COST OF ENERGY**

By

**CHOK EU-TJIN**

A thesis submitted to the Department of Electrical and Electronic Engineering,  
Lee Kong Chian Faculty of Engineering and Science,  
Universiti Tunku Abdul Rahman,  
in partial fulfillment of the requirements for the degree of  
Master of Engineering Science  
September 2017



## **ABSTRACT**

### **A NOVEL ALGORITHM FOR OPTIMAL OPERATION AND SIZING OF GENERATOR-PHOTOVOLTAIC-ENERGY STORAGE SYSTEM FOR MINIMIZING COST OF ENERGY**

**Chok Eu-Tjin**

There are still many off-grid areas in Malaysia and they mainly depend on standalone diesel generators for electricity. Situated in a tropical region, Malaysia receives an abundance of solar irradiance throughout the year and photovoltaic (PV) systems can be one of the possible energy sources to complement the diesel generators in the remote areas, to reduce the reliance on diesel generators. This translates into the reduced fossil fuel consumption, hence bringing an economic benefit to residents in the remote areas. However, one issue associated with photovoltaics is the intermittency its power generation. Energy storage system (ESS) offers a solution which can be used in conjunction with the generator-PV system. The ESS ensures energy supply security and reliability by storing up excess solar energy for later use in the energy deficit situation. In addition to the generator-PV-ESS system, other systems such as the PV-ESS, generator-ESS, generator-PV are modelled in Matlab Simulink. The main purpose of the study is to obtain the optimal system size and control strategy which yields the minimum cost of energy (COE) while reliably supplying electricity to the inhabitants it is intended for. Optimal system component sizing is an important factor in keeping system costs low. Oversizing of components such as PV and ESS might incur additional costs

while under sizing of these components might cause power supply reliability issues as system might not be able to meet the load demand. Load following and cycle charging control strategies, which are commonly used in other literatures are devised for the generator-PV-ESS system. Other than that, a novel fuzzy control dispatch strategy was also designed for the generator-PV-ESS system. A total of four different fuzzy configurations were devised and tested in this study. The generator-PV-ESS system produced the lowest COE compared to other types of system. Other than that, the fuzzy control dispatch strategy achieved a system with lower COE compared to the load following and cycle charging dispatch strategy. Various component sizes for PV, ESS and generator were simulated for these different types of system. This work assumes perfect knowledge of daily solar irradiance pattern as well as load demand. Simulation results show that using the developed control strategies, COE reduction achieved using the generator-PV-ESS system over that of a standalone generator system is promising.

## **ACKNOWLEDGEMENTS**

I would like to express my gratitude to my supervisor, Dr. Chua Kein Huat for providing me with a platform and opportunity to undertake this interesting research area. I have gained a wide array of knowledge and wisdom from him throughout the entire academic research journey of mine. I would also like to thank my co-supervisor, Prof. Ir. Dr. Lim Yun Seng for his patience, encouragement and constructive feedback while undertaking this research. His kindness in providing me with a conducive space to carry out my research is something that I am thankful for. His vast experience in the academic research arena is something that I have gained and benefitted in the form of valuable feedback for my research project. I would like to show my special gratitude to Dr. Stella Morris for her constructive feedback on my research work.

I would also express my gratitude to my parents for their support while I pursue my postgraduate studies. They are the ones brought me into this world and carefully nurtured me until adulthood. I will work even harder in the future to bring them pride.

Finally, I would like to thank my colleagues who are also pursuing their postgraduate studies. Having them throughout my journey here meant a lot to me as all of us cheered each other on to overcome challenges that we have faced throughout our research work.

## APPROVAL SHEET

This dissertation/thesis entitled “A NOVEL ALGORITHM FOR OPTIMAL OPERATION AND SIZING OF GENERATOR-PHOTOVOLTAIC-ENERGY STORAGE SYSTEM FOR MINIMIZING COST OF ENERGY” was prepared by CHOK EU-TJIN and submitted as partial fulfillment of the requirements for the degree of Master of Engineering Science at Universiti Tunku Abdul Rahman.

Approved by:

\_\_\_\_\_  
(Dr. CHUA KEIN HUAT)

Date:.....

Supervisor

Department of Electrical and Electronic Engineering  
Lee Kong Chian Faculty of Engineering and Science  
Universiti Tunku Abdul Rahman

\_\_\_\_\_  
(Prof. Ir. Dr. LIM YUN SENG)

Date:.....

Professor/Co-supervisor

Department of Electrical and Electronic Engineering  
Lee Kong Chian Faculty of Engineering and Science  
Universiti Tunku Abdul Rahman

**LEE KONG CHIAN FACULTY OF ENGINEERING AND SCIENCE**  
**UNIVERSITI TUNKU ABDUL RAHMAN**

Date: \_\_\_\_\_

**SUBMISSION OF THESIS**

It is hereby certified that **CHOK EU-TJIN** (ID No: *14UEM06555* ) has completed this thesis entitled “**A Novel Algorithm for Optimal Operation and Sizing of Generator-Photovoltaic-Energy Storage System for Minimizing Cost of Energy**” under the supervision of Dr. Chua Kein Huat (Supervisor) from the Department of Electrical and Electronic Engineering, Lee Kong Chian Faculty of Engineering and Science, and Prof. Ir. Dr. Lim Yun Seng (Co-Supervisor) from the Department of Electrical and Electronic Engineering, Lee Kong Chian Faculty of Engineering and Science.

I understand that University will upload softcopy of thesis in pdf format into UTAR Institutional Repository, which may be made accessible to UTAR community and public.

Yours truly,

\_\_\_\_\_  
(*Chok Eu-Tjin*)

## **DECLARATION**

I (CHOK EU-TJIN) hereby declare that the dissertation is based on my original work except for quotations and citations which have been duly acknowledged. I also declare that it has not been previously or concurrently submitted for any other degree at UTAR or other institutions.

Name: Chok Eu-Tjin

Date: September 2017

## TABLE OF CONTENTS

	<b>Page</b>
<b>ABSTRACT</b>	<b>iv</b>
<b>ACKNOWLEDGEMENTS</b>	<b>vi</b>
<b>APPROVAL SHEET</b>	<b>vii</b>
<b>SUBMISSION SHEET</b>	<b>viii</b>
<b>DECLARATION</b>	<b>ix</b>
<b>LIST OF TABLES</b>	<b>xiv</b>
<b>LIST OF FIGURES</b>	<b>xvi</b>
<b>LIST OF ABBREVIATIONS/NOTATION</b>	<b>xix</b>
<b>CHAPTER</b>	
<b>1.0 INTRODUCTION</b>	<b>1</b>
1.1 Research Background	1
1.2 Research Objectives	3
1.3 Research Methodology	4
1.4 Thesis Organization	6
1.5 List of Publications	8
<b>2.0 LITERATURE REVIEW</b>	<b>9</b>
2.1 Introduction	9
2.2 Power Generation in Remote Areas	9
2.3 Feasibility of Hybrid Energy Systems	11
2.4 Essential elements for a Hybrid Energy System	13
2.4.1 Diesel Generator	14
2.4.2 Photovoltaic (PV) Cells	14
2.4.3 Energy Storage System	15

2.5	Assessment of HES	15
2.5.1	Technical Considerations	15
2.6	Optimal System Component Sizing	17
2.6.1	Intuitive Method	18
2.6.2	Iterative Technique	19
2.6.3	Graphical Method	21
2.6.4	Probabilistic Method	22
2.6.5	Linear Programming Method	22
2.6.6	Genetic Algorithm	23
2.7	Dispatch and Control Strategies	25
2.7.1	Dynamic Control	26
2.7.2	Dispatch Control	27
2.7.3	Role of Artificial Intelligence in HES Control	31
2.8	Homer	33
2.9	Summary	34
<b>3.0</b>	<b>ARCHITECTURE OF HYBRID ENERGY SYSTEM</b>	<b>35</b>
3.1	Introduction	35
3.1.1	Matlab/Simulink	36
3.1.2	Simulation Type	40
3.2	Diesel Generator	41
3.2.1	Calculation of Generator Parameters	43
3.3	Energy Storage System	46
3.3.1	Battery Lifetime	48
3.3.2	ESS Energy	49
3.4	Solar Photovoltaic (PV)	50
3.5	Bi-directional Converter	52
3.6	Load Demand	54
3.7	Power to Current Conversion	57
3.8	System Sizing	60
3.9	Economic Feasibility Study	62
3.9.1	Calculation of COE in Microsoft Excel	66
3.9.2	Calculation of Payback Period	67

3.10	Simulation and Optimization Process	67
3.11	Summary	69
<b>4.0</b>	<b>CONTROL ALGORITHM IN HYBRID ENERGY SYSTEM</b>	<b>71</b>
4.1	Introduction	71
4.2	Control and Operation	72
4.2.1	Generator-ESS System	73
4.2.2	Generator-PV System	74
4.2.3	PV-ESS System	75
4.3	Generator-PV-ESS System	77
4.3.1	Load Following and Cycle Charging Strategy	77
4.4	Fuzzy Control Dispatch Strategy	85
4.4.1	Design of Fuzzy Control Dispatch Strategy	91
4.5	Summary	95
<b>5.0</b>	<b>RESULTS AND DISCUSSION</b>	<b>96</b>
5.1	Introduction	96
5.2	Technical Feasibility Studies for Different System Configurations	96
5.2.1	Generator-PV System	97
5.2.2	Generator-ESS system	99
5.2.3	PV-ESS system	102
5.3	Performance of Generator-PV-ESS System	104
5.3.1	Case Study 1: Load Following Operation with Varying ESS Size	104
5.3.2	Case Study 2: Cycle Charging Operation with Varying Solar Irradiance	107
5.3.3	Case Study 3: Fuzzy Control Operation	110
5.3.4	Case Study 4: Comparison of the Fuzzy Control Dispatch Strategy with the Load Following and Cycle Charging Strategies under Various Solar Irradiance	113
5.4	Economic Considerations	118

5.4.1	Economic Analysis of Generator-PV System	118
5.4.2	Economic Analysis of Generator-ESS System	121
5.4.3	Economic Analysis of PV-ESS System	122
5.5	Economic Analysis of Generator-PV-ESS System	123
5.5.1	Generator Size at 40 kW	124
5.5.2	Generator Size at 50 kW	126
5.5.3	Generator Size at 60 kW	128
5.5.4	Economic Comparison for Load Following and Cycle Charging	130
5.6	Fuzzy Control Dispatch Strategy	133
5.6.1	Economic Analysis of Fuzzy Control Dispatch Strategy	134
5.6.2	Economic Comparison for Fuzzy Control Dispatch Strategy	138
5.7	Fuzzy Control Dispatch Strategy using different Load Profiles	140
5.7.1	Fuzzy Control Dispatch Strategy in Load Profile 2	140
5.7.2	Fuzzy Control Dispatch Strategy in Load Profile 3	143
5.8	Summary	146
<b>6.0</b>	<b>CONCLUSIONS AND FUTURE WORKS</b>	<b>148</b>
6.1	Conclusion	148
6.2	Limitation and Future Work	151
	<b>LIST OF REFERENCES</b>	<b>153</b>
	<b>APPENDICES</b>	<b>158</b>

## LIST OF TABLES

<b>Table</b>		<b>Page</b>
1.1	List of publications	8
3.1	Description of the data types supported by “To Workspace” block	39
3.2	Diesel generator fuel consumption	42
3.3	Energy generated at various generator loading factor	43
3.4	Diesel generator fuel consumption in terms of liter/hour	44
3.5	ESS string size and its corresponding kWh value	46
3.6	Converter size at various PV size	54
3.7	Comparison between the different load profiles	57
3.8	Component sizes used in the study	61
3.9	Component lifetime and costs for COE calculation	65
4.1	Fuzzy rule 1	94
4.2	Fuzzy rule 2	95
5.1	Power flow equation for the system in load following operation with varying ESS size	107
5.2	Power flow equation for the system in cycle charging operation during low and high PV output	108
5.3	Power flow equation for the system in fuzzy control operation during low and high PV output	113
5.4	Economic analysis for generator-PV system	119
5.5	COE values for generator-ESS system	121
5.6	COE values for PV-ESS system	122
5.7	Economic summary for load following dispatch strategy	131

5.8	Economic summary for cycle charging dispatch strategy	131
5.9	Economic summary of fuzzy control dispatch strategy	138
5.10	Economic comparison between standalone diesel generator system and generator-PV-ESS system using fuzzy control dispatch strategy for load profile 2	141
5.11	Economic comparison between standalone diesel generator system and generator-PV-ESS system using fuzzy control dispatch strategy for load profile 3	144

## LIST OF FIGURES

<b>Figure</b>		<b>Page</b>
2.1	(a) Load following dispatch strategy (b) Cycle charging dispatch strategy	28
3.1	(a) generator-PV system (b) generator-PV-ESS system (c) generator-ESS system (d) PV-ESS system	36
3.2	Screenshot of Matlab software	38
3.3	To Workspace block for data logging	39
3.4	To Workspace block parameter setting menu	40
3.5	Three-phase source Simulink block	41
3.6	Simulink block diagram of the lookup table block, for the calculation of generator fuel consumption	43
3.7	Lookup table parameter setting box	44
3.8	Calculation of generator runtime	45
3.9	Block diagram for calculation of SOC	47
3.10	Block diagram for calculation of ESS energy	49
3.11	Block diagram for PV source generation	51
3.12	PV deloading operation	52
3.13	Daily power output for a 100kW PV installation (365 days)	53
3.14	Load profile 1	55
3.15	Load profile 2	56
3.16	Load profile 3	56
3.17	Block diagram for conversion of power to current	58
3.18	Three unbalanced vectors of three-phase system resolved into three balanced systems of vectors	59
3.19	Block diagram for conversion of power to current	60

3.21	Process of simulation and optimization	69
4.1	Dispatch strategy flowchart for generator-ESS system	74
4.2	Dispatch strategy flowchart for generator-PV system	75
4.3	Dispatch strategy flowchart for PV-ESS system	77
4.4	Regions of operation for generator-PV-ESS system	78
4.5	Flowchart for the load following dispatch strategy	83
4.6	Flowchart for the cycle charging dispatch strategy	84
4.7	System in (a) cycle charging dispatch strategy (b) fuzzy control dispatch strategy	88
4.8	Flowchart for fuzzy control dispatch strategy	90
4.9	Fuzzy inference system	91
4.10	Input and output of fuzzy logic controller	92
4.11	Input membership function for (a) solar irradiance (b) battery SOC	93
4.12	Output membership function (a) MF1 (b) MF2	94
5.1	Generator-PV system with small PV size	98
5.2	Generator-PV system with large PV size	99
5.3	Generator-ESS system with small ESS size	100
5.4	Generator-ESS system with large ESS size	101
5.5	PV-ESS system under high solar irradiance	102
5.6	PV-ESS system under low solar irradiance	103
5.7	Load following operation of system having 50 kW generator, 80 kW PV (Scenario 1: ESS size of 5 strings)	105
5.8	Load following operation of system having 50 kW generator, 80 kW PV (Scenario 2: ESS size of 3 strings)	106

5.9	System in cycle charging operation with 50 kW generator, ESS size of 3 strings, PV size of 60 kW at (a) low PV output day	108
5.10	System in cycle charging operation with 50 kW generator, ESS size of 3 strings, PV size of 60 kW at (b) high PV output day	109
5.11	System in fuzzy control operation with 50 kW generator, ESS size of 3 strings, PV size of 60 kW at (a) low PV output day	111
5.12	System in fuzzy control operation with 50 kW generator, ESS size of 3 strings, PV size of 60 kW at (b) high PV output day	112
5.13	Low solar irradiance operation in (a) load following (b) cycle charging (c) fuzzy control	115
5.14	High solar irradiance operation in (a) load following (b) cycle charging (c) fuzzy control	117
5.15	COE of generator-PV system	119
5.16	Generator runtime vs generator replacement	120
5.17	COE values for 40 kW generator (a) load following (b) cycle charging	125
5.18	COE values for 50 kW generator (a) load following (b) cycle charging	127
5.19	COE values for 60 kW generator (a) load following (b) cycle charging	129
5.20	Fuzzy control dispatch strategy (a) Rule 1- MF 1 (b) Rule 1- MF 2	135
5.21	Fuzzy control dispatch strategy (a) Rule 2- MF 1 (b) Rule 2- MF 2	137
5.22	COE values obtained with fuzzy control dispatch strategy in load profile 2 (a) Rule 1-MF 1 (b) Rule 1-MF 2 (c) Rule 2-MF 1 (d) Rule 2-MF 2	143
5.23	COE values obtained with fuzzy control dispatch strategy in load profile 3 a) Rule 1-MF 1 (b) Rule 1-MF 2 (c) Rule 2-MF 1 (d) Rule 2-MF 2	146

## LIST OF ABBREVIATIONS/ NOTATION

HES	Hybrid Energy System
O&M	Operation and maintenance
ESS	Energy Storage System
COE	Cost of Energy
LCOE	Levelised Cost of Electricity
PV	Photovoltaic
STC	Standard test conditions
DOD	Depth of discharge
LPSP	Loss of power supply probability
LLP	Loss of load probability
UL	Unmet Load
TED	Total Energy Deficit
TNPC	Total Net Present Cost
EC	Energy cost
ENS	Energy Not Supplied
LCE	Life cycle emissions
MILP	Mixed-integer linear program
AI	Artificial Intelligence
GA	Genetic Algorithm
SOC	State of Charge
NPC	Net Present Cost
DPP	Discounted Payback Period
FLC	Fuzzy Logic Controller

# CHAPTER 1

## INTRODUCTION

### 1.1 Research Background

There are many rural areas without utility grid connection as they are geographically too far from the cities. With low population and low overall demand for electricity, the high cost of grid connection to these areas is not justified. These rural areas depend on standalone diesel generators for electricity generation which are often very costly in the long run.

To solve this problem, hybrid energy system (HES) can be a viable system for these rural areas. HES is advantageous when compared to single source energy systems as it has higher reliability and efficiency, lower energy storage requirement due to complementary behaviour of different sources, and minimum electricity generation cost when optimum system design is used (Sinha and Chandel, 2014).

In the research, the energy sources considered are the PV, energy storage system (ESS) and the diesel generator. The feasibility of HES using a combination of these energy sources are also reviewed. Systems with PV remain a popular option as PV has a significantly lower maintenance cost as compared to that of the standalone diesel generator. However, energy generation using PV is

intermittent and its output is dependent on meteorological variables. The ESS can be used to store excess energy from the PV and this energy can be discharged whenever needed.

An important design aspect of HES is that they must be economically feasible, while reliably supplying electricity to the inhabitants it is intended for. The type and capacity of the energy sources used will impact the system cost as well as the lifetime of the energy sources. In other words, optimal system component sizing is an important factor in keeping system costs low. Oversizing of components such as PV and ESS might incur additional costs. On the other hand, under sizing of these components might cause power supply reliability issues as system might not be able to meet the load demand.

Apart from that, the control and dispatch strategies of all HES are also studied. Dispatch control simulation is based on solving the energy balance between the energy generated, consumed and stored (Mandelli et al., 2016). The dispatch strategy of each of the HES type is designed, and they include those for the generator-PV, generator-ESS, PV-ESS and the generator-PV-ESS system. For the generator-PV-ESS system, there are two widely used dispatch strategies, namely the load following and cycle charging dispatch strategies.

In the load following strategy, the generator will supply power enough to meet the load demand. On the other hand, in the cycle charging strategy, generator will operate at a high loading factor in order to produce surplus power to be charged into the ESS. Load following and cycle charging are widely used

dispatch strategies and its application can be found in the works of (Ma et al., 2015), (Basir Khan et al., 2015), (Kolhe et al., 2015), (Ngan and Tan, 2012), (Adaramola et al., 2014). A novel fuzzy control dispatch strategy is proposed in this study. The fuzzy control dispatch strategy aims to reduce PV energy wastage due to insufficient ESS capacity while reducing generator turn-on time.

The optimal component size, combined with a good dispatch strategy will ensure that a minimum cost of electricity (COE) is achieved. In this study, COE is used as a performance indicator for comparison between different configurations of HES systems. The COE of the fuzzy control dispatch strategy is compared against that of the load following and cycle charging dispatch strategy.

## **1.2 Research Objectives**

The objectives of this research work are as follows:

1. To determine the optimal size for each component in the HES.
2. To develop control strategies for the operation of HES to achieve a minimal cost of energy.
3. To evaluate the performance of the control strategies developed for the HES.

### **1.3 Research Methodology**

This research aims to determine the optimal component sizing and dispatch strategy for the Generator-PV-ESS system in order to achieve minimum COE. Each of the HES models in study are designed and simulated in Matlab Simulink. Using a wide range of component sizes, each HES is simulated and the outputs are recorded in order to calculate the COE of each system. These outputs include the generator runtime, fuel consumption and the ESS throughput. Other than that, control strategies for the HES were also developed for the generator-PV-ESS system, which are the widely used load following and cycle charging dispatch strategy. A novel fuzzy dispatch strategy is developed and its performance is compared against that of the load following and cycle charging dispatch strategy. Different cases and scenarios are used to evaluate and compare the performance of the control algorithms. The research methodology is divided into 4 steps as follows:

#### *Step 1: Literature review*

Review of existing options for off-grid power systems in remote areas, where grid extension is not feasible. The challenges in providing electricity to these remote areas using standalone diesel generator are highlighted. A thorough review of HES implemented in other literature is done. Various dispatch strategies for the HES were also reviewed. The components for the HES are also briefly introduced.

*Step 2: Design and development of various HES in modelling software*

All the HES which are developed include the generator-PV, generator-ESS, PV-ESS, and generator-PV-ESS system. All the components including the diesel generator, PV, ESS and load were modelled in Matlab Simulink.

*Step 3: Development of dispatch strategies for HES*

Dispatch strategies for the generator-PV, generator-ESS, PV-ESS and generator-PV-ESS are developed. For the generator-PV-ESS system, the widely used load following and cycle charging dispatch strategies were developed. A novel fuzzy control dispatch strategy is developed which reduces the COE of the system. The fuzzy control dispatch strategy reduces energy wastage due to PV curtailment and also reduces the generator turn-on time.

*Step 4: Performance evaluation of dispatch strategies*

Each of the HES systems was evaluated in terms of its technical and economic feasibility. In the technical feasibility study, several case studies with different operating conditions were investigated. Economic feasibility study is carried out by having each system compared against each other in terms of the COE produced. A system with an optimum component size and well-designed dispatch strategy will yield a low COE.

## **1.4 Thesis Organization**

The structure of the thesis is organized as follows:

Chapter 2 of this thesis introduces the problems associated with electricity generation in rural areas without utility grid connection. These areas rely on expensive and inefficient diesel generators for power generation. The chapter also summarizes the literature review of existing Hybrid Energy System (HES) used in these rural areas. Essential elements of the HES such as PV, ESS and diesel generator are also introduced. The technical assessment for HES as well as the optimal system component sizing is also discussed in this chapter. Dispatch strategies for the HES are also discussed, along with a review of the role of artificial intelligence in the control of HES.

Chapter 3 describes the system design developed in Matlab Simulink. The details of each component such as the generator, PV, ESS and bi-directional converter are explained. The parameters including the generator runtime, fuel consumption, as well as the ESS throughput are considered in the calculation of COE, which is an economic feasibility indicator used in the study.

Chapter 4 describes the dispatch strategies involved in all the type of systems simulated. In this study, the generator-PV-ESS system and various combination of hybrid energy system (HES) such as generator-PV, generator-ESS, and PV-ESS system are studied. The control and operation for each of these systems are presented and explained in detail. The dispatch strategies formulated is based

on the availability of the energy source. For example, in this case it would be the availability of the solar PV source. In the generator-PV-ESS system, the load following and cycle charging dispatch strategies are outlined and presented. Both of these dispatch strategies are widely used in other literature when dealing with generator-PV-ESS systems. Other than that, a novel fuzzy control dispatch strategy is introduced which addresses the shortcomings of the load following and cycle charging dispatch strategy. The fuzzy control dispatch strategy makes use of PV prediction data as well as the state of charge (SOC) of the ESS in order to determine the generator turn-off time. Using this dispatch strategy, the generator turn-off time is maximized while PV curtailment/wastage is minimised. These control algorithms are developed and simulated in the Matlab Simulink software.

Chapter 5 discusses the operation of each system simulated based on different operating scenarios. For example, in a generator-PV system, the system operation under different PV sizes were discussed. Other than evaluating the systems in terms of its technical feasibility, the systems were also evaluated in terms of its economic feasibility. The performance of the fuzzy-based dispatch strategy is compared with the performance of the load following and cycle charging strategy using the COE values. The results for the economic feasibility are presented and discussed in this chapter.

Finally, conclusions are drawn in Chapter 6. The key findings of the research and their implications are summarized. The limitations and opportunities for future improvement of the energy storage system are also elaborated.

## 1.5 List of Publications

The research findings have been published in peer review journals and international conferences and they are as listed in Table 1.1.

**Table 1.1: List of publications**

No	Title/ Status/ Link	Status	Journal (J)/ Proceeding (P)/ Conference (C)	Index/ Impact factor
1	Control Strategies in Energy Storage System for Standalone Power Systems <a href="http://digital-library.theiet.org/content/conferences/10.1049/cp.2016.1268">http://digital- library.theiet.org/c ontent/conferences/ 10.1049/cp.2016.1 268</a>	Accepted	(C): 4 <sup>th</sup> IET International Conference on Clean Energy and Technology 2016	SCOPUS
2	Novel Fuzzy Controller for Standalone Power Systems for Minimum Cost of Electricity and Carbon Emissions	Under Review	(J): Energy	ISI/ 4.292

## **CHAPTER 2**

### **LITERATURE REVIEW**

#### **2.1 Introduction**

This chapter presents a review on the application of standalone hybrid energy systems (HES) in remote areas, where grid extension is costly and not feasible. Technical and economic feasibility of such a system is presented, along with issues often associated with HES. A thorough overview of the component sizing methods used in other researches is also reviewed. Various operation and control strategies using classical and advanced approach are compared.

#### **2.2 Power Generation in Remote Areas**

There are many rural areas in Malaysia, particularly East Malaysia, which do not have access to the electricity grid because these areas are geographically remote from the cities. These rural areas have to depend on the standalone diesel generators for electricity generation as the grid extension to these areas requires a significantly high cost. Low population density and low overall electricity demand do not make a good justification for huge investments associated with infrastructure for electricity grid connection (Veldhuis and Reinders, 2015). An example of such remote area is Pulau Perhentian, one of

the smallest island in Malaysia which is powered by 200 kW diesel generators (Ashourian et al., 2013). Other examples such as Pulau Tioman, Pulau Redang, and Pulau Layang-layang (Lau et al., 2015). There are also a fair share of off-grid areas on the mainland as well, with examples such as Kemar in Perak (Aziz and Shamsudin, 2013), Kalabakan in Sabah (TNB Energy Services, n.d.), Kampung Denai in Pahang, and Kampung Opar in Sarawak (Fadaeenejad et al., 2014).

Although the initial investment on diesel generators are low, however the operation and maintenance (O&M) costs over time is significantly high. Other than that, relatively high O&M costs are attributed to the transportation costs factored into the price of the diesel fuel. In some areas, the fuel price can be 400% more expensive than the retail price due to the high transportation costs involved (Lau et al., 2010). In another part of the world for instance, the residents in rural areas who depend on diesel generator systems frequently experience blackouts due to the high fuel cost and the discontinuous fuel supplies (Ma et al., 2015). A similar blackout situation was also experienced by schools as highlighted in (Ajan et al., 2003) when maintenance had to be done on the school's standalone generator system. Approximately 800 out of 10,000 schools in Malaysia are not supplied with 24 hour electricity. Most of them are located in East Malaysia, and no plans are in place for them to be connected to the grid in the next 5 to 10 years (Borhanazad et al., 2013). (Mahmud, 2010) also reported on the state of these schools without electricity grid connection in the state of Sabah, where 79 out of 276 schools have been installed with hybrid photovoltaic (PV) systems which not only increases the supply reliability but

also reduce dependency on the costly diesel generators. Another problem with the standalone diesel generators is when they are often operated at low loading factor, which increases the cost of energy (COE) produced (Merei et al., 2013)

### **2.3 Feasibility of Hybrid Energy Systems**

In the study carried out by (Ngan and Tan, 2012), the technical and economic feasibility of hybrid energy systems were analyzed. Six types of systems are introduced, namely the generator-PV system, generator-wind turbine system and the generator-wind turbine-PV system, all of them with and without the energy storage system (ESS). As compared to the standalone diesel generator system, these HES are feasible only when the fuel cost is high. (Ashourian et al., 2013) proposed a generator-PV-ESS-wind turbine system for an island resort in Malaysia. It was found that the system is low in economic feasibility as compared to the standalone generator system because of the high component cost. Although the HES brought about savings in generator fuel and runtime, the high material and installation cost of PV and batteries are the main barrier when evaluating the HES against standalone generator system.

The COE of the generator-PV-ESS systems in Northern Nigeria are found to be 7.9% lower as compared to the standalone generator systems, based on simulations using HOMER (Adaramola et al., 2014). The generator-PV-ESS system is also found to be the most economically viable option as compared to the generator-ESS and generator-PV system. The authors performed the

simulation using the current fuel price as well as the solar irradiance data for that particular area in Northern Nigeria. Although the COE for the HES is higher than that of the electricity tariff for the region in study, it is concluded that it is more economically viable as compared to the COE after accounting for the cost of grid extension.

The authors of (Ajan et al., 2003) have presented the feasibility studies of using the hybrid system of generators, PV and ESS instead of the standalone generators in the rural areas. Anticipating future drop in PV prices, the generator-PV-ESS system would be economically more viable than the standalone generator system. However, the issues of the PV systems are the intermittency of the power output as well as the PV power generation profile not matching with the demand profile of the customers. ESS can be used in order to store excess energy for later use. Several studies have been carried out with regards to using ESS in generator-PV systems. A feasibility study done in Indonesia for the generator-PV-ESS system (Veldhuis and Reinders, 2015) shows that the Levelised Cost of Electricity (LCOE) is 19% lower than that of standalone diesel generator systems.

As (Sinha and Chandel, 2014) sums it up, the advantages of hybrid energy system in comparison to single source energy systems are: higher reliability and efficiency, reduced energy storage capacity due to the complementary behavior of different energy sources, as well as minimum electricity generation cost when optimum system design is used.

However, ESS contributes to a high system cost, as they can take up to 52% of the total system cost (Jakhrani et al., 2012). The price of PV and ESS is expected to continue to decrease in the near future, providing HES a competitive edge against standalone diesel generators in terms of energy cost.

#### **2.4 Essential Elements for a Hybrid Energy System**

A HES consists of more than two electricity generation sources, of which they can be renewable energy based or fossil fuel based. Being blessed with the abundance of solar irradiance in Malaysia, solar energy has a huge potential to provide electricity for off-grid rural areas. The natural resources required for solar energy generation is essentially free, abundant, and inexhaustible.

One popular option for energy generation is through PV systems because they have a significantly lower maintenance cost as compared to that of the standalone diesel generator. However, PV based systems may incur high initial costs, and its sunshine dependent nature is not able to supply electricity on a 24 hour basis (Shaahid and El-Amin, 2009). PV system's performance is intermittent and is greatly dependent on meteorological input such as solar irradiance and temperature. PV systems are a good complement to the existing standalone diesel generator systems as it is capable of providing a greater system reliability at reduced energy generation costs (Ameen et al., 2015).

### **2.4.1 Diesel Generator**

Power generation using diesel generators is a popular option in many rural areas without power grid connection. However, the high operational and maintenance cost of diesel generator systems remain as one of the drawbacks of this method of energy generation.

### **2.4.2 Photovoltaic (PV) Cells**

A PV cell converts sunlight into direct current (DC) electricity. Energy generation through PV cells is generally regarded as one of having a low maintenance. However, the high price of PV cells is a prohibitive factor when it comes to energy generation using PV. Other than that, another drawback of electricity generation through PV is that it is intermittent in nature. A PV cell is a semiconductor device which converts solar energy into DC electricity through the photovoltaic effect. A PV panel consists of multiple connected PV cells and is modular in nature. The power rating of each PV panel is specified in terms of peak Watts ( $W_p$ ) by the manufacturer at standard test conditions (STC) at a defined cell junction temperature of  $25^{\circ}\text{C}$  and irradiance of  $1000\text{ W/m}^2$ .

### **2.4.3 Energy Storage System**

There are three important factors which need to be considered when evaluating the cycle life of the ESS (Gallo et al., 2016). They are the depth of discharge (DOD), charge and discharge rate, as well as ambient operating temperature. A 100% DOD indicates that the ESS is fully depleted while 0% DOD indicates fully charged ESS. A high DOD cycling will result in a shorter battery lifetime. Generally, the ESS lifetime will be reduced when it is charged or discharged at a higher rate than that specified by the manufacturer. Meanwhile, as ambient operating temperature of the ESS increases, battery lifetime will be reduced.

## **2.5 Assessment of HES**

### **2.5.1 Technical Considerations**

There are multiple technical parameters which need to be considered when designing a HES. This is due to the fluctuating nature of renewable energy sources, such as the PV. It is essential that the system meets the load demand.

One of the technical parameters is the loss of power supply probability (LPSP). It is the probability that the power supply is unable to meet the load demand and indicates the reliability of a power supply. LPSP is calculated by dividing all loss of power supply over time ( $LPS(t)$ ), over the total load demand ( $LD(t)$ ). Mathematically, it can be expressed in the following manner: A LPSP value of

0 indicates that load demand is fully met. The degree of LPSP can vary from system to system, and ranges from 0 to 1. The following equation expresses the LPSP:

$$LPSP = \frac{\sum_{t=1}^N LPS(t)}{\sum_{t=1}^N LD(t)} \quad (2.1)$$

Where,

$$LPS(t) = LD(t) - E_{sys}(t) \quad (2.2)$$

Where  $E_{sys}(t)$  is total energy generated from the system and  $LD(t)$  the total load demand of the system.

In some literature, a similar index to the LPSP is known as the Loss of load probability (LLP). It is an indicator of how often the occurrence whereby a system is unable to meet the load demand (Ismail et al., 2014). Alternatively, it is the percentage of the mean load unmet by the system and can be expressed as the ratio of the total energy deficit to the total load demand over a specific time period. The following formula expresses the LLP:

$$LLP = \frac{\sum_{t=1}^N ED(t)}{\sum_{t=1}^N LD(t)} \quad (2.3)$$

Where  $ED(t)$  is the energy deficit, which is the energy not able to be supplied by system.

Unmet Load (UL) refers to the load not met, divided by the total sum of load over a time period (Bernal-Agustín and Dufo-López, 2009). In (Borowy and Salameh, 1996), the authors performed optimization on the size of PV and ESS in a PV-wind-ESS system, while considering the desired UL value. The number

of PV and ESS were varied and each combination are assessed economically, while complying to the maximum UL value specified.

In (T. Givler and P. Lilienthal, 2005), the authors concluded that by allowing a small percentage of unserved load, PV-ESS system can be more cost competitive than a generator-PV-ESS system over a larger range of loads. In applications which allow for some capacity shortage to occur, capital cost can be significantly reduced. The cost competitiveness of the PV-ESS system over the generator-PV-ESS system would significantly increase even with a 0.5% of capacity shortage.

## **2.6 Optimal System Component Sizing**

The most vital aspect in the design of an off-grid hybrid energy system is that they must be economically feasible while supplying reliable electricity to inhabitants in remote areas. The type of generation sources and components used as well as their capacity size greatly impacts the system cost and its lifetime. Hence, correct system component sizing is crucial in the design of HES. Oversizing of components such as generator, PV, ESS might incur additional cost which is unnecessary. Other than that, sizes of components which are non-complementary to each other might also be an issue. For example, when PV is sized to be significantly larger than the capacity of the ESS, wastage might occur as excess energy from PV could not be utilised fully.

Unit sizing refers to the method of determining the correct size of the HES components by minimizing the system costs, while ensuring system reliability. The component sizing in this study is to determine the generator size, the PV size, as well as the ESS capacity. Over sizing of system components will incur additional system costs, while under sizing can result in the system being unable to meet the load demand, resulting in a power outage. Based on literature review done, there are six popular methods of sizing for HES: intuitive method, iterative method, graphical method, probabilistic method, linear programming method, as well as genetic algorithm based method.

There are multiple traditional approaches used in various literature. Other than that, artificial intelligence based approaches are proposed when it comes to system component sizing. This section will discuss these approaches and provide an insight of how system sizing is done in other studies.

### **2.6.1 Intuitive Method**

The intuitive method is the most basic sizing method for HES which takes into account mean or generalised values of the solar irradiance. This method does not consider the relationship between subsystems or the intermittent nature of solar irradiance (Sidrach-de-Cardona and Mora López, 1998). Sizing done using this method refers to the worst month method, one which uses meteorological data of a particular month that has the lowest solar energy yield. Alternatively, this can be based on the average annual solar energy production

values. However, one major disadvantage of such a method is that under or over sizing of system might occur, resulting in poor system reliability or high COE (Khatib et al., 2013).

### **2.6.2 Iterative Technique**

The iterative technique is a mathematical procedure which produces approximate solutions for problems in a recursive manner. The recursive process is halted when the best configuration is reached and is within the size boundaries defined by the designer. In (Diaf et al., 2007), the authors used the iterative technique to determine the best size of a PV-wind turbine system based on the lowest LCOE to meet the required system reliability. The iterative optimization method is computationally more taxing as compared to other methods (Sinha and Chandel, 2015).

In terms of optimal sizing of components in a HES, the authors of (Kaabeche and Ibtouen, 2014) developed a sizing model based on iterative approach for a generator-wind-PV-ESS standalone system. The suggested model considers three sub-models, which are the Total Energy Deficit (TED), Total Net Present Cost (TNPC) and Energy Cost (EC). The study evaluated various component sizes with TED of 0%, which basically are the systems which do not allow any energy deficit. The financial indicators TNPC and EC are then evaluated for these systems. The authors further concluded the generator-wind-PV-ESS

system is economically more feasible compared to the wind-PV-ESS system or standalone generator system.

The iterative method can be further divided into the stochastic and deterministic methods. In stochastic method, the intermittent nature of solar resource and load demand is considered by using the hourly solar irradiance and the load profile data in the simulation. Meanwhile, the deterministic method uses daily averaged solar irradiance and load demand as these data are difficult to obtain for the particular area in study.

The work by (Mandelli et al., 2016) introduces a stochastic method, where the authors introduced an off-grid PV-ESS system sizing methodology while considering the effects of load profile uncertainty. In achieving this, the authors developed an innovative stochastic method which produces varying daily load profiles based on a single load data. Different degrees of uncertainty can be selected in the model in order to study the effects of load uncertainty to the optimum sizing of components. Steady state simulation using hourly step time data was also used to perform techno-economic analysis for the system, and the optimum system size was determined based on the net present cost and loss of load probability.

### **2.6.3 Graphical Method**

A graphical construction method is presented in (Borowy and Salameh, 1996) to obtain the best component size of a PV-wind turbine system, utilising long-term meteorological data. The study was done based on residential load profile and at a desired LPSP. The study obtained the optimum component sizes, which was based on the minimum system cost. This method is also used in (Markvart, 1996) in designing a PV-wind system, based on monthly wind and solar data. The graphical construction technique is easily understandable and non-complex. However, the drawback of such a method is that it is inflexible and is based on assumptions and the coefficients of mathematical equations are difficult to derive (Sinha and Chandel, 2015).

The authors in (Arun et al., 2008) introduced a sizing method for a PV-ESS system using such a technique. In the study, it utilizes a sizing curve which connects the combination of PV sizes and the resulting minimum ESS capacity required to meet the load demand. Doing so enables the system designer to identify the entire range of feasible system configurations, or rather the configurations which meet a specified reliability level. Such a method was also in (Khatib et al., 2012) , where sizing method using sizing curve for optimum PV size at different LLP and optimum ESS size for different PV sizes are presented.

#### **2.6.4 Probabilistic Method**

The probabilistic approach is such that where multiple possible outcome exists for different degrees of uncertainty of occurrence of parameters, such as the fluctuating nature of solar parameters as well as the load demand. The probabilistic approach enables uncertainty to be quantified not in fixed values, but by using distributions. However, the main disadvantage of such a method is that it cannot represent the dynamic changing performance of the hybrid system. This method is used in (Tina et al., 2006) where the authors used the probabilistic approach to assess the long term performance of the solar-wind hybrid system, both for grid-connected and off-grid applications. Sizing is based on the Energy Expected Not Supplied (EENS), a probabilistic index used for systems integrating renewable energy sources, and happens during the condition where load exceed available generation. It is found that when the probabilistic method is compared to the iterative technique based on a simulation program developed in Matlab Simulink, difference in the EENS is only up to 1.9%.

#### **2.6.5 Linear Programming Method**

The linear programming method is based on mathematical model represented by linear relationships and is suitable for solving complex problems (Sinha and Chandel, 2015). In (Chedid and Rahman, 1997), the authors used the linear programming technique to obtain the lowest cost of electricity while ensuring the supply reliability for a PV-wind system. (Nogueira et al., 2014) presented a

sizing methodology using linear programming for a PV-ESS-wind system. The proposed system is effective in producing remote systems with minimum cost and high reliability. The system designed enables various LPSP to be defined and the optimal sizing will be the result of the required LPSP level.

(Dufo-López et al., 2011) describes a multi-objective optimization of a standalone generator-wind-PV-generator-battery system, with the aim at minimizing carbon dioxide life cycle emissions (LCE) and the levelised cost of energy (LCOE). Evolutionary algorithms were also used to search for best combination of components in terms of LCOE and LCE. (Al Busaidi et al., 2016) presents three techniques for the component sizing of a wind-PV energy system. They are the annual monthly average sizing technique, most unfavorable month technique, and the LPSP technique. The LPSP technique is also used by other literature in (Yang et al., 2008). In (Shen, 2009), LPSP was employed in the optimal sizing of a PV-ESS system in Malaysia. (Khalilpour and Vassallo, 2016) developed a decision support tool for optimal sizing and operation scheduling for grid-connected PV-ESS system. A multi-period mixed-integer linear program (MILP) is developed with the aim at maximizing the net present value of the cash flow and minimizing operational costs.

#### **2.6.6 Genetic Algorithm**

In hybrid energy systems, the optimal sizing of the components is a non-convex and non-linear optimization problem. In effectively solving such problems,

heuristic algorithms which are derived as a branch of artificial intelligence (AI) is needed. (Maleki and Pourfayaz, 2015, p. maleki)

Genetic Algorithm (GA) is a search process which imitates the natural selection process. Solutions are generated by using techniques derived from the natural evolution process, such as crossover, mutation and inheritance. It excels in solving problems with various solutions and is easily understandable. However, the limitation of GA is that it has a tendency to converge towards the local optimum point rather than the global optimum point.

In (Dufo-López and Bernal-Agustín, 2005), the sizing methodology for a generator-PV system is presented. GA is used to optimize the system, where variables such as number of PV panels, type of PV panel, number of batteries, type of battery, generator size, inverter size, as well as dispatch strategies. The GA developed is made up of two parts, where the first part optimizes the system component configuration needed to meet the load demand satisfactorily while the second part performs component operation optimization based on configuration obtained in the first part. The methodology also calculates the COE for the optimized configuration.

GA excels in scenarios where classical optimization cannot perform well, due to complexity present in HES such as non-linear characteristics of components and uncertainty in renewable energy productions and load demand. GA is also used in the sizing of the components in the work by (Bala and Siddique, 2009).

## 2.7 Dispatch and Control Strategies

In a HES, two forms of control are present, namely the dynamic control and dispatch control. Dynamic control is concerned with the parameters such as frequency and voltage magnitude of the system while dispatch control deals with energy flow between components within the system (Gupta et al., 2011). Dispatch control simulation is based on solving the energy balance between the energy generated, consumed and stored (Mandelli et al., 2016). Using such a simulation method, the case study over a year can be performed, using hourly step time data. In comparison, a whole year dynamic control simulation would not be feasible due to the vast amount of computational resource needed.

This is also in parallel to the two different kinds of simulations which can be carried out when it comes to energy dispatching. They are the short term and long term simulations (Torreglosa et al., 2015). Short term simulation focuses on the dynamics of each of the energy sources which make up the system and takes into consideration on the net power variations due to load power changes or renewable energy source disturbances. Simulations such as these usually done in a short time period, from 200 seconds to a day. Meanwhile, long term simulations are used when the objective is to show the operation of the system during a significant period of time, and may be from months to the total lifetime of the system. Currently, attention is shifted towards other parameters such as operation costs, degradation of sources, level of charge of energy storage, instead of the dynamics of the energy sources.

### 2.7.1 Dynamic Control

The authors in (Gan et al., 2016) presented a novel control algorithm which optimizes the operation of diesel generator in a generator-wind turbine-ESS system using genetic algorithm (GA). The total simulation time used is 24 hours. Using day-ahead wind speed and load demand data, the generator operation is optimized according to constraints defined by the system designer. The following are the constraints used. At each time step:

- a. Total power generated by generator, ESS and wind turbine should be greater than or equal to load demand
- b. Energy charged into ESS is the excess energy between total power generation and load demand
- c. SOC of ESS should be greater than or equal to 20%
- d. Power produced by generator should be less than or equal to its maximum power output

Another literature focused on dynamic control is highlighted in (Chong et al., 2016) where the authors presented an optimal control strategy using fuzzy logic controller for standalone PV system with ESS and supercapacitor hybrid ESS. Results show that the proposed system is able to reduce the ESS peak current and ESS peak power by 16% and 15% respectively, effectively reducing battery charge and discharge cycle and dynamic stress level of battery. Other than that, the proposed system increases the supercapacitor's level of utilization by up to 687%.

### 2.7.2 Dispatch Control

In 1995, Barley proposed operation strategies for a generator-PV-ESS system. The work was one of the pioneering works regarding the operation of HES, one which would pave the way for many other works. Hourly intervals were used in the simulation, in which parameters remain constant during that particular time period. Ideal battery model was considered in the study, ignoring battery losses or the effect of battery cycling towards the lifetime of battery. Three main control strategies were proposed in the study:

- a. Zero-charge strategy (load following): the generator never charges the battery. Setpoint of the state of charge (SOC\_setpoint) takes the value of 0
- b. Full cycle-charge strategy (cycle charging): battery is charged to 100% of its capacity whenever the diesel generator is turned on (SOC-setpoint) is 100%
- c. Predictive control strategy: battery charging action depends on the predicted load demand and expected energy generated by renewable sources.

The authors of (Ameen et al., 2015) presents a simplified Matlab model of a generator-PV-battery system. The load following and cycle charging control strategies were considered in the study. Both of these control strategies are first introduced by (C.D. Barley and C.B.Winn, 1995), and have become of great importance to software tools such as HYBRID2, HOMER, and HOGA (Bernal-Agustín and Dufo-López, 2009). Load following strategy ensures that the

generator will supply power enough to meet the load demand and any excess power from the PV is charged into the battery. In the cycle charging strategy, any excess power from both PV and generator will be charged into the battery. The generator will operate at high loading factor in order to produce surplus power to be charged into the battery. At higher loading factor, energy generated per liter of fuel is greater. Load following and cycle charging are widely used dispatch strategies and its application can be found in the works of (Ma et al., 2015), (Basir Khan et al., 2015), (Kolhe et al., 2015), (Ngan and Tan, 2012), (Adaramola et al., 2014). Figure 2.1 shows an example of system in load following and cycle charging dispatch strategy.

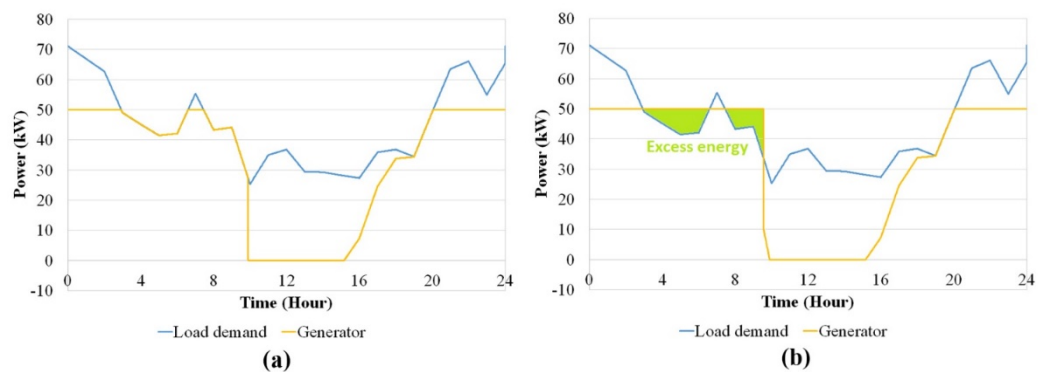


**Figure 2.1: (a) Load following dispatch strategy (b) Cycle charging dispatch strategy**

The cycle charging strategy can reduce the fuel consumption and generator operation time to be lower than that of the load following strategy (Ameen et al., 2015). However, fuel consumption and generator running time should not be the only indicators for assessing the performance of the different strategies. The fuel consumption metric was also used for comparison in (Tazvinga et al., 2013) where load following dispatch strategy has been employed for a generator-PV-

ESS system. It was found that the hybrid system is able to achieve up to 82% fuel savings when compared to a standalone generator system. Similar fuel savings were also reported in (Kusakana, 2015) where the author devised modified versions of the load following and cycle charging dispatch strategy. It achieved up to 81% fuel cost reduction compared to standalone generator system.

(Upadhyay and Sharma, 2016) considers three types of dispatch strategy for HES in an Indian rural area. The dispatch strategies considered are load following, cycle charging and peak shaving strategy. Simulation results show that the cycle charging strategy provides the best results in terms of minimum COE. Sizing is done using each dispatch strategies optimized with genetic algorithm, particle swarm optimization and biogeography technique.

(Dufo-López et al., 2011) presented a multi-objective optimization of a standalone PV-wind turbine-generator-ESS system, minimizing the LCOE and the equivalent carbon dioxide (CO<sub>2</sub>) and LCE. A total of 62,370 possible combination of components were considered. For each combination of the components, four control variables were optimized:

- a. Generator minimum output power: the diesel specific power consumption (liter/kWh) for low output power is higher than that of high output power. An optimal generator minimum output power might exist other than the value recommended by manufacturer (usually 30% rated power)

- b. ESS minimum SOC: battery lifetime is calculated using the rainflow counting method, which is a type of cycle counting method. Since the EES is often charged and discharged in partial cycles, the rainflow counting method is useful in determining the number of charge and discharge full cycles in the ESS operation. This means that an optimal minimum SOC might exist, which is higher than that specified by the manufacturer
- c. Generator critical power limit setpoint and ESS SOC setpoint for generator stop action: when load demand is lower than the generator critical power limit setpoint, it is more economical to produce higher power output. The surplus power can be used to charge the battery up to the SOC setpoint, where the generator will be switched off once it is reached

(Abedi et al., 2012) presented a novel power management strategy (PMS) for the optimal design and operation of a HES. The PMS is able to simultaneously minimize overall system cost, reduce unmet load and carbon emissions, while considering intermittent renewable energy sources. Fuzzy logic technique is used to handle the mixed-integer multi objective optimization problem.

(Yap and Karri, 2015) presented an algorithm for the generator-PV system to reduce the fuel consumption as much as possible. The system consists of multiple generators of varying sizes and controlled in a way to have a minimum runtime in order to prevent engine cycling, which is damaging to the generator.

### **2.7.3 Role of Artificial Intelligence in HES Control**

Artificial intelligence (AI) techniques provides an alternative to conventional classical techniques in solving complicated practical problems in various applications. AI techniques have increasingly found its use in modeling, optimization, prediction and forecasting, identification, as well as system control.

Fuzzy set (FS), introduced by Zadeh in 1965 is a generalization of conventional set theory. It provides a mathematical tool dealing with variables in a linguistic manner. There are two main characteristics of fuzzy systems which makes it excel in certain applications compared to other techniques. Firstly, fuzzy logic allows estimated values to be used in decision making, even when there is uncertainty or incompleteness in the information at hand. Another important characteristic of fuzzy logic is such it is suitable for approximate reasoning, in applications where a mathematical model is complex and difficult to derive. It enables the translation of qualitative knowledge to quantitative knowledge, in control and automation applications.

(Abadlia et al., 2016) applied fuzzy logic controller in a standalone PV-ESS-fuel cell system. The fuzzy based power management system controls charging/discharging action, as well as the power delivery from the fuel cell. The system is found to be effective in meeting the load demand and maximizing hydrogen production for the fuel cell operation.

In the work of (Fossati et al., 2015), the authors presented an algorithm utilizing fuzzy logic in order to reduce the operating cost of microgrids consisting of diesel generator, micro-turbine, fuel cell, wind turbine, and ESS. The proposed algorithm determines the day-ahead schedule of the microgrid operation, whereby power output of the storage system is controlled. Two genetic algorithms were used; one which generates the microgrid scheduling, and another which tunes the fuzzy membership functions. The proposed algorithm can produce savings of up to 3.3%.

Artificial neural Network (ANN) is a mathematical model which has learning ability as well as parallel data processing. The ANN consists of multiple layers of neurons which performs computations. These neurons are linked to one another based on weight factor. ANN is advantageous in control systems as it has a nonlinear and adaptive structure and generalization skills and can be designed independent from system parameters.

However, the ANN lacks rules for defining the structure of its cells and layers due to its “blackbox” nature. Another drawback of control strategy based on ANN is such that it requires a significant amount of historical data for the learning and tuning process.

In (Al-Alawi et al., 2007), an ANN based controller is presented to control the diesel generator on/off action. The ANN controller aims to maintain a predefined minimum generator loading factor while under light load condition and high solar irradiance level. The ANN model performs prediction on the

action which should be taken by the generator including the time it should be switched off, as well as the optimum power needed by the generator. The key objectives are to reduce fuel dependency, engine wear and tear, as well as greenhouse gases (GHG). Results show that the ANN model developed can achieve an accuracy of up to 97%, and clearly demonstrates that ANN can be used with high degree of confidence when it comes to the control of the diesel generator.

Genetic Algorithm is capable of solving problems with multiple solutions. It is a stochastic algorithm which mimics the natural process of biological evolution (Rich and Knight, 1990). The algorithm imitates the process whereby living organisms adapt to harsh conditions, through evolution and inheritance. The GA technique is an optimum search technique which implements concepts such as natural selection and survival of the fittest. The GA technique generally has a low development complexity. However, this technique is prone to premature convergence.

## **2.8 Homer**

Many research done throughout the world uses HOMER to optimize their HES. HOMER was developed by the National Renewable Energy Laboratory. HOMER is able to evaluate various design options for grid connected and standalone remote systems. Three main tasks which HOMER is capable of is simulation, optimization, and sensitivity analysis. Based on the components

selected by the user, Homer simulates the system using predefined range of values of each of these components. Systems in Homer are simulated by performing hourly energy balance calculations for a whole year period. Other than that, energy flow between each component in the system are also considered based on energy demand and generation difference. A comprehensive literature review reveals that HOMER is the most preferred and used optimization tool.

## **2.9 Summary**

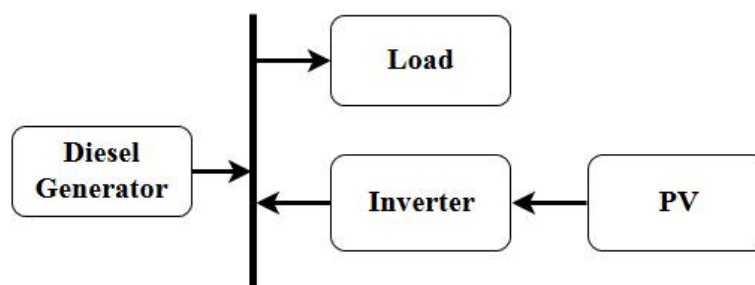
Hybrid energy systems reduce generator fuel dependence and reduces overall cost of energy provided to the inhabitants compared to that of standalone generator systems. The ESS is a vital component in the HES whereby it stores energy during conditions of excess energy production and uses it during a later time. Optimal component sizing is important in HES as oversizing incurs additional cost while undersizing causes system reliability issues. In the generator-PV-ESS system, the load following and cycle charging dispatch strategies are commonly used in other literatures. However, dispatch strategies which involve the use of artificial intelligence are also more commonly used and shows good performance in ensuring optimal and cohesive operation of components in the HES.

## CHAPTER 3

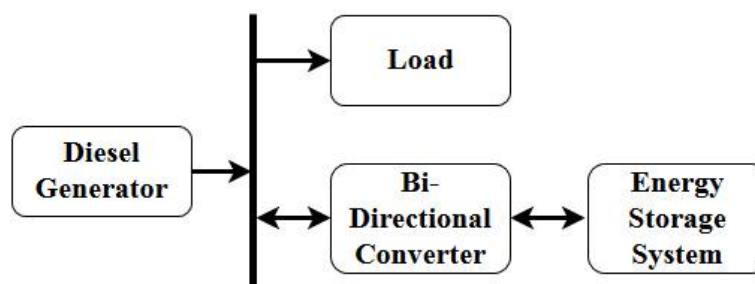
### ARCHITECTURE OF HYRID ENERGY SYSTEM

#### 3.1 Introduction

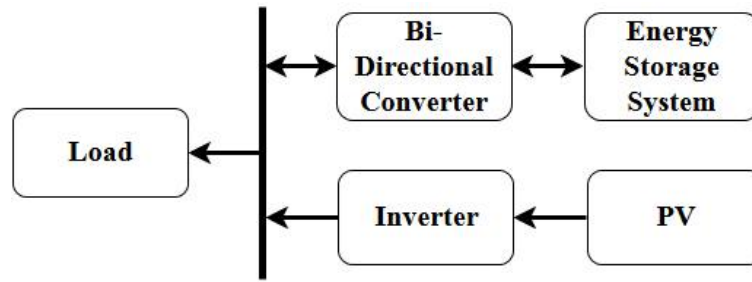
In this chapter, various hybrid energy systems (HES) were evaluated, utilizing a combination of diesel generator, PV, and ESS. The hybrid systems evaluated are the generator-PV system, generator-ESS system, PV-ESS system, the generator-PV-ESS system as illustrated in Figure 3.1.



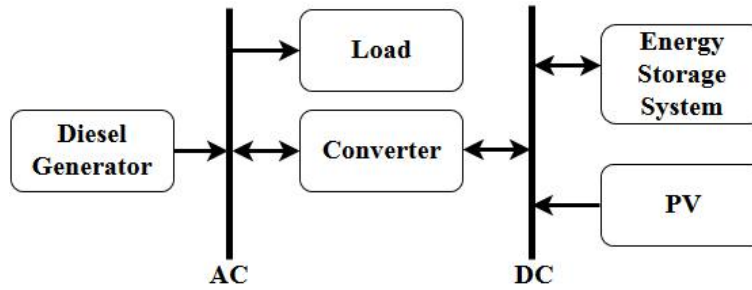
(a)



(b)



(c)



(d)

**Figure 3.1: (a) generator-PV system (b) generator-PV-ESS system (c) generator-ESS system (d) PV-ESS system**

These HES are modelled in Matlab Simulink. Parameters obtained from the simulation are used to calculate the cost of energy (COE) in order to determine the most cost effective HES configuration. The system uses parameters obtained from the simulation in order to calculate the COE, which determines the most cost effective HES configuration.

### 3.1.1 Matlab Simulink

Matlab, developed by Mathworks, is a high level programming language and interactive platform for numerical computation, visualisation and programming.

Matlab is a computational tool widely used in various fields of science and engineering.

Simulink is a block diagram environment for multi-domain simulation and Model-Based Design. Its main interface is a graphical block editor, which can be used with a wide range of customisable block libraries and solvers for the simulation and modelling of dynamic systems. It is integrated with Matlab, where algorithms devised can be implemented in Simulink and simulation results exported to Matlab for analysis and processing. It also features data and scope displays to view simulation results.

In this study, Matlab is used as a management platform where the component sizes are fetched from Excel spreadsheets for use in the Simulink model. Other than that, Matlab is also used to automate simulations in Simulink as well as to fetch generated simulation results to calculate economic feasibility of any particular system.

MAT-files are binary MATLAB formatted files, where all the variables needed for used in the simulation are used. Examples of such variables are the load profile data as well as the solar irradiance.

Figure 3.2 shows a screenshot of the Matlab software. Section 1 represents the file directory path, where Simulink or Matlab files can be searched and opened from the window. One precaution which needs to be taken is that the for the read and write process into Excel worksheets using Matlab commands, the file



are in time-series, array, structure, as well as a structure with time data. The following table summarizes the type of formats which can be saved by the block.

**Table 3.1: Description of the data types supported by “To Workspace” block**

Data type	Description
Timeseries	Data vectors sampled over time, often in order and in fixed intervals. Timeseries analysis finds its use in identifying patterns, modelling patterns, and forecasting values
Array	Input signals are saved as N-dimensional arrays
Structure	Arrays with related data grouped in fields, and can contain data of varying types and sizes
Structure with time	Similar to the structure type, with the addition of a time field which stores the simulation time hits

The “To Workspace” block is as shown in Figure 3.3 , while the setting menu for this block is as shown in Figure 3.4. In the setting menu, the variable name can be specified, along with the data format and sample time for the block. The sample time in this study here is set to be at 60 seconds, where the input to the block will be sampled every 60 seconds. It has been found from initial tests that sample time of 60 seconds provides the best balance between data resolution and simulation time.

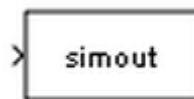


**Figure 3.3: To Workspace block for data logging**

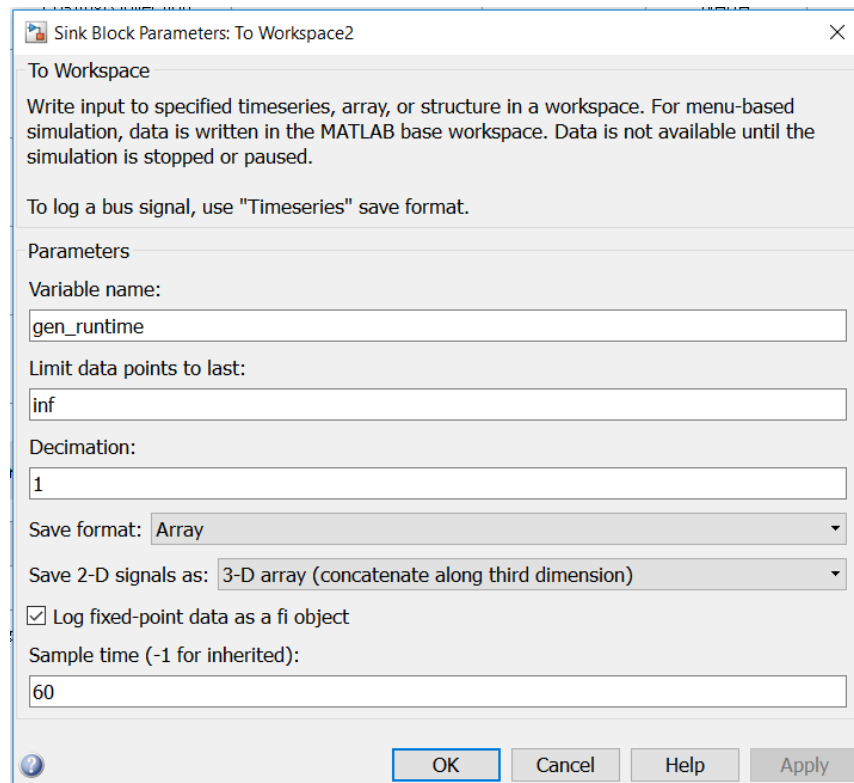


**Figure 3.4: To Workspace block parameter setting menu**

### 3.1.2 Simulation Type

There are a total of four methods which can be used for the simulation of power systems. They are the continuous, continuous ideal switch, discrete, as well as the phasor solution methods. In this study, the phasor solution method is used. Most of the time the phasor solution method is used in areas where electromechanical oscillations occur within power systems consisting of large motors and generators. However, the phasor solution method is not only limited to the study of transient stability of generator and motors, but can also be used to solve any linear system. This is especially true when one is only interested with the magnitude and phase changes occurring in all voltages and currents,

where all differential equations resulting from RLC elements do not need to be solved. Instead, all which is solved is a much simpler set of algebraic equations utilising the voltage and current phasors. When this happens, the simulation time of any particular system can be reduced, resulting in a much faster simulation. The nature of simulations which are designed to be solved using phasor solution method is such that the time scale of interest for such simulations can be now in terms of multiple days. In this study, simulations are run for up to a month and requires less than 3 minutes for each simulation.

### 3.2 Diesel Generator

The diesel generator is represented using the three-phase source block in Simulink as shown in Figure 3.5. The block applies a three-phase balanced voltage source having an internal R-L impedance. The three internal voltage sources are in Y connection, where its neutral can be accessed or be internally grounded.

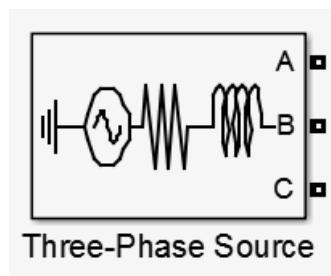


**Figure 3.5: Three-phase source Simulink block**

In the model, the three-phase source is configured in such a way that it supplies the load demand while leaving no deficit load demand. In other words, the

demand will always be met. For example, during a time when PV source is supplying to the load and is lower than the load demand, the generator represented by the three-phase source block will supply the difference between the PV and load demand.

For all the diesel generator sizes considered, there is a fuel consumption curve specified by the manufacturer. Table 3.2 summarizes the fuel consumption curve of generator size 40 kW, 50 kW, 60 kW, and 70 kW based on the datasheet found in (Cummins Power, n.d.). Fuel consumption is specified using the generator loading factor values from 0 to 1. Loading factor of 1 means that the generator is supplying at its rated power output while loading factor of 0 means that the generator outputs zero power.

**Table 3.2: Diesel generator fuel consumption**

Fuel Consumption (liter/hour)				
Generator size (kW)	Generator Loading Factor			
	0.25	0.5	0.75	1.0
40kW	4.9	7.6	10.6	13.2
50kW	4.9	8.3	12.1	16.1
60kW	5.8	9.8	14.4	18.5
70kW	6.9	12.1	16.9	21.2

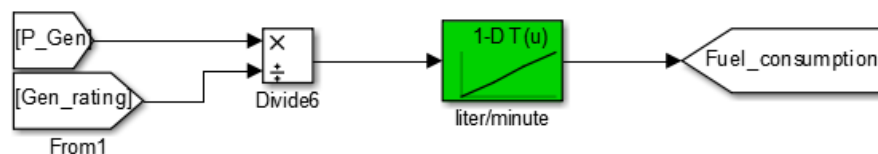
While it can be observed that fuel consumption increases with generator loading factor, it is important to note the amount of energy unit produced (kWh) per liter fuel consumed. The greater the loading factor, the greater the amount of energy generated for every liter of fuel used and it is as illustrated in Table 3.3. Therefore, it provides an incentive to run the diesel generator at the highest possible loading factor.

**Table 3.3: Energy generated at various generator loading factor**

Energy Generated(kWh/liter)				
Generator size (kW)	Generator Loading Factor			
	0.25	0.5	0.75	1.0
40kW	2.0	2.6	2.8	3.0
50kW	2.6	3.0	3.1	3.1
60kW	2.6	3.1	3.1	3.2
70kW	2.5	2.9	3.1	3.3

### 3.2.1 Calculation of Generator Parameters

In order to calculate the generator fuel consumption throughout the simulation, the n-D Lookup Table block is used. The lookup table block maps the input connected to it and outputs a value by looking up or interpolating a table of values defined in the parameter box. In this case, it has been configured to be a one-dimension lookup table. By specifying the fuel consumption at the four loading factors, the block plots a function which maps to an output when input is specified. Other than that, the fuel consumption data is specified in terms of liter per minute instead of liter per hour. If the liter per hour values were to be used, it would be highly inaccurate as generator power output does not change hourly in the simulation. Instead, generator output changes by the minute during the simulation. Figure 3.6 illustrates the Simulink block diagram implementing the lookup table block in calculating the generator fuel consumption.



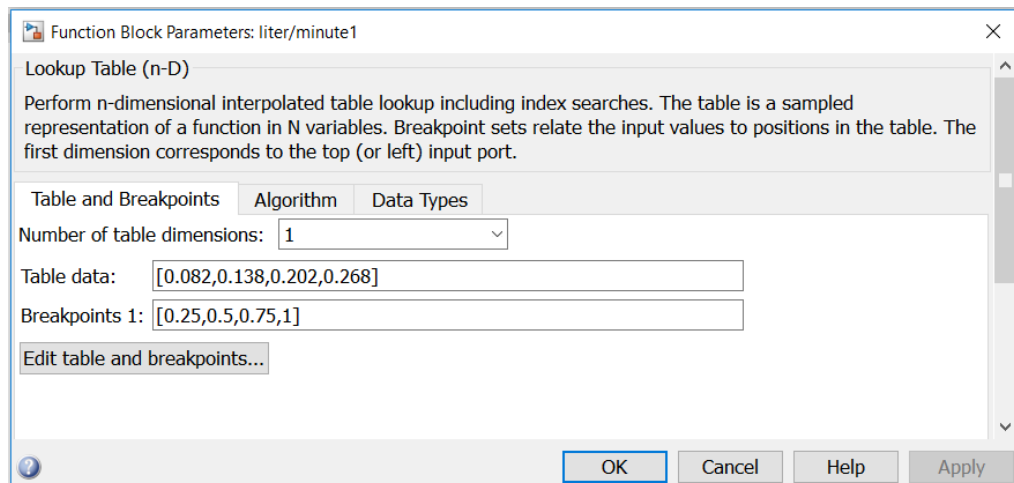
**Figure 3.6: Simulink block diagram of the lookup table block, for the calculation of generator fuel consumption**

Table 3.4 shows the fuel consumption of the diesel generator at different loading factor in terms of liter/hour.

**Table 3.4: Diesel generator fuel consumption in terms of liter/hour**

Generator size (kW)	Fuel Consumption (liter/minute)			
	Generator Loading Factor			
	0.25	0.5	0.75	1.0
40kW	0.082	0.127	0.177	0.220
50kW	0.082	0.138	0.202	0.268
60kW	0.097	0.163	0.240	0.308
70kW	0.115	0.202	0.282	0.353

In the lookup table block parameter setting box, the fuel consumption values at each generator loading factor can be entered, as shown in Figure 3.7 where the table data section represents the liter/minute values while Breakpoint 1 is where generator loading factor values are entered.



**Figure 3.7: Lookup table parameter setting box**

First, the generator loading factor is calculated based on Equation 3.1. The loading factor is the ratio of the generator power output ( $P_{Gen}$ ) and the generator size in terms of kW which used in the system.

$$\text{loading factor} = \frac{P_{Gen}}{\text{Generator size}}$$

3.1

The lifetime of each diesel generators are rated at 15,000 hours. Once the lifetime has been reached, replacement of the generator is required.

There is no built-in function which records and monitors the generator runtime. Hence, a separate function is used in order calculate the generator runtime. When  $P_{Gen}$  is supplying power, the function outputs 1 and while it is turned off, it outputs 0. The values of 1 and 0 are stored in a workspace variable is called the “gen\_hour” for every minute of the in-simulation time. At the end of each simulation, all the values of the variables are summed up in order to obtain the total number of minutes the generator is running.

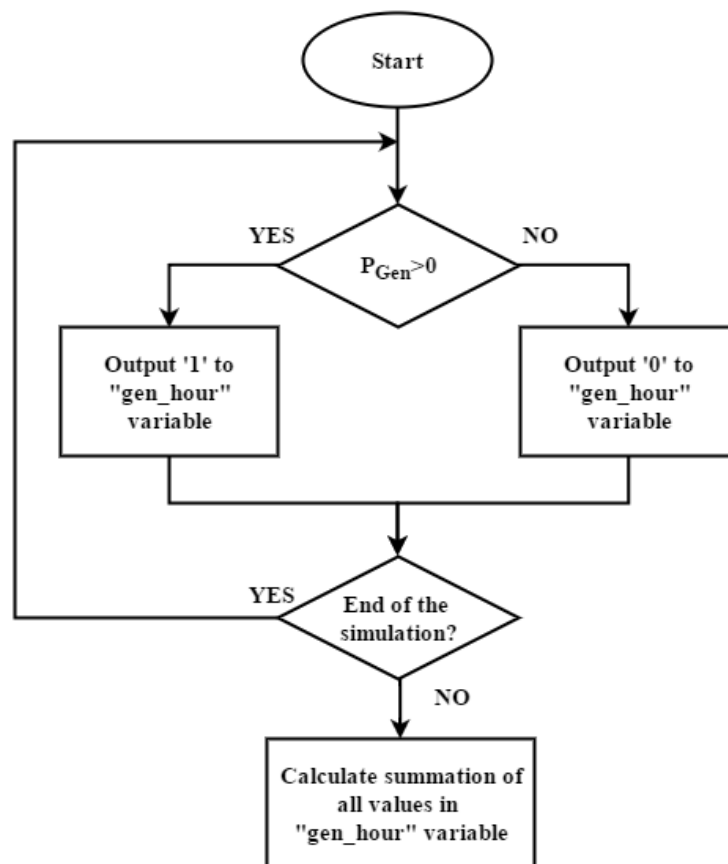


**Figure 3.8: Calculation of generator runtime**

### 3.3 Energy Storage System

The Energy Storage System (ESS) is made up of lead acid batteries and bi-directional converters. Lead acid battery technology is more suitable in the application of a HES as it capable of providing high charge/discharge cycles at the lowest cost as compared to other battery technologies. The ESS consists of a string of 8 lead acid batteries connected in series to produce a battery bus voltage of 48V. Table 3.5 shows a the ESS string size and its corresponding capacity in terms of kWh.

**Table 3.5: ESS string size and its corresponding kWh value**

ESS size (strings)	ESS size (kWh)
1	55.52
2	111.04
3	166.56
4	222.08
5	277.6
6	333.12
7	388.64
8	444.16
9	499.68
10	555.2
11	610.72
12	666.24
13	721.76
14	777.28
15	832.80

The operation of the battery is dependent on its state-of-charge (SOC). The SOC can be expressed as follows:

$$SOC = \int P_{Batt} dt \times \frac{1}{E_{rated}} \times 100\% \quad 3.2$$

Where  $P_{Batt}$  is the power flowing in or out of battery during charging/discharging and  $E_{rated}$  is the capacity rating of the battery in kWh.

Figure 3.9 shows the block diagram for the calculation of SOC in Simulink.

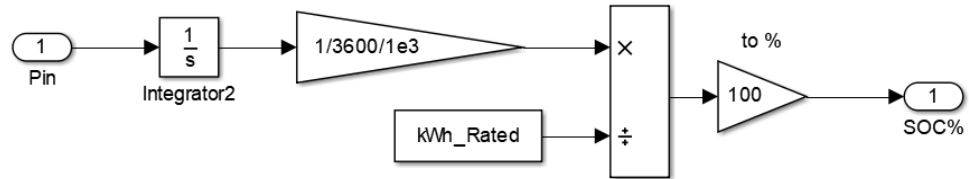


**Figure 3.9: Block diagram for calculation of SOC**

Battery SOC should be within limits in order to prevent overcharging and undercharging of batteries described as follows:

$$SOC_{min} < SOC < SOC_{max} \quad 3.3$$

Where  $SOC_{Max}$  is the maximum threshold for battery SOC in order to prevent overcharging while  $SOC_{Min}$  is the minimum threshold for battery SOC in order to prevent undercharging the batteries. The  $SOC_{Min}$  and  $SOC_{Max}$  used in the study is 30% and 90% respectively, which are commonly used values and can be found in (Fossati et al., 2015) and (Yahyaoui et al., 2014).

The ESS is commonly used to store an excess of renewable energy, where in this case it is the PV energy. However, it can also be used when the generator is unable to meet the load demand. In this condition, the ESS will be discharged in order to meet the deficit in power generation, according to the equation:

$$P_{Load} = P_{Gen} + P_{ESS} \quad 3.4$$

### 3.3.1 Battery Lifetime

In this study, battery lifetime is limited by its throughput. It is assumed that the battery replacement will be needed once fixed amount of energy cycles has taken place in the battery, regardless of the DOD of battery. The study uses the lifetime throughput value in order to calculate the lifetime of batteries. Hence, the amount of energy cycling through the battery will be monitored and recorded during system simulation.

Factors limiting the lifetime of the battery bank can be either from the lifetime throughput or float life. The equation used to calculate the battery life is as shown in equation 3.5.

$$R_{batt} = \min\left(\frac{N_{batt} Q_{lifetime}}{Q_{throughput}}, R_{batt,f}\right) \quad 3.5$$

where  $R_{batt}$  is the battery bank life (year),  $N_{batt}$  the number of batteries in the battery bank,  $Q_{lifetime}$  the lifetime throughput of a single unit battery (kWh),  $Q_{throughput}$  the battery throughput in a year (kWh/year) and  $R_{batt,f}$  the battery float life (year) as specified in the manufacturer specification sheet. The battery life is the minimum value between either the lifetime throughput and the battery float life.

The ESS is assumed to be pre-charged, and has a SOC of 80% at the beginning of all the simulation performed in this study.

### 3.3.2 ESS Energy

The energy flowing in and out of the ESS can be calculated by using equation 3.6, where the energy is obtained by calculating the area under the power.

$$e(t) = \int_0^t p(t) dt \quad 3.6$$

where  $e(t)$  refers to the energy while  $p(t)$  refers to the power value. The ESS energy is modelled using the combination of mathematical blocks in Simulink. In the model, the ESS power during discharge operation takes a negative value while the charging operation takes a positive value. Figure 3.10 illustrates the blocks used to calculate the ESS energy for both the charge and discharge energy values.

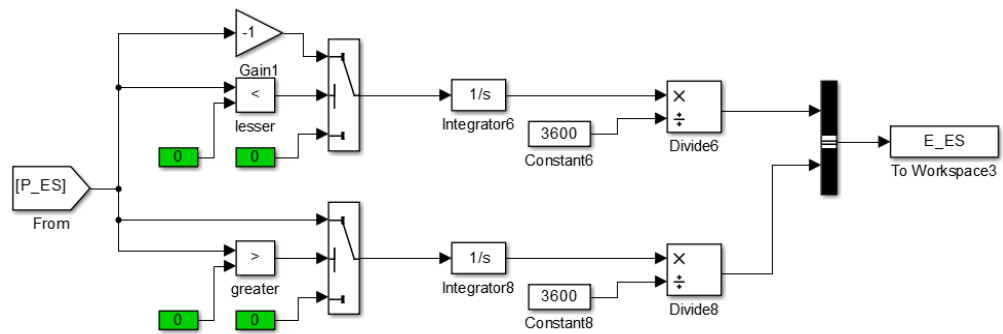


**Figure 3.10: Block diagram for calculation of ESS energy**

### 3.4 Solar Photovoltaic (PV)

The power rating of a PV panel is defined in terms of  $W_p$  (peak Watts) produced at a temperature of 25°C and solar irradiance of 1000 W/m<sup>2</sup>. PV output can be expressed by the following equation:

$$P_{PV} = A_{PV} \times I \quad 3.7$$

Where  $A_{PV}$  is the total area of the solar PV panel installation in m<sup>2</sup> and  $I$  is the solar irradiance expressed in W/m<sup>2</sup>. The Malaysian solar irradiance data was obtained from National Renewable Energy Laboratory at (National Renewable Energy Laboratory, n.d.) and they are hourly solar irradiance values. These values are placed in a MAT-file, which are loaded into the Matlab workspace whenever the simulation in Simulink is started.

An inverter converts the DC output of the PV into AC. In most cases, the usual lifetime for PV modules are 20-25 years (Branker et al., 2011). Although some literatures have reported of PV modules having lifetime beyond 25 years, this study uses a PV lifetime of 25 years.

Figure 3.11 shows the Simulink block diagram for the PV power output generation. From the left on diagram, there is a time block which output the simulation time. The simulation time, which natively is the unit of seconds is then passed through a gain block, which converts seconds value into hourly values. This is done by specifying a gain of 1/3600 in the block. Next, the hourly values are summed to a constant of '1' as the values specified in the lookup table for the irradiance value starts from time of hour 01 instead of hour 00. The

new time value is then passed to the lookup table containing solar irradiance values, of which is mapped to the input. The output of the lookup table block is then multiplied with a gain block containing the size of PV specified for that particular simulation.

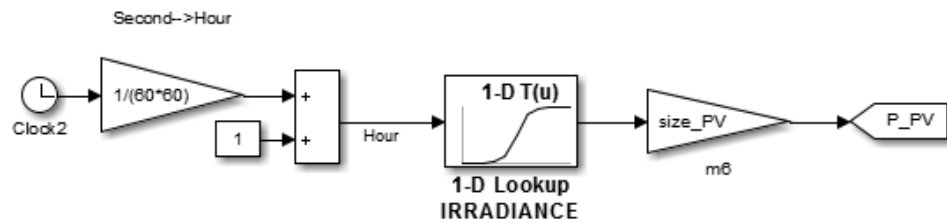


**Figure 3.11: Block diagram for PV source generation**

PV deloading is performed when there is an excess of PV energy which cannot be stored into the Energy Storage System (ESS) when  $SOC_{Max}$  has been reached. In the simulation, there will be instances where there will be excess PV energy even when the diesel generator is switched off. In the PV deloading operation, a lower PV power can be produced by operating the  $V_{DC}$  of the PV system at a value higher than the  $V_{MPP}$  (voltage at maximum power point). This can be seen in Figure 3.12. The PV deloading operation is implemented in both literature (Malla and Bhende, 2014) and (Zarina et al., 2014).

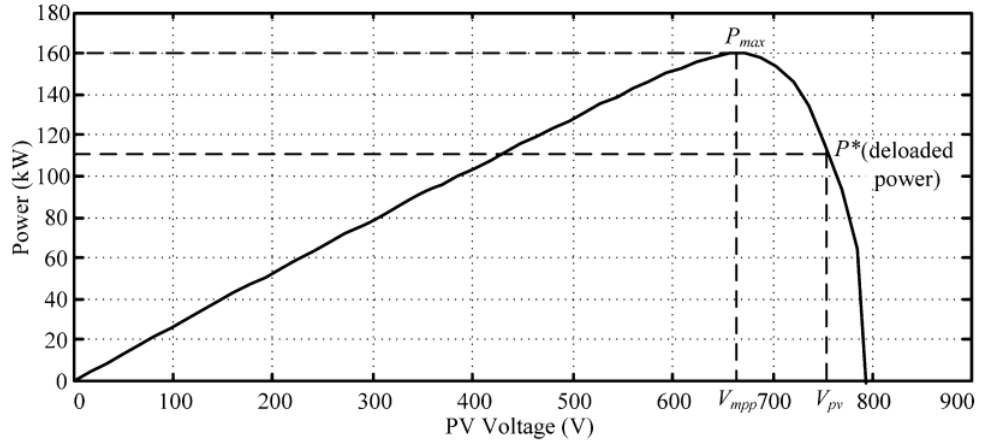


**Figure 3.12: PV deloading operation**

### 3.5 Bi-Directional Converter

A bi-directional converter is needed in order to charge and discharge the ESS. The size of the bi-directional converter plays an important role in the system as inadequate size will limit charge/discharge capacity while over sizing will incur additional costs. The equation used to determine the bi-directional converter size is as follows:

$$S_{converter} = \max(P_{discharge}, P_{charge}) \quad 3.8$$

Where  $P_{discharge}$  is calculated according to the equation:

$$P_{discharge} = P_{max\ load} - P_{gen\ rating} \quad 3.9$$

Where  $P_{charge}$  is calculated according to the equation:

$$P_{charge} = P_{PV\ max} - P_{min\ load} \quad 3.10$$

Where  $S_{converter}$  is the bi-directional converter size,  $P_{max\ load}$  the maximum load demand,  $P_{gen\ rating}$  the diesel generator size,  $P_{PV}$  the PV power and  $P_{min\ load}$  the load demand.  $P_{PV\ max} - P_{min\ load}$  refers to the maximum value of the difference

between PV and load demand. The maximum  $P_{PV}$  will always be lower than actual PV size used.

For example, a 100 kW PV installation in the system. Using the Malaysian solar irradiance data, there are only 8 instances throughout the year where  $P_{PV}$  is greater than 80kW. This is as shown in Figure 3.13. Hence, 80 kW is selected as the maximum  $P_{PV}$  magnitude that has to be catered for. Using this as a benchmark, maximum  $P_{PV}$  can also be determined for other sizes of PV used in the system. Maximum  $P_{PV}$  is determined using the following:

$$P_{PV\ max} = 0.8 \times P_{PV\ rating} \quad 3.11$$

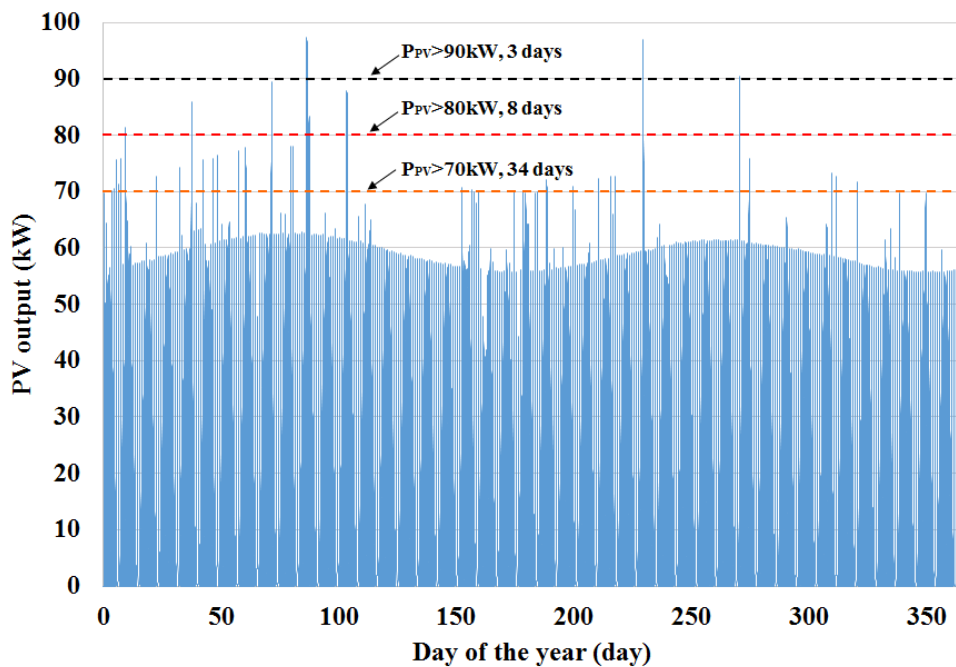


**Figure 3.13: Daily power output for a 100 kW PV installation (365 days)**

The  $P_{\min\ load}$  based on the load profile used in this study is 25 kW. Hence, the value  $P_{PV\ max} - P_{\min\ load}$ , which is the magnitude of excess PV power to be charged in to the battery can be determined. The section  $P_{\max\ load} - P_{gen\ rating}$  refers

to the maximum power magnitude to be discharged whenever load demand exceeds the maximum power output of the diesel generator. In essence, the converter is sized in order to accommodate for the maximum value of either ESS charge or discharge power. The converter size determined using equation 3.8 is presented in Table 3.6 below.

**Table 3.6: Converter size at various PV size**

PV size (kW)	Converter size (kW)		
	Diesel Generator size (kW)		
	40	50	60
30	40	30	20
40	40	30	20
50	40	30	20
60	40	30	30
70	40	40	40
80	40	40	40
90	50	50	50
100	60	60	60
110	70	70	70
120	80	80	80

### 3.6 Load Demand

In this study, the type of load employed is that of a residential rural area load profile. Residential load profile differs from commercial load in the sense that maximum load demand in commercial load occurs between morning and evening, while that of residential load occurs somewhere from the evening until early morning.

There are a total of 3 load profiles used in this study, two of which are recorded from a residential area in Malaysia, while the other obtained from (Kolhe et al., 2015). Each of these load profiles have different energy consumption per day

but similar maximum load demand, and will provide a platform for comparison in the later part of this study. Different load profiles are used in order to test the robustness of the developed dispatch strategy, and how the shape of the load profile affects the COE of the system. Load profile 1 is used as the main load profile to compare the various types of HES as well as the different dispatch strategies. Load profile 2 and 3 are used to validate and compare findings obtained from load profile 1. Figure 3.14, Figure 3.15 and Figure 3.16 shows the load profile 1, 2 and 3 respectively.

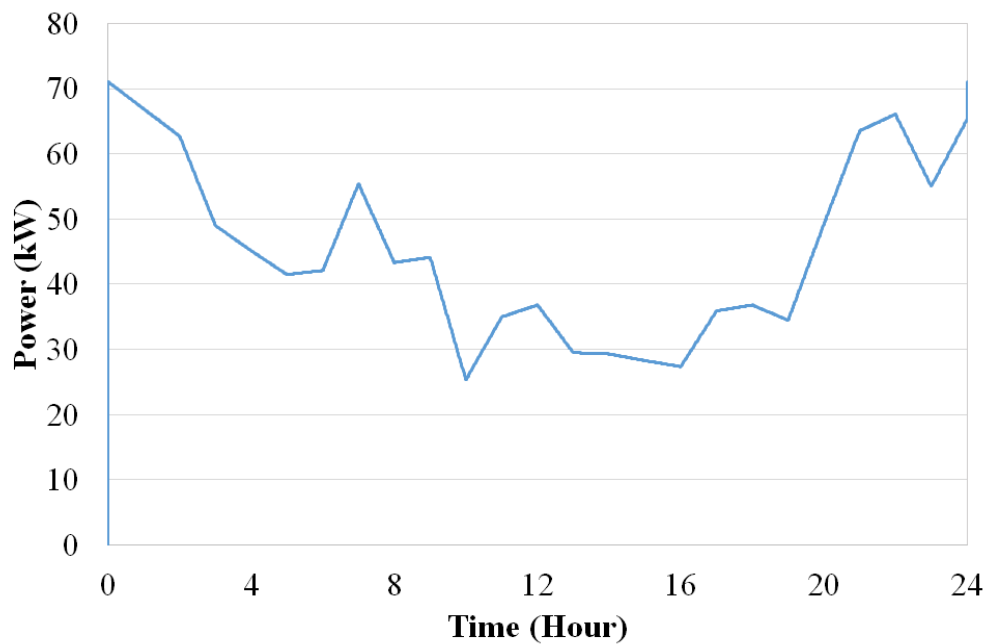


**Figure 3.14: Load profile 1**

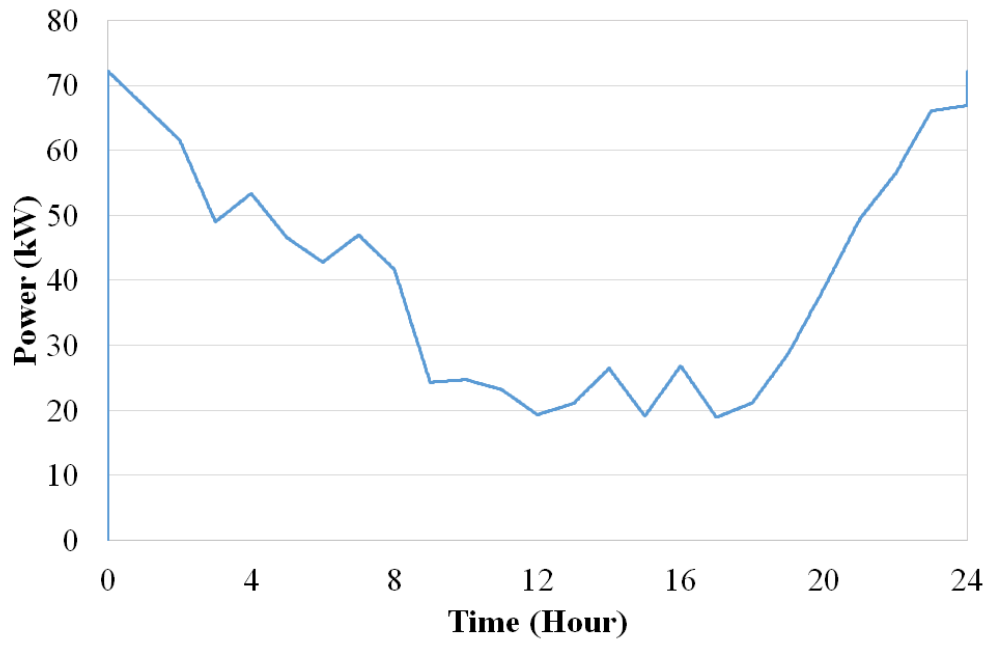


**Figure 3.15: Load profile 2**

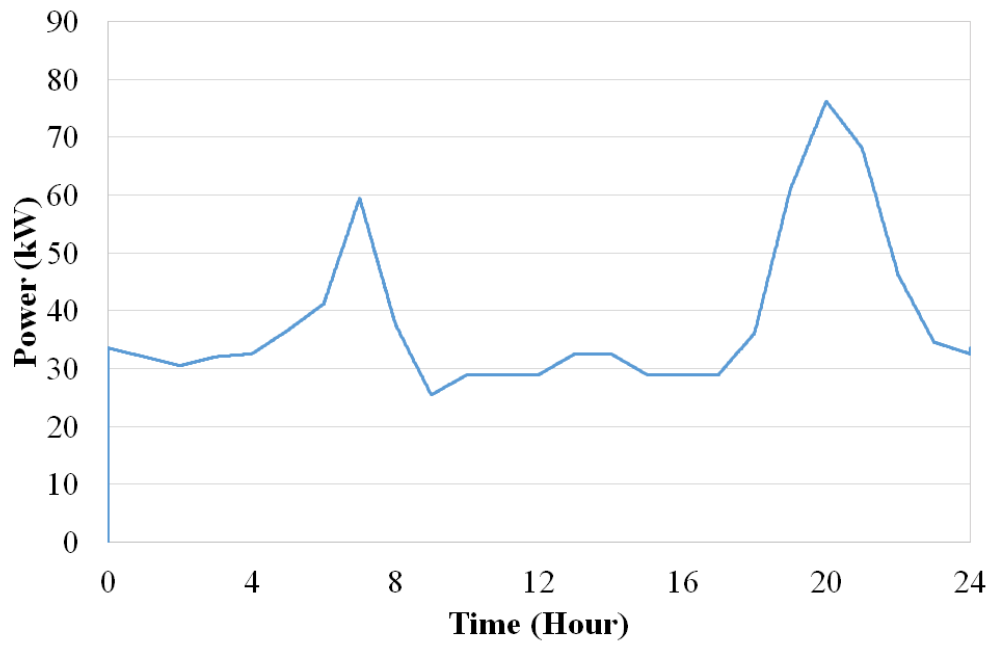


**Figure 3.16: Load profile 3**

**Table 3.7: Comparison between the different load profiles**

	Load profile 1	Load profile 2	Load profile 3
Peak demand (kW)	71	72	76
Minimum demand (kW)	25	19	25
Energy (kWh/day)	1070.8	942.8	921.7

The load data can be entered by the user using a Matlab script. After the script is run, its values will be updated in a MAT-file. During each simulation, Simulink will create a variable out of this MAT file and place it as a workspace variable. A n-D (n-dimension) lookup table reads this workspace variable and plots the load profile to be used in the simulation.

### **3.7 Power to Current Conversion**

In the model used, each component within the system are modelled using a set of blocks which convert power values into current values which are exchanged between components in the whole system. The current values are supplied by the current source block, labelled as 'CsA' and 'CsB' in Figure 3.17. In the set of blocks,  $V_{ab}$  and  $V_{bc}$  are measured using the built in voltage measurement block, which are placed between points AB and BC respectively.

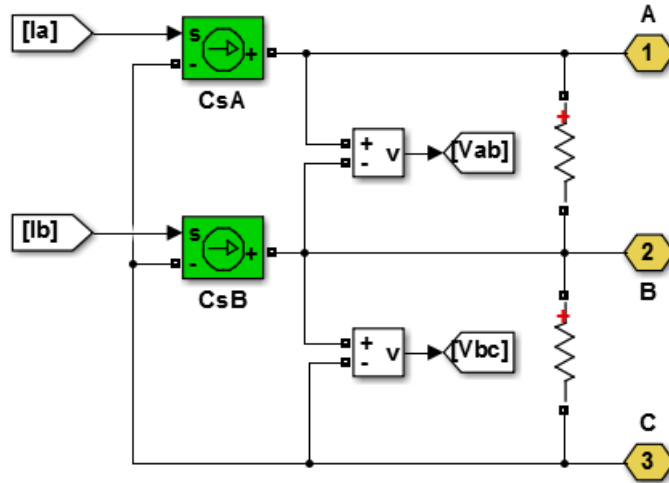


**Figure 3.17: Block diagram for conversion of power to current**

Then, using equation as shown below,  $I_a$  and  $I_b$  are obtained and is passed on to the current source blocks.

$$S = 3V_{rms}I_{rms} \quad 3.12$$

$$S = \frac{3V_p I_p}{2} \quad 3.13$$

Where,

$$V_{rms} = \frac{V_p}{\sqrt{2}} \quad 3.14$$

$$I_{rms} = \frac{I_p}{\sqrt{2}} \quad 3.15$$

Power systems can be represented by the positive, negative and zero sequence voltage. The positive sequence voltage is used in order to calculate the current values needed.

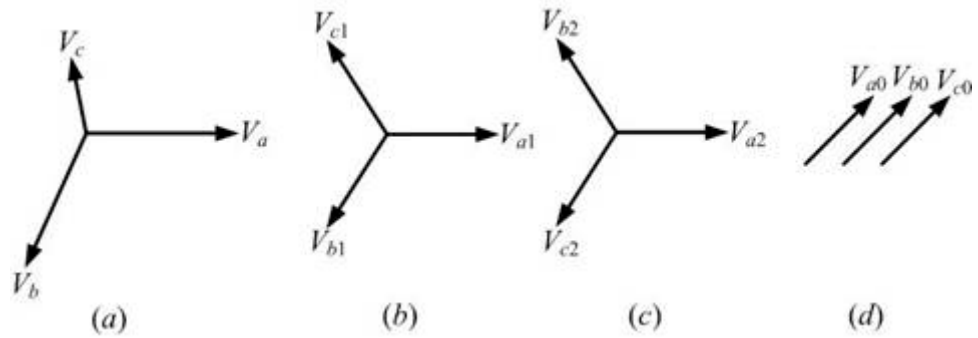


**Figure 3.18: Three unbalanced vectors of three-phase system resolved into three balanced systems of vectors**

The positive sequence component can be derived as the following:

$$V_{a1} = \frac{1}{3}(V_a + aV_b + a^2V_c)$$

$$V_{a1} = \frac{1}{3}(V_a + V_b \angle 120^\circ + V_c \angle 240^\circ)$$

$$V_{a1} = \frac{1}{3}(V_a - V_b \angle -60^\circ + V_c \angle 240^\circ)$$

$$V_{a1} = \frac{1}{3}(V_a - V_b(1 + a^2) + a^2V_c)$$

$$V_{a1} = \frac{1}{3}(V_a - V_b - a^2V_b + a^2V_c)$$

$$V_{a1} = \frac{1}{3}(V_{ab} - a^2V_{bc}) \quad 3.16$$

$$V_1 = \frac{1}{3}(V_{ab} - e^{-\frac{j2\pi}{3}}V_{bc}) \quad 3.17$$

Figure 3.19 shows the Simulink block diagram which converts the calculated power values into current values needed.

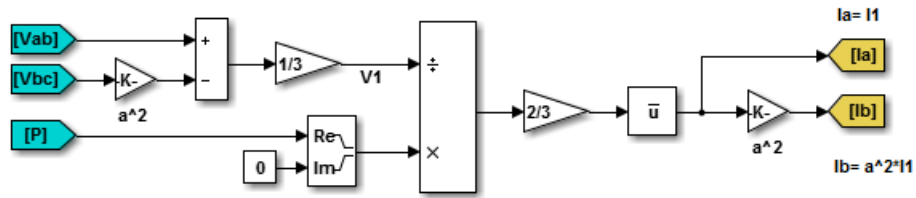


**Figure 3.19: Block diagram for conversion of power to current**

### 3.8 System Sizing

In this study, optimal system sizing is obtained by simulating the system with all possible component sizes, over a range of sizes specified beforehand. Should a particular combination of components (generator, PV, ESS, bi-directional converter) result in unmet load during simulation, that particular combination will be considered as not feasible.

System sizing is an integral part of the design of any HES utilising any type of renewable energy. A common misconception is that having a bigger size of say PV source would contribute to higher system COE. However, the truth is that while generally increasing size of PV source increases the COE, a system having a larger PV size might have a lower COE compared to a system having a lower PV size in cases where the diesel generator is switched off for a longer duration.

Each simulation is run based on pre-set component sizes determined beforehand. They make up the search space, which is a set of all potential solutions. It is a n-dimensional space with an axis corresponding to each

variable to be searched. The minimum and maximum values along each of these axis is defined by the user. For example, in a generator-PV-ESS system, the variables on each of these axis are generator, PV and ESS. At the beginning of each simulation, the model will fetch the values for each component sizes needed for that particular configuration.

In the study, the maximum load demand for the selected load profile used is 71 kW. Should a standalone diesel generator system be used to serve this load, the generator should be sized at 80 kW. However, in generator-PV-ESS system, generator can be sized much smaller as the deficit can be served by the PV and ESS. The generator sizes considered are 40, 50 and 60 kW respectively. Meanwhile, PV sizes considered are from 30 – 120 kW, with a step size of 10 kW between each options. Other than that, ESS sizes considered are from 1 – 15 strings, with each string consisting of 8 pieces of 6.94 kWh lead acid battery.

**Table 3.8: Component sizes used in the study**

Generator (kW)	PV (kW)	Converter (kW)	ESS (string)	ESS Capacity (kWh)
40	30	30	1	55.52
50	40	40	2	111.04
60	50	50	3	166.56
	60	60	4	222.60
	70	70	5	277.6
	80	80	6	333.12
	90		7	388.64
	100		8	444.16
	110		9	499.68
	120		10	555.2
			11	610.72
			12	666.24
			13	721.76
			14	777.28
			15	832.8

After each of the possible combination of components are simulated, parameters such as generator runtime, generator fuel consumption, and battery throughput are logged into a spreadsheet, all of which will be used in evaluating the economic feasibility of the particular combination of components.

### **3.9 Economic Feasibility Study**

Economics play an important role in this study, where a system is operated in such a way to minimise its total net present cost, as well as to search for the system configuration with the lowest total net present cost. System configuration here can cover either the component sizes used in that particular system or the dispatch strategy used. This section describes the use of life-cycle cost as a metric for comparison for systems with different configurations as well as the calculation of the total net present cost.

Non-renewable energy sources such as diesel generator tend to have a lower initial capital cost and higher operating costs than that of the renewable sources. In searching for the system with the best configuration, the economics of systems having different capacity of renewable and non-renewable energy sources should be compared. In doing so, such comparisons must be done in a way which take into account the capital and operating costs. This can be performed through the life-cycle cost analysis, one which includes all the costs occurring within the system lifetime.

In this study, the total net present cost (NPC) is used to represent the life-cycle cost of a particular system. This is also the case for the software such as HOMER and HOGA. The total NPC accumulates various type of costs and revenues which occur during project lifetime into one lump sum in today's monetary value. In doing so, future cash flows are discounted back to the present using a discount rate.

For each component in the system there are a few parameters which has to be specified. They include the initial capital cost, which is the upfront payment which occurs in year zero, the replacement cost, which occurs when a component has reached it lifetime and replacement is needed and the operating and maintenance (O&M) cost, which occurs yearly throughout the duration of the project lifetime.

Each system configuration is evaluated based on its Cost of Energy (COE) and is defined as the average cost per kilowatt hour (\$/kWh) of energy served by the system. The COE of a system can be calculated by using the following:

$$COE = \frac{C_{ann,tll}}{E_{tll}} \quad 3.18$$

where  $C_{ann,tll}$  is the total annualized cost and  $E_{tll}$  is the total energy served in kWh. The total annualized cost refers to cost which were to occur equally in every year throughout the project lifetime. It is given by the following equation:

$$C_{ann,tll} = C_{NPC}CRF(i, R_{proj}) \quad 3.19$$

Where NPC is the Net Present Cost of a system and CRF the capital recovery factor. The NPC is calculated using the following:

$$NPC_{comp} = I_{comp} + \sum_{n=1}^N \frac{AC}{(1 + DR)^n} - \frac{S}{(1 + DR)^n} + \frac{R}{(1 + DR)^n} \quad 3.20$$

Where  $I_{comp}$  is the initial cost of the component, AC the annual cost, N the project lifetime, DR the discount rate, S the component salvage cost and R the component replacement cost.

Capital recovery factor refers to a ratio used in calculating the present value of a series of annual cash flows. The capital recovery factor can be calculated as follows:

$$CRF(i, N) = \frac{1(1 + i)^N}{(1 + i)^N - 1} \quad 3.21$$

Where  $i$  is the real interest rate and N the number of years of the project lifetime. In this project, the N value used is 25 years. Meanwhile, the real interest rate is calculated using the equation below.

$$i = \frac{i' - f}{1 + f} \quad 3.22$$

Where  $i$  is the real interest rate,  $i'$  the nominal interest rate, and  $f$  the annual inflation rate.

The salvage value is the value remaining for a component at the end of the project duration. Salvage value of each component is calculated at the end of project lifetime using the following equation: -

$$S = C_{rep} \times \frac{R_{rem}}{R_{comp}} \quad 3.23$$

Where  $S$  is the salvage value,  $C_{rep}$  the component replacement cost,  $R_{rem}$  the component remaining life, and  $R_{comp}$  the component lifetime. Once the lifetime of a particular has been reached, the component will have to be replaced. For example, if the project lifetime specified is 25 years and the PV lifetime is also 25 years, the salvage value of the PV at the end of the project will be zero. In another scenario, if the PV lifetime of 30 years is used in a 20 year project lifetime, salvage value of the PV at the end of the project is one-third of the PV replacement cost.

Table 3.9 summarizes the costs for each component for the calculation of COE:

**Table 3.9: Component lifetime and costs for COE calculation**

Component	Lifetime	Capital cost	Replacement cost	O&M
Generator	15,000 hours <sup>-a</sup>	\$500/kW <sup>a</sup>	\$500/kW <sup>a</sup>	\$0.025/kW/hour <sup>a</sup>
Bi-directional converter	15 years <sup>a</sup>	\$550/kW <sup>a</sup>	\$550/kW <sup>a</sup>	\$10/kW/year <sup>a</sup>
Battery	9645 kWh <sup>a,c</sup>	\$1100/unit <sup>a</sup>	\$1100/unit <sup>a</sup>	\$10/unit/year <sup>a</sup>
PV	25 years <sup>b</sup>	\$2000/kW <sup>b</sup>	\$2000/kW <sup>b</sup>	\$10/kW/year <sup>b</sup>
PV inverter	15 years <sup>a</sup>	\$350/kW <sup>d</sup>	\$350/kW <sup>d</sup>	\$10/kW/year <sup>a</sup>

Footnotes:

a- Data collected from (Lau et al., 2015)

b- Data collected from (C.D. Barley, 1996)

c- Battery throughput for one unit of battery

d- Data collected from (Kolhe et al., 2015)

### **3.9.1 Calculation of COE in Microsoft Excel**

The COE of each system with its particular combination of components is calculated in a Microsoft Excel spreadsheet. The spreadsheet has all the required formulas, and is based on example spreadsheets generated by HOMER software, which is as shown in Appendix E.

In the spreadsheet, each year within the whole project is laid out and in this study, it is up to 25 years. For each component required in the system, there are the capital, fuel, operating, replacement, as well as the salvage cost. Capital cost refers to the initial cost required to purchase the particular component, and this is logged in year 0. It is only beginning from year 1 which all the other costs are taken into consideration. Fuel cost is applicable for the diesel generator used in this system. The replacement cost exists for all components except for the PV as the project lifetime is taken to be 25 years, which is the exact lifetime for the PV. However, in the case of components such as the ESS, diesel generator, converter, replacements are required throughout the project lifetime. By the end of the project, some components might not have reach its operational lifetime yet, and salvage cost is calculated.

The nominal total cost is the sum off all the cost occurring in that particular year. Based on the nominal cost, the discounted cost is calculated by multiplying the discount factor obtained for every year. The sum of the discounted total cost is then the Net Present Cost (NPC).

### 3.9.2 Calculation of Payback Period

Other than the NPC and COE, another parameter which will be calculated is the payback period. The payback period is defined as the length of time required to recover the cost an investment in a project. However, one major disadvantage of the simple payback period is that it does not account for the time value of money. The alternative which can be used is the discounted payback period (DPP), which accounts for time value of money by discounting project cash inflows. The DPP can be calculated by using the following formula:

$$DPP = A + \frac{B}{C} \quad 3.24$$

Where A is the last period (year) with a negative values of discounted cumulative cash flow, B the value of the discounted cumulative cash flow at the end of period A, and C the discounted cash flow after period A. The discounted cash flow can be calculated using the following formula:

$$Discounted\ Cash\ Flow = \frac{Nominal\ Cash\ Inflow}{(1 + i)^N} \quad 3.25$$

Where i is the discount rate while N is the period (year) which the cash inflow occurs.

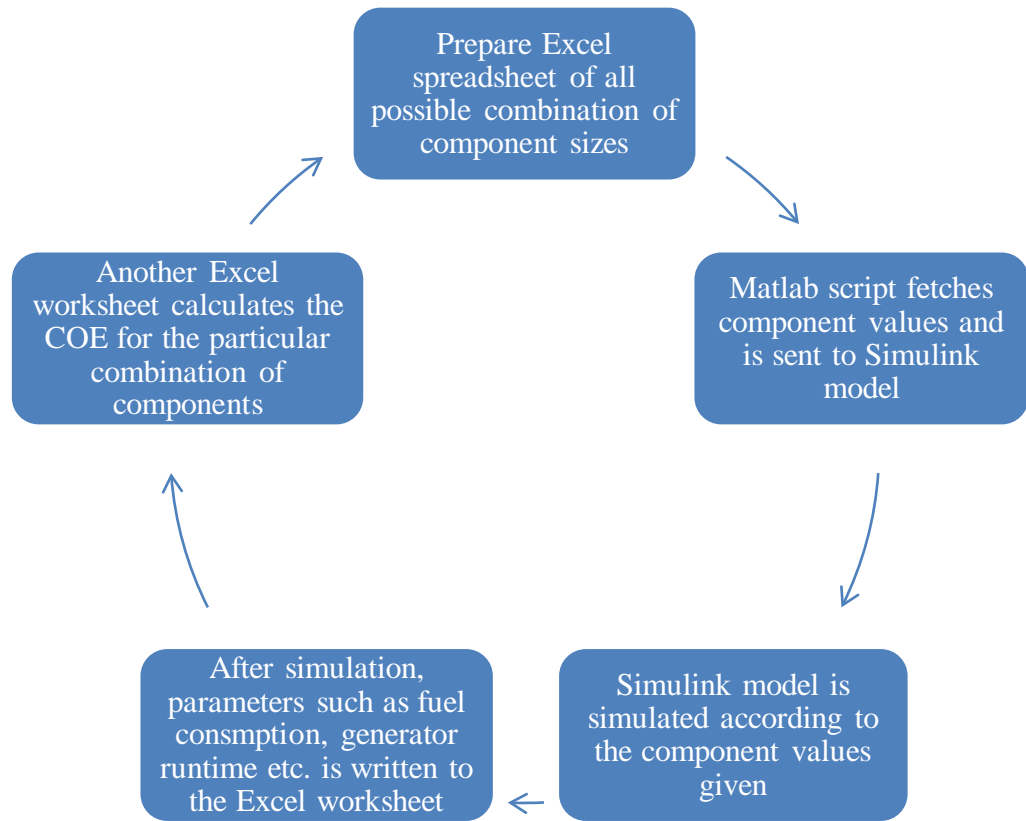
### 3.10 Simulation and Optimization Process

Figure 3.19 shows the steps involved in the simulation and optimization of the various HES in this study. The simulation process begins with preparing an Excel worksheet of all the possible combinations of the components, which

includes the generator, PV, bi-directional converter, as well as the ESS. All possible combinations are arranged in rows, in ascending order of the component sizes used.

Next, a Matlab script is executed and it will fetch a particular combination of component sizes to be used by the Simulink Model. Each component in the Simulink model takes the value of the rating specified in the Excel worksheet previously. The HES in Simulink is then simulated. Once simulation is completed, parameters such as generator runtime, generator fuel consumption, battery throughput are obtained and logged into the Excel worksheet along the corresponding component sizes used.

Another Matlab script will fetch the all the previously logged results and place them in an Excel worksheet for the calculation of cost of energy (COE). Other than that, component sizes will also be specified within the worksheet, where predefined formulas in the worksheet calculates the cost of the components as well.



**Figure 3.20: Process of simulation and optimization**

### 3.11 Summary

In this chapter, various types of HES were introduced along with the components which they are made up from. These components, which are all simulated in Matlab Simulink were introduced and they are the generator, ESS, PV, bi-directional component and the load component. A detailed explanation of the modelling of these components was presented in this chapter. Furthermore, three different load demand profiles which are considered in the later part of this study were introduced. Parameters which influence the economic feasibility of the HES were also introduced in this chapter. The COE

acts as an economic indicator for the feasibility of a particular configuration of a HES.

## CHAPTER 4

### CONTROL ALGORITHMS FOR HYBRID ENERGY SYSTEM

#### 4.1 Introduction

There are various HES types studied, which includes the generator-ESS, generator-PV, PV-ESS, as well as the generator-PV-ESS system. Dispatch strategies were devised and discussed in detail for each HES type. The dispatch strategy determines how the component should operate and at what power output, as well as whether to charge or discharge the ESS to achieve the optimal COE.

The HES types which only have two energy source such as the generator-ESS, generator-PV and PV-ESS system have much simpler dispatch strategy as compared to the generator-PV-ESS system. Generally, the more energy sources in a system, the more sophisticated the control and operation will be.

The generator-PV-ESS system requires a more sophisticated control than other HES because the system consists of three energy sources. The load following and cycle charging dispatch strategy which is widely used for the generator-PV-ESS system is discussed. Other than that, a fuzzy control dispatch strategy is also formulated and aims to minimize generator runtime and PV power curtailment.

## 4.2 Control and Operation

Control and operation strategy plays an important role in HES. The control strategy is related to the net load, the difference between the actual load demand and the renewable energy power output. In designing the control strategy for HES, the balance of net load must be ensured so the load demand is always met. An optimal control strategy ensures that a low COE for HES can be achieved.

The operation of HES such as the generator-PV, generator-ESS and PV-ESS system is straightforward and non-complex as there are only two energy sources. When one source fails to meet the load demand, the other energy source will complement the other energy source to supply power to the load. One important consideration when devising the dispatch strategy for HES is the utilization of each component within the system. One such example is the pattern of use of generators, where it should be operated at high loading factor whenever possible. Other than that, ESS should be well utilized as it should be charged whenever possible.

The operation of all components has to be coordinated in order to achieve an optimal COE. The COE provides a platform for comparison in order to determine which is the best type of HES. The SOC of the ESS in the operation of all the HES is kept to be within 30% ( $SOC_{Min}$ ) and 90% ( $SOC_{Max}$ ). The following are the different types of HES considered and simulated in this study for performance comparisons:

1. Generator-ESS system
2. Generator-PV system
3. PV-ESS system

#### **4.2.1 Generator-ESS System**

The flowchart for the dispatch strategy implemented in the generator-ESS system is as illustrated in Figure 4.1. The algorithm starts off by determining if the load demand ( $P_{Load}$ ) is greater than the generator maximum power output ( $P_{GenMax}$ ). If this condition is true, the generator will operate at maximum power output while ESS will be discharged in order to meet the difference  $P_{Load}$  and  $P_{GenMax}$  while ESS SOC is greater than 30%.

On the other hand, if  $P_{Load}$  is smaller or equal to  $P_{GenMax}$ , the generator will operate at maximum power output, of which the excess power will be charged into the ESS whenever SOC is below 90%. If the SOC has reached 90%, the generator will supply just enough power to meet the load demand. In this case, the ESS will be idle.

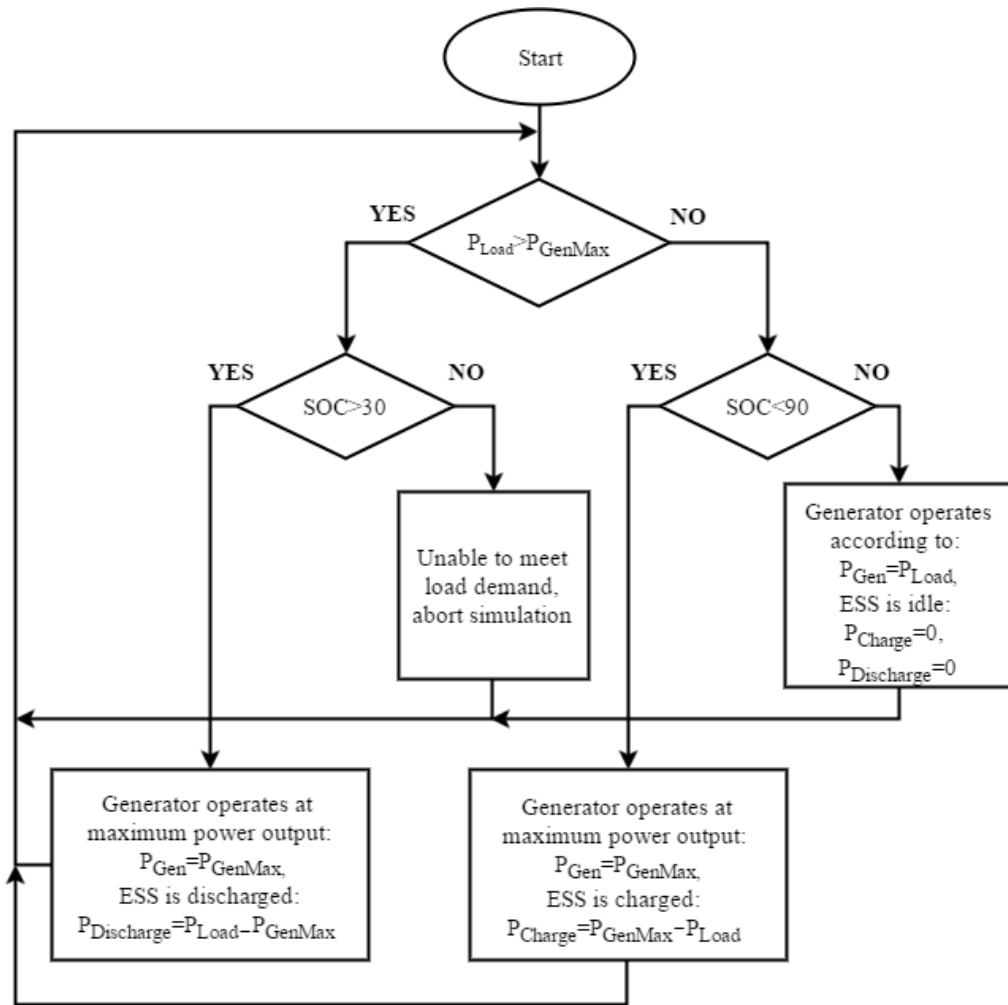


**Figure 4.1: Dispatch strategy flowchart for generator-ESS system**

#### 4.2.2 Generator-PV System

The flowchart for the dispatch strategy implemented in the generator-PV system is as illustrated in Figure 4.2. In the dispatch strategy for the generator-PV system, the algorithm first starts off to determine if there is any output from the PV. When there is an output from the PV, the system moves on to test the condition if the PV output is greater than the load demand. If this condition is true, the generator will be switched off while the PV fully meets the load

demand. However, since there are no storage devices to store the excess PV power, the PV will undergo deloading operation while keeping its output to match the load demand. Meanwhile, if  $P_{PV}$  is lesser than the  $P_{Load}$ , the generator will operate in such a way that it supplies the difference between  $P_{Load}$  and  $P_{PV}$ . During the condition when there is no output from the PV, the generator will fully meet the load demand.

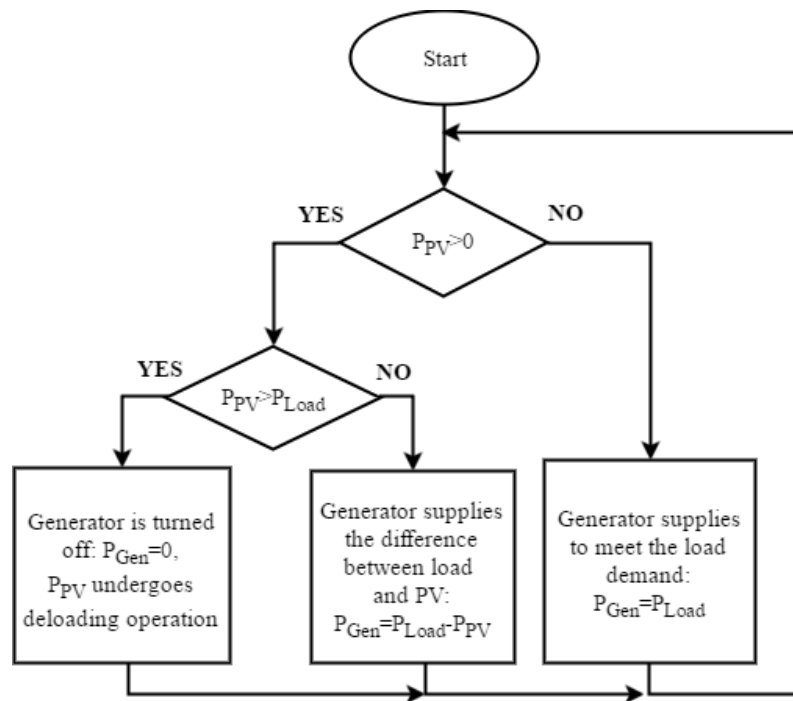


**Figure 4.2: Dispatch strategy flowchart for generator-PV system**

### 4.2.3 PV-ESS System

The flowchart for the dispatch strategy implemented in the generator-ESS system is as illustrated in Figure 4.3. In the dispatch strategy for the PV-ESS system, the algorithm determines if there is PV power output. If no  $P_{PV}$  is produced, ESS will be discharged to meet load demand if SOC is above 30%.

If SOC is not above 30%, then the system is not able to meet the load demand and simulation is aborted.

During the condition where  $P_{PV}$  is greater than  $P_{Load}$ , ESS will be charged according to the difference between  $P_{PV}$  and  $P_{Load}$  while SOC is less than 90%. Once SOC has reached 90% ESS will stop charging and PV will undergo deloading. When  $P_{PV}$  is lesser than  $P_{Load}$ , ESS will be discharged to supply the difference between  $P_{Load}$  and  $P_{PV}$  while SOC is above 30%. If during this condition the SOC is not above 30%, the system is unable to meet the load demand and the simulation will be aborted.

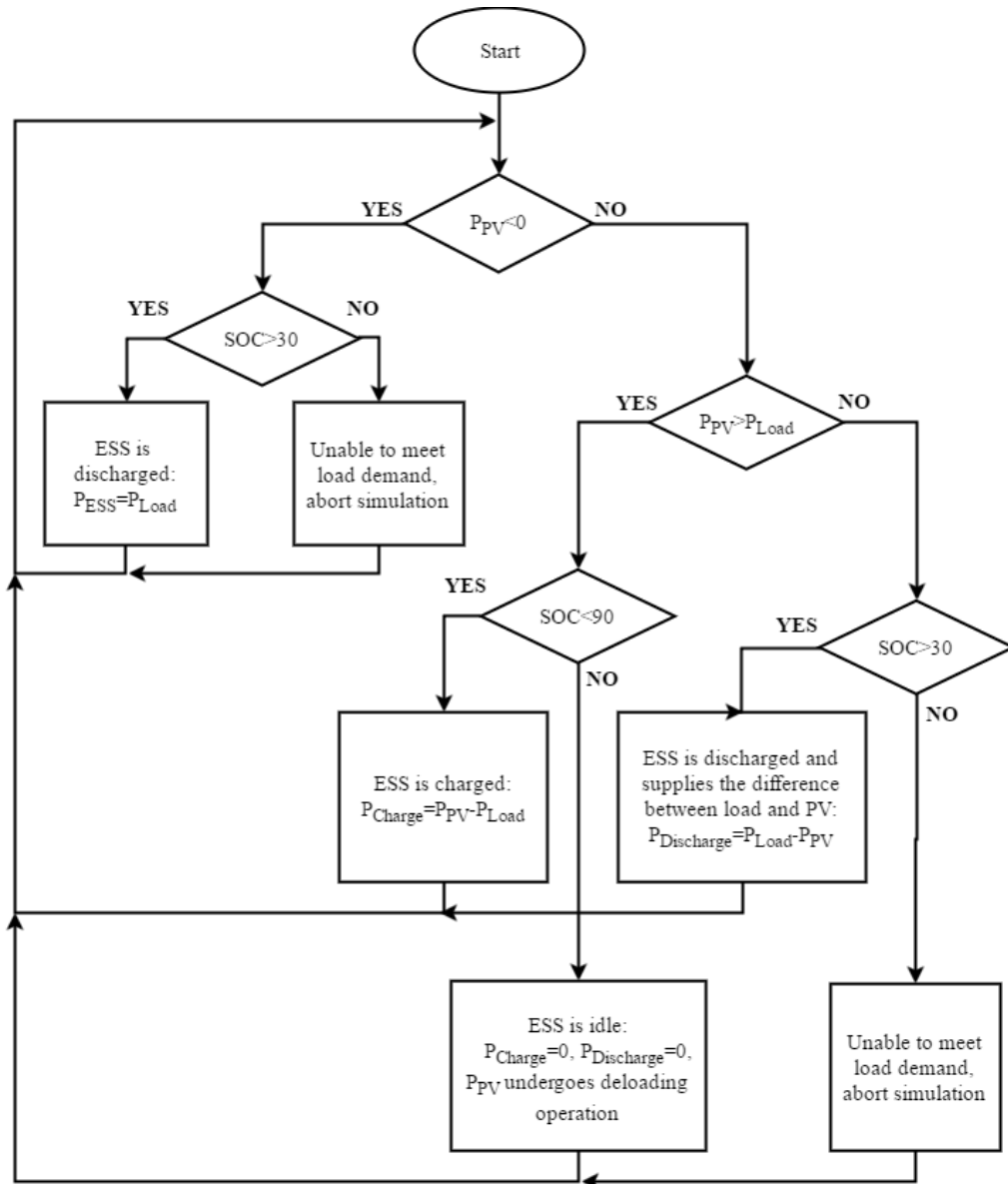


**Figure 4.3: Dispatch strategy flowchart for PV-ESS system**

### 4.3 Generator-PV-ESS System

#### 4.3.1 Load Following and Cycle Charging Strategy

In the load following dispatch strategy, generator supplies enough power just to meet the load demand. Excess PV power ( $P_{PV}$ ) is used to charge the ESS. On

the other hand, in the cycle charging dispatch strategy, generator will produce excess power in order to charge the ESS, in addition to charging of ESS by excess  $P_{PV}$ .

The generator-PV-ESS operational control is based on 5 distinct states which depend on the values of  $P_{PV}$  and  $P_{Load}$ , where they are the power generated by PV and load demand respectively. Figure 4.4 illustrates the various regions of operation of the generator-PV-ESS system. At these states, ESS SOC is constantly monitored in order to determine the charge and discharge action of ESS. The generator maximum power output ( $P_{GenMax}$ ) is also used as a reference in the control algorithm.

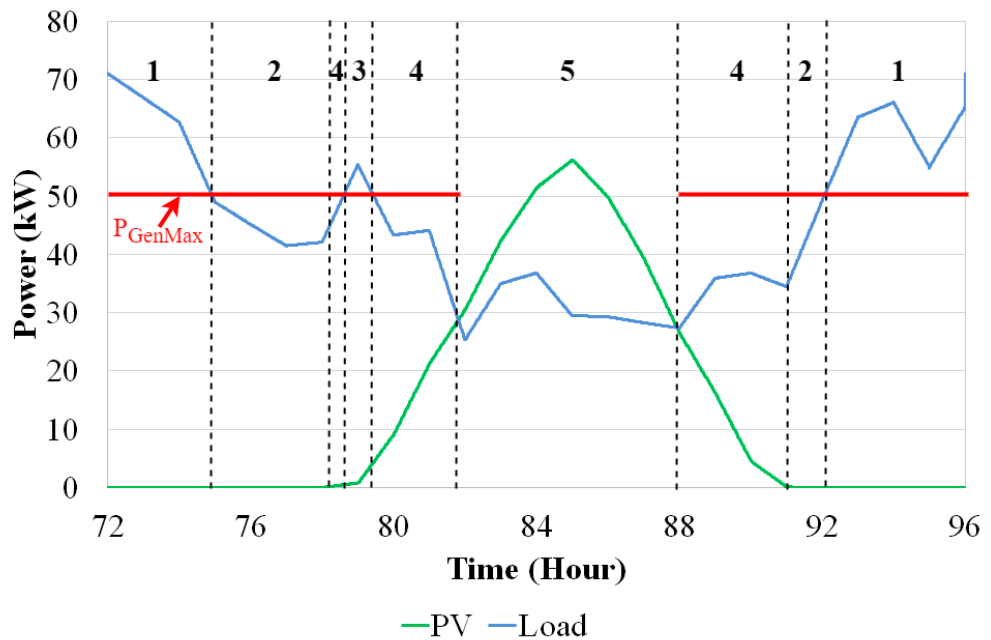


**Figure 4.4: Regions of operation for generator-PV-ESS system**

The following section explains in detail each operating states based on Figure 4.4.

1.  $P_{Load} > P_{GenMax}$

In this case, the load demand is greater than the maximum generator power output. When this occurs, the ESS will be discharged in order to meet the deficit in energy supply. For example, at a particular time step where  $P_{Load}$  is 70 kW and with system having a  $P_{GenMax}$  of 50 kW, the ESS will have to discharge 20 kW. This is done according to the equation:

$$P_{Load} = P_{GenMax} + P_{ESS} \quad 4.1$$

2.  $P_{Load} < P_{GenMax}$

During this condition, the load demand is less than the maximum generator power output. Depending on whether the system is operating in load following or cycle charging dispatch strategy, the generator can be operated in such a way that it supplies power just enough to meet the load demand, or it can operate at high loading factor in order to generate surplus energy to be charged into the ESS. In load following dispatch strategy, generator supplies the load demand and the equation is as follows:

$$P_{Load} = P_{Gen} \quad 4.2$$

In the cycle charging dispatch strategy, the ESS is charged from generator's surplus power while the SOC is below 80% and the equation is as follows:

$$P_{Load} = P_{GenMax} - P_{ESS} \quad 4.3$$

### 3. $P_{PV} > 0$ and $P_{Load} - P_{PV} > P_{GenMax}$

During this condition, there is PV output power while the net load demand ( $P_{Load} - P_{PV}$ ) is greater than the maximum generator power output. When this happens, ESS will have to be discharged. Load demand is also met by the generator operating at  $P_{GenMax}$ , as well as the PV power output. This is carried out according to the following equation:

$$P_{Load} = P_{GenMax} + P_{PV} + P_{ESS} \quad 4.4$$

### 4. $P_{PV} > 0$ and $P_{Load} - P_{PV} < P_{GenMax}$

During this condition, there are two processes which the ESS can undergo. The first option is where the PV can be used to charge the ESS and the second option would be to not charge the ESS and leave the ESS in idle mode. In this section, ESS will be charged when SOC is below a threshold SOC set ( $SOC_{Mid}$ ). In this study, the  $SOC_{Mid}$  for the load following dispatch strategy is 60% while that  $SOC_{Mid}$  for cycle charging dispatch strategy is at 80%. This means the ESS SOC level will be close to the  $SOC_{Mid}$  before the condition  $P_{PV} > P_{Load}$  happens. Although setting the threshold SOC during this condition would mean that only a small range of ESS SOC capacity would be available for charging during the  $P_{PV} > P_{Load}$  condition, an empirical assessment done has shown that the best  $SOC_{Mid}$  for load following and cycle charging dispatch strategy are 60% and 80% respectively as they produce the lowest COE for each dispatch strategy. Even with the  $P_{PV}$  possibly being curtailed during PV deloading in the condition  $P_{PV} > P_{Load}$ , the benefits of a lower COE outweigh the amount of  $P_{PV}$  curtailed when SOC has reached  $SOC_{Max}$  of 90%.

During condition where SOC is less than SOC<sub>Mid</sub> of 60%, in load following strategy:

$$P_{Load} = P_{Gen} \quad 4.5$$

ESS will be charged by the during the same time:

$$P_{Charge} = P_{PV} \quad 4.6$$

During condition where SOC is less than SOC<sub>Mid</sub> of 80%, in cycle charging strategy:

$$P_{Load} = P_{GenMax} - P_{ESS} \quad 4.7$$

ESS will be charged by both the surplus power from generator and PV power during the same time:

$$P_{Charge} = P_{PV} + (P_{GenMax} - P_{Load}) \quad 4.8$$

For both load following and cycle charging, once SOC has reached 60% and 80% respectively, the load demand will be met by both the generator and PV power:

$$P_{Load} = P_{Gen} + P_{PV} \quad 4.9$$

##### 5. $P_{PV} > P_{Load}$

In this condition, the PV power output is greater than the load demand and will be the sole energy source to meet the load demand. The diesel generator will be turned off to prolong its lifetime. Excess PV power will be used to charge the ESS until the SOC reaches 90%.

$$P_{Load} = P_{PV} - P_{ESS} \quad 4.10$$

At any time during the simulation, the load demand is met by the generator, PV and ESS.

$$P_{Load} = P_{Gen} + P_{PV} + P_{ESS} \quad 4.11$$

Figure 4.5 and Figure 4.6 shows the flowchart of the load following and cycle charging dispatch strategy respectively.

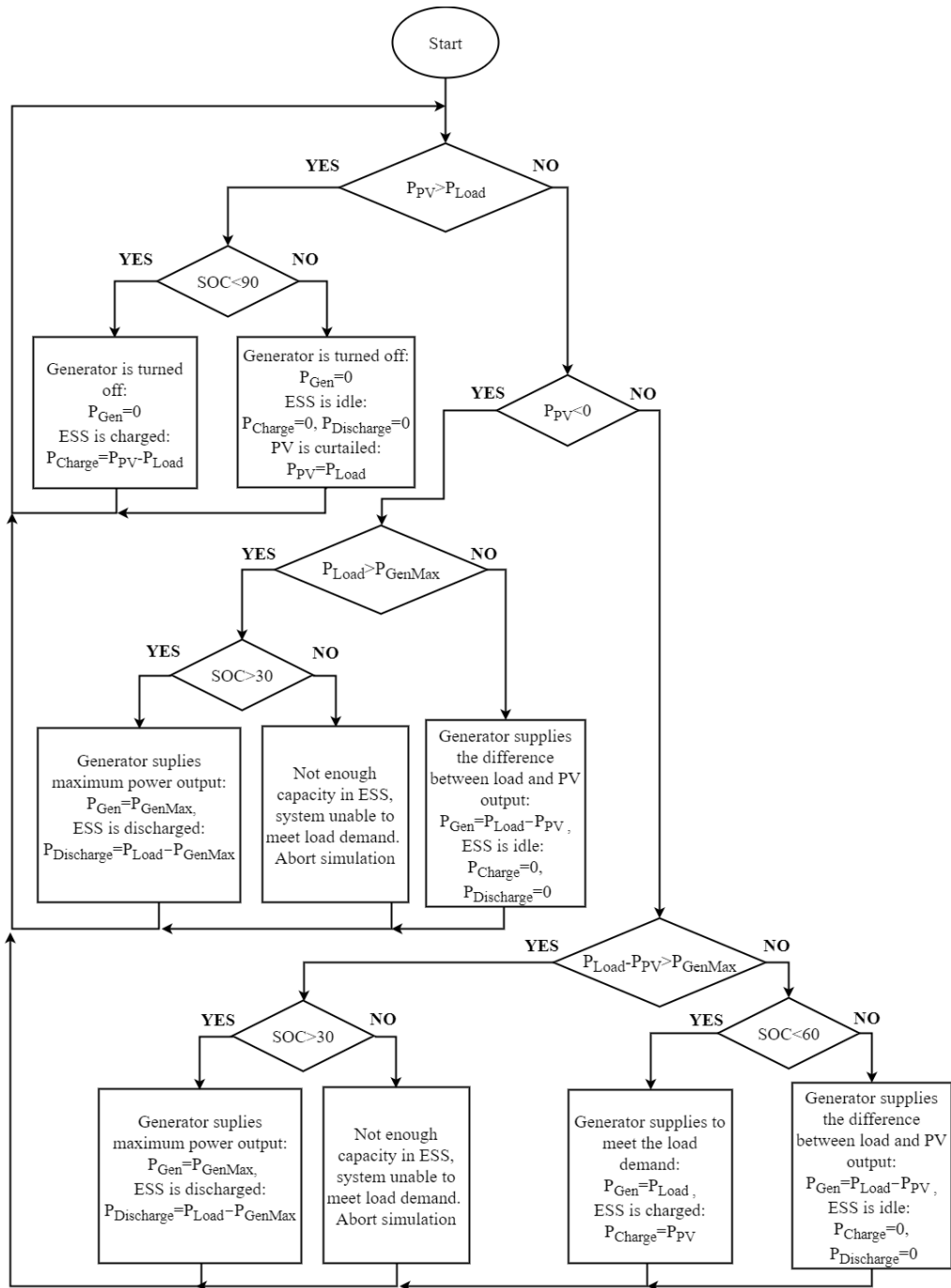


**Figure 4.5: Flowchart for the load following dispatch strategy**

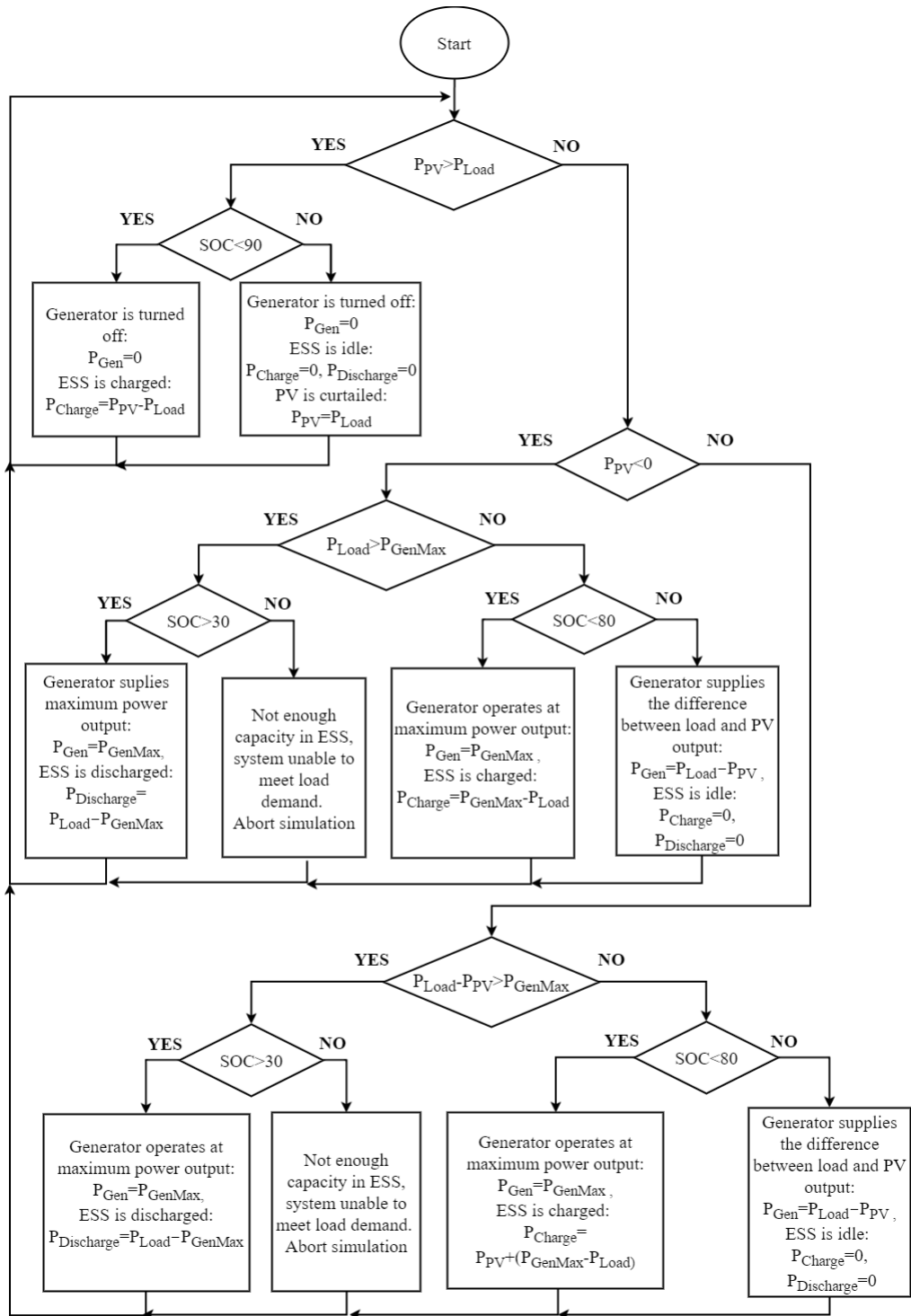


**Figure 4.6: Flowchart for the cycle charging dispatch strategy**

#### **4.4 Fuzzy Control Dispatch Strategy**

Fuzzy logic control is widely used in industrial process control as it does not require an accurate model of the plant model. It is generally difficult to obtain an accurate plant model as there are various uncertainties as well as lack of perfect knowledge on all parameters which affects plant operation. Fuzzy control is often implemented in system where there is difficulty in deriving accurate mathematical model of the plant, where its dynamic characteristics cannot be easily quantified. Fuzzy logic can be seen as an extension of ordinary logic, where it goes beyond ordinary logic utilising simple true/false statements. Variables in fuzzy logic take the form of degrees of membership function in which it can be any values between zero and one.

Fuzzy logic describes plants in numeric and linguistic terms, which makes algorithms easier to be understood compared to conventional complex mathematical models. Using intuitive and easily understood linguistic description of the system, fuzzy logic algorithms also enables a shorter development time compared to conventional algorithm design methods.

However, in applications where precise mathematical models are available, conventional controllers would perform better than that of fuzzy logic controllers. There is also a challenge in determining the most optimal fuzzy inference system as there are many different fuzzy system configurations which can be formed depending on how the membership function and fuzzy rules are designed.

The fuzzy control dispatch strategy is developed based upon the load following and cycle charging dispatch strategies. In the load following and cycle charging dispatch strategy, charging of the ESS by the PV is done only when  $P_{PV}$  is in excess ( $P_{PV} > P_{Load}$ ). Moreover, the generator will be turned off when this condition is met.

However, the results of the load following and cycle charging strategy have been evaluated and it is found that generator can be turned off even before  $P_{PV} > P_{Load}$  condition is met. This in turn reduces the overall generator runtime, which is one of the parameter vital in improving the COE of the system. This is due to less often generator replacement needed when the generator runtime is lower.

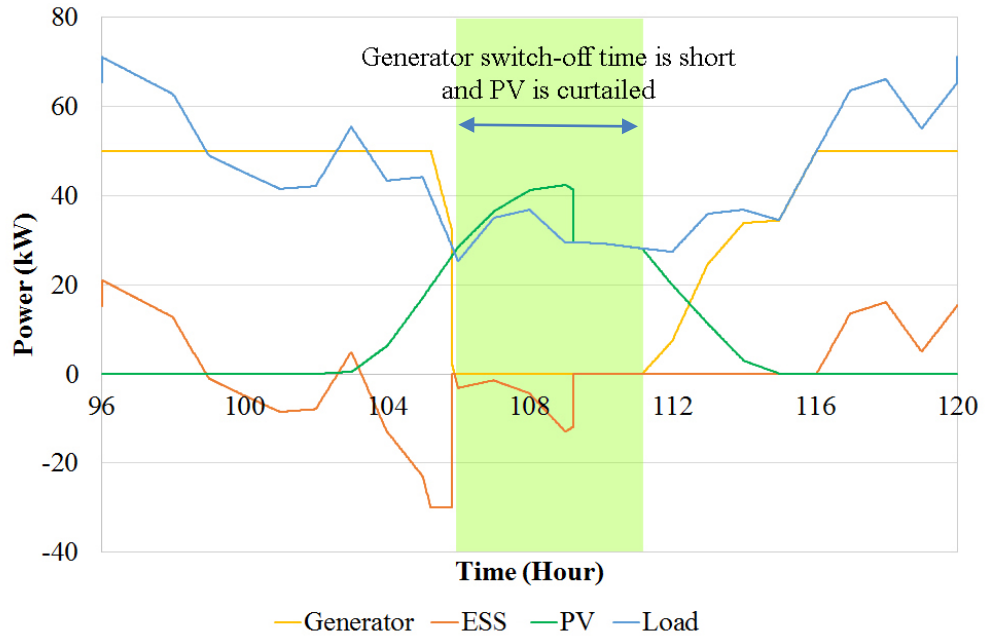
There are two weaknesses present in the load following and cycle charging dispatch strategy formulated. The first weakness is when there is an excess PV power and the ESS has reached  $SOC_{Max}$ , the PV will undergo deloading operation and its power output will be curtailed and wasted. Another weakness is that the generator will only be turned off when  $P_{PV}$  is greater than  $P_{Load}$ . In many cases, the generator can be turned off earlier before this condition is met. In other words, generator can be turned off when  $P_{PV}$  is not greater than  $P_{Load}$ . When such a scenario occurs, ESS will be utilised to supply the difference between PV power and load demand. Using ESS in this condition is also beneficial as discharging the ESS will ensure more capacity for charging during the condition of  $P_{PV} > P_{Load}$ .

In the fuzzy control dispatch strategy, both the concept from load following and cycle charging dispatch strategy will be utilized. This means that when the generator is turned on, it will be run at maximum output power, while when ESS has reached  $SOC_{Max}$ , generator will supply power just to meet the load demand.

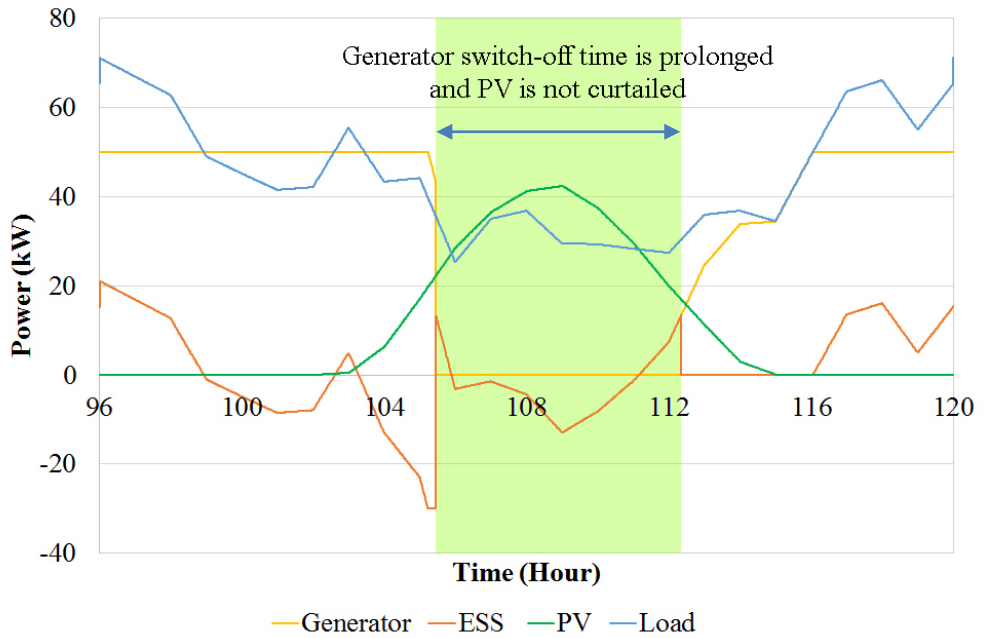
However, the fuzzy control dispatch strategy will also include mechanisms which address the two main weaknesses of load following and cycle charging strategies. The first feature is that the fuzzy control dispatch strategy will be able to utilize the forecasted PV output and ensure that the ESS has a low enough SOC level in order to have enough capacity for the next day. As a result, more excess PV power can be stored into the ESS and the occurrence of PV curtailment can be reduced.

The fuzzy control dispatch strategy can reduce the generator runtime by switching off the generator for a longer period of time, while ensuring that load demand is met. This is done by generating a parameter called  $P_{Fuzzy}$  each day based on the SOC and day ahead solar irradiance value.

As mentioned earlier, the fuzzy control dispatch strategy enables a lower generator runtime and prevents wastage of PV power. Figure 4.7 shows the results of using cycle charging dispatch strategy as compared to that of using the fuzzy control dispatch strategy. It is observed that when the fuzzy control dispatch strategy was used, the generator has a longer switch off time and PV output is not curtailed.



(a)



(b)

**Figure 4.7: System in (a) cycle charging dispatch strategy (b) fuzzy control dispatch strategy**

The fuzzy control dispatch strategy flowchart is shown in Figure 4.8. The first condition is such that instead of comparing if  $P_{PV}$  is greater than  $P_{Load}$ , the condition now compares whether  $P_{PV}$  is greater than the difference between  $P_{Load}$  and  $P_{Fuzzy}$ . In order to obtain the  $P_{Fuzzy}$ , the system will need to use the predicted solar irradiance data as an input to the FLC. Since the study does not cover prediction methods for the solar irradiance, the predicted solar irradiance data used is the next day hourly solar irradiance data obtained from (National Renewable Energy Laboratory, n.d.).

When this condition is met, the algorithm compares if  $P_{PV}$  is greater than  $P_{Load}$ . If this condition is met, generator will be switched off. ESS will be charged according to the difference between  $P_{PV}$  and  $P_{Load}$  while SOC is below 90%. During the condition when  $P_{PV}$  is not greater than  $P_{Load}$ , generator will be switched off if the SOC is greater than 30% and ESS will be discharged to meet the load demand according to the difference between  $P_{Load}$  and  $P_{PV}$ . However, if SOC is not greater than 30%, generator will be used to supply for the difference between  $P_{Load}$  and  $P_{PV}$ . In this case, the ESS will be idle with no charge or discharge operation.

During the next condition when difference between  $P_{Load}$  and  $P_{Fuzzy}$  is greater than  $P_{PV}$  and when  $P_{Load}$  is greater than  $P_{GenMax}$ , generator will operate at its maximum loading factor and ESS will be discharged to meet the load demand. The power to be discharged is calculated as the difference between  $P_{Load}$ ,  $P_{PV}$  and  $P_{GenMax}$ .

The final condition is such that when SOC is less than 80% and the difference between  $P_{Load}$  and  $P_{Fuzzy}$  is greater than  $P_{PV}$ . When this condition is true, the system will operate similar to the cycle charging strategy when its third condition is met. Generator will operate at maximum loading factor and excess power is charged into the ESS. When this condition is not met, generator will supply just enough power to meet the load demand.

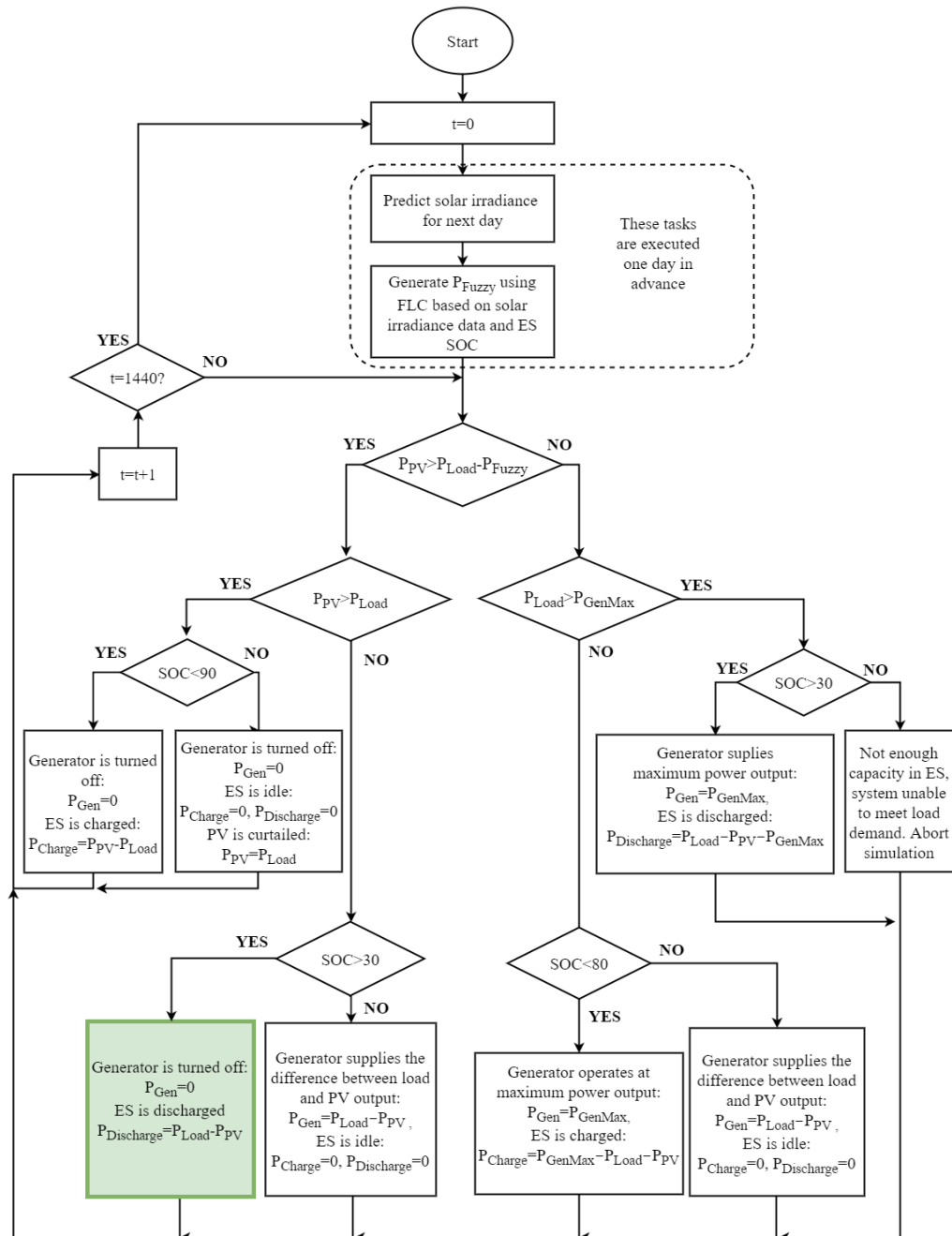
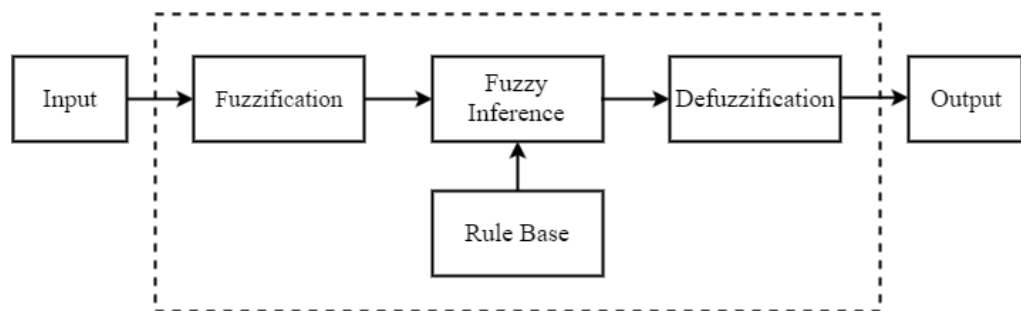


Figure 4.8: Flowchart for fuzzy control dispatch strategy

#### 4.4.1 Design of Fuzzy Control Dispatch Strategy

The proposed fuzzy logic controller (FLC) consists of three main parts as shown in Figure 4.9. They include the fuzzification, interference engine, as well as defuzzification. Fuzzification is a process whereby the input in the form of crisp quantity is converted into degrees of membership of the input fuzzy set and they take on values between zero and one.



**Figure 4.9: Fuzzy inference system**

The inference engine is vital part of the FLC, where it has the capacity to interpret and apply expert's decision on how to best operate under conditions it is put in. The inference engine uses "IF-THEN" rules which can be tabulated by the designer. Defuzzification is a process which converts the conclusion into crisp values to be used as output of the system.

Figure 4.10 shows the input to the fuzzy logic controller, battery SOC and solar irradiance. The output generated is  $P_{\text{Fuzzy}}$ .

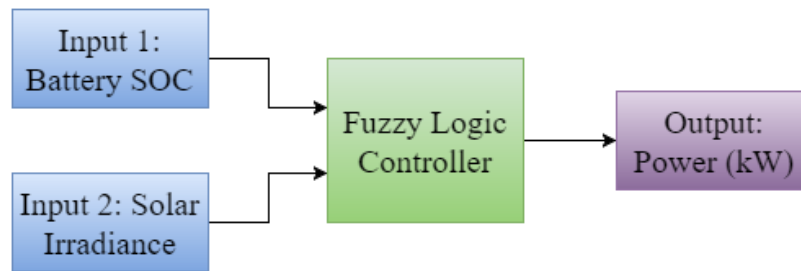
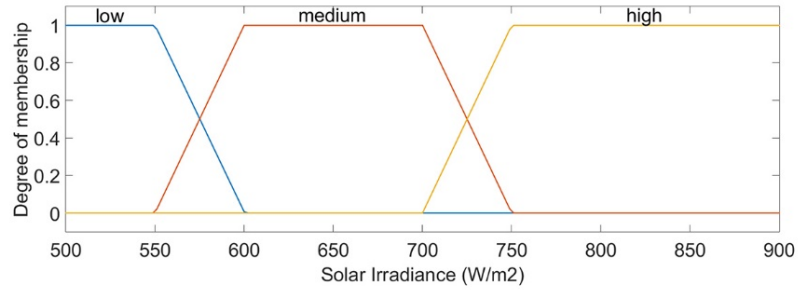


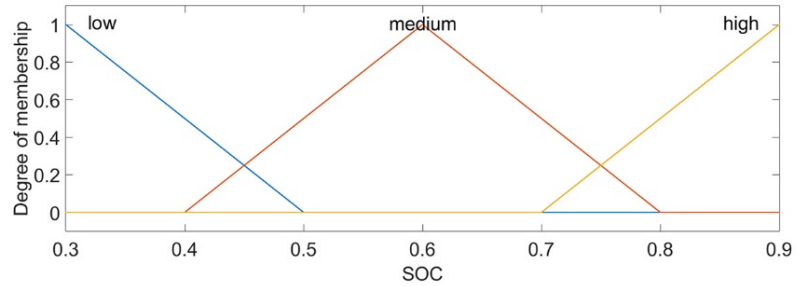
**Figure 4.10: Input and output of fuzzy logic controller**

There are three membership functions for battery SOC and they take the form of a triangular function. They can be categorized as low, medium and high. The input variable is constrained to minimum SOC of 30% and maximum SOC of 90%, which are the  $SOC_{Min}$  and  $SOC_{Max}$  used throughout the study.

Meanwhile, the membership function for the input variable solar irradiance is categorised as low, medium and high. The solar irradiance range has a minimum value of  $500 \text{ W/m}^2$  and maximum value of  $900 \text{ W/m}^2$ . Based on the Malaysian solar irradiance historical data, there were no instances where solar irradiance could reach a value of  $1000 \text{ W/m}^2$ . In Malaysia, the occurrence of solar irradiance above  $900 \text{ W/m}^2$  happens only 3 times within a year. This can be seen from solar irradiance data obtained from (National Renewable Energy Laboratory, n.d.) which is presented in Appendix D at page 162.. Figure 4.11 shows the input membership function for solar irradiance and battery SOC.



(a)



(b)

**Figure 4.11: Input membership function for (a) solar irradiance (b) battery SOC**

There are two types of output membership function designed for the purpose of the system control using fuzzy logic controller. In both types, there are four membership categorised as low, medium, high and very high. The output ranges from 0 to 40 kW and is denoted as  $P_{Fuzzy}$ . The larger the  $P_{Fuzzy}$ , the longer the generator will be turned off. In designing the output membership function, each of them were tested empirically using maximum output range of up to 20 kW, 30 kW, 40 kW, and 50 kW. It was found that system performance is the best when 40 kW is used. Beyond 40 kW, the performance of the system deteriorates. Figure 4.12 illustrates the both output membership functions.

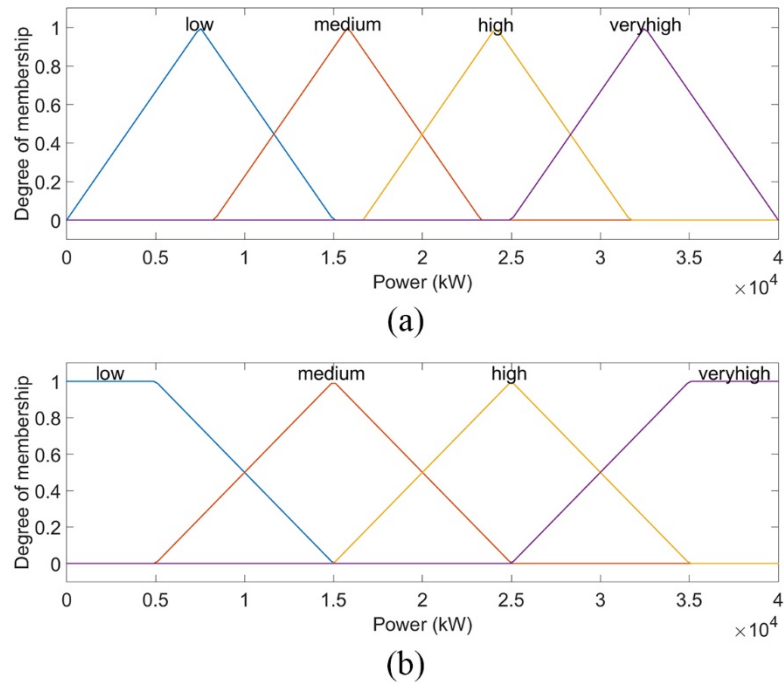


**Figure 4.12: Output membership function (a) MF 1 (b) MF 2**

Table 4.1 and Table 4.2 shows the fuzzy rule used in the fuzzy control dispatch strategy, where Rule 1 tends to output a lower  $P_{Fuzzy}$  while Rule 2 tend to output a higher  $P_{Fuzzy}$ . However, this is at the expense of the number of system configurations which can meet the load demand where Rule 1 produces more system configurations which can meet the load demand compared to Rule 2. The  $P_{Fuzzy}$  value generated will be constant throughout the day, or least for a duration lasting longer than the  $P_{PV}$  when it produces an output.

**Table 4.1: Fuzzy rule 1**

Battery SOC	Solar Irradiance		
	Low	Medium	High
Low	Low	Low	Medium
Medium	Low	Medium	High
High	Medium	High	Very High

**Table 4.2: Fuzzy rule 2**

Battery SOC	Solar Irradiance		
	Low	Medium	High
Low	Low	Medium	High
Medium	Medium	High	Very High
High	High	Very High	Very High

#### **4.5 Summary**

The dispatch strategy for HES plays an important role in the operation of such systems and has a profound impact onto the COE of a particular system. This chapter presents the dispatch strategies for the different HES systems such as the generator-PV, generator-ESS, PV-ESS, as well as the generator-PV-ESS system.

A novel control algorithm based on fuzzy logic is developed to reduce generator runtime and PV power curtailment in the generator-PV-ESS system. This is done by utilising next-day PV power output and ESS SOC as input to the fuzzy logic controller. There are a total of two different output membership functions and fuzzy rules respectively developed for the purpose of comparison. Compared to the load following and cycle charging dispatch strategy, the fuzzy control dispatch strategy excels in producing a system with lower NPC and COE.

## **CHAPTER 5**

### **RESULTS AND DISCUSSION**

#### **5.1 Introduction**

The performance of all the system simulated in this study is evaluated in terms of its technical and economic feasibility. They include the generator-PV, generator-ESS, PV-ESS, and the generator-PV-ESS system. In assessing the technical feasibility of each system, the operation of the various systems will be presented and discussed. Parameters pertaining to the system will also be varied in order to observe how the system will work in different cases. Other than that, the results for the economic feasibility are presented and discussed in this chapter. Ideally, the best system to be implemented in an off-grid rural area would be the one with the lowest COE value.

#### **5.2 Technical Feasibility Studies for Different System Configurations**

In this section, the operation of the different types of HES is discussed in detail. Case studies are also presented, where different operating scenarios will be compared. An example of such a scenario is when there are different daily solar irradiance values or when different ESS capacities are used. These comparisons

will provide a better understanding on what actually happens during operation of the generator-PV-ESS system.

In describing the operation of the system, each figure introduced here are divided into multiple sections, each representing a certain set of operations by generator, PV and ESS. The section aims to introduce various cases where the system would operate in order to show the diversity in operation and control undertaken by the system.

### **5.2.1 Generator-PV System**

This section describes the operation of the generator-PV system. Since the generator has to be sized to meet the peak demand, only the size of the PV can be varied. The two cases below illustrate the operation when PV size is varied.

#### **Case 1: Generator-PV System with Small PV Size**

Figure 5.1 shows the operation of the generator-PV system with small PV size of 40 kW, and it is divided into 5 sections.

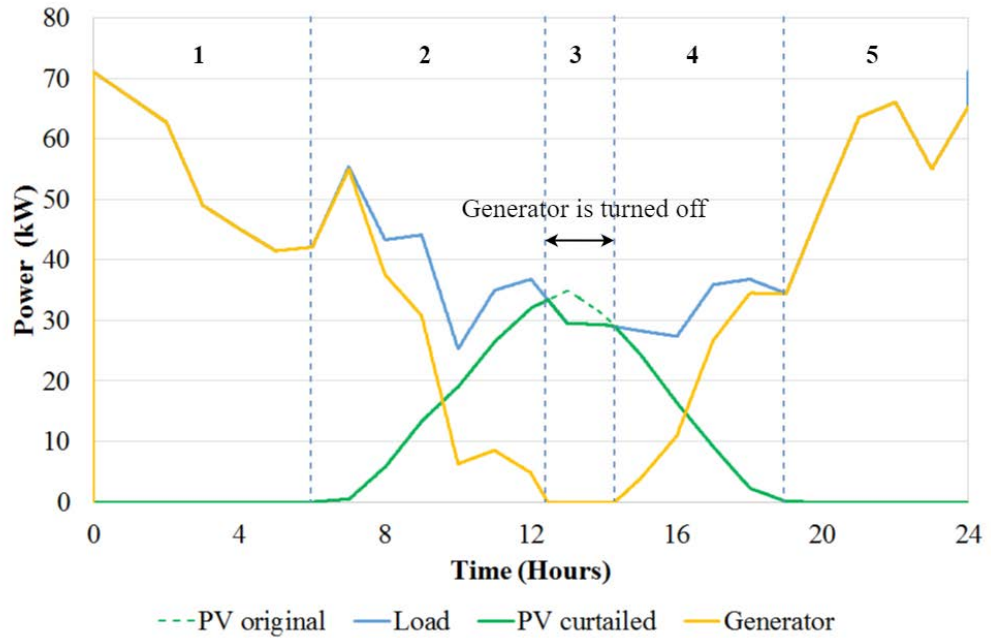


**Figure 5.1: Generator-PV system with small PV size**

In section 1, load demand,  $P_{Load}$  is served by the generator only. As PV starts producing power in section 2, the load demand is now served by both the generator,  $P_{Gen}$  and PV,  $P_{PV}$ . In section 3,  $P_{PV}$  exceeds  $P_{Load}$  and generator is turned off as  $P_{PV}$  fully meets the load demand. Since there is no ESS in this system, this causes the PV to be curtailed. In section 4, both  $P_{PV}$  and  $P_{Gen}$  meets the load demand, similar to that in section 2. In section 5, generator fully meets the load demand as there is no  $P_{PV}$  produced.

### Case 2: Generator-PV System with Large PV Size

Figure 5.2 shows the operation of the generator-PV system with large PV size of 70 kW.

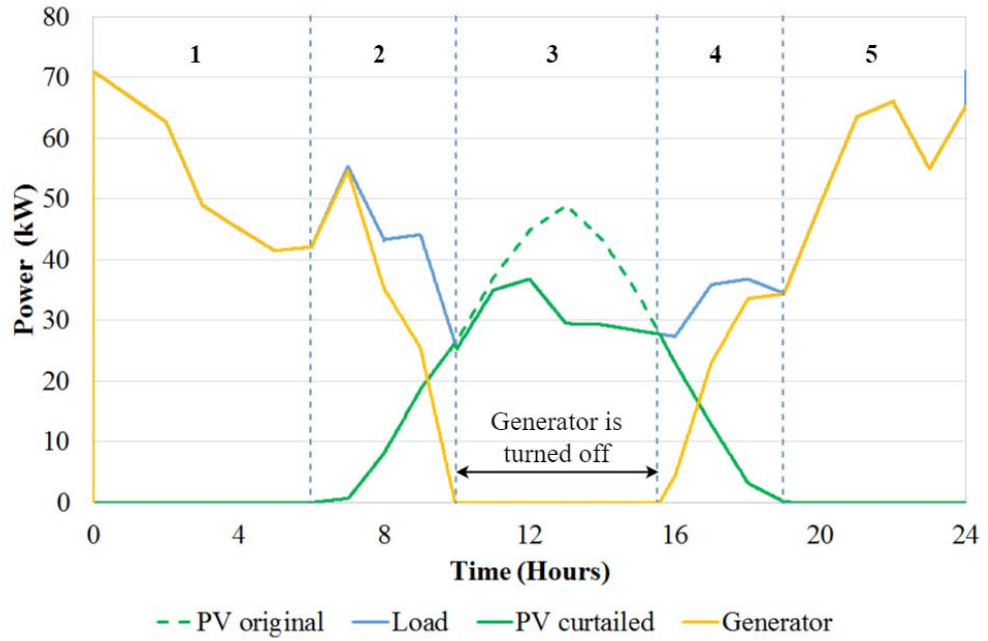


**Figure 5.2: Generator-PV system with large PV size**

The operation of the system is divided into 5 sections. In the generator-PV with large PV size, the operation is similar to that of a generator-PV with small PV size. This is true for sections 1 to 5. However, the difference is that in this case, the generator is switched off for a longer time period compared to that in case 1. This happens because in a system with large PV size,  $P_{PV}$  exceeds  $P_{Load}$  at a much earlier time compared to a system with small PV size. The large  $P_{PV}$  produced ensures that the condition of  $P_{PV} > P_{Load}$  is met for a longer time period, where generator will be turned off during this condition.

### 5.2.2 Generator-ESS System

This section describes the operation of the generator-ESS system. The two cases below illustrate the operation when ESS size is varied.

### Case 3: Generator-ESS System with Small ESS Size

Figure 5.3 shows the generator-ESS system with small ESS size of 3 strings (166.56 kWh) and its operation is divided into 6 sections.

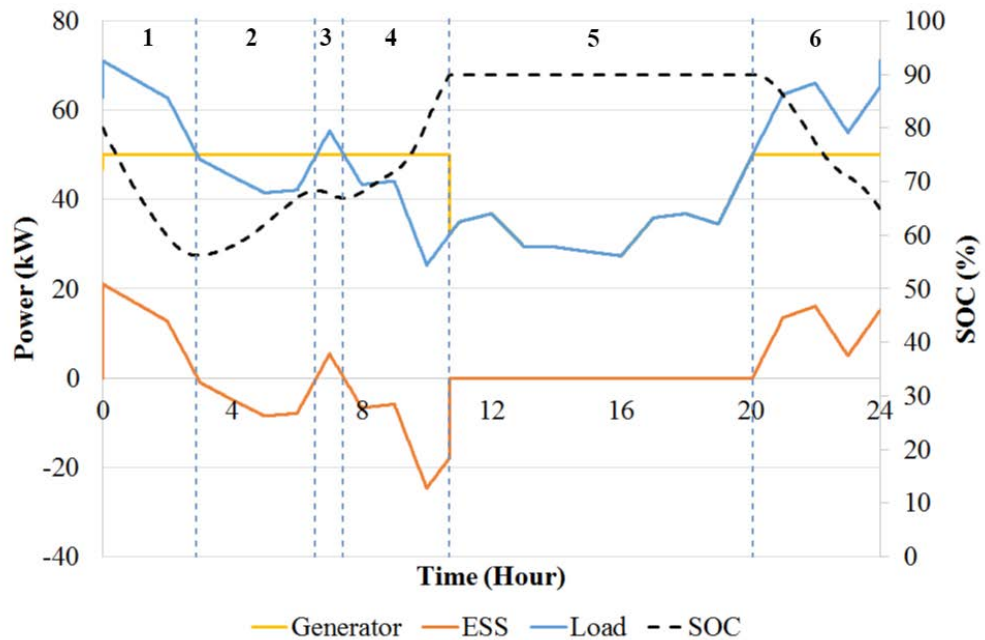


**Figure 5.3: Generator-ESS system with small ESS size**

In section 1, load demand is greater than the generator maximum output,  $P_{GenMax}$ . This causes the ESS to discharge, while generator runs at its maximum loading factor in order to meet the load demand. Section 1 and 3 is similar in operation. In section 2, load demand is lesser than the  $P_{GenMax}$  and SOC is below  $SOC_{Max}$  of 90%. This causes the generator to run at  $P_{GenMax}$  and the excess power is used to charge the ESS. In section 4, load demand is lesser than the  $P_{GenMax}$ . Generator is run at  $P_{GenMax}$  and excess power is used to charge the ESS. At section 5, the SOC has reached 90%, which causes the generator to supply power enough to only meet the load demand. In section 6, a condition similar

to that in section 1 occur. In this case, generator runs at  $P_{GenMax}$  and ESS is discharged to meet the load demand.

#### Case 4: Generator-ESS System with Large ESS Size

Figure 5.4 shows the generator-ESS system with large ESS size of 8 strings (444.14 kWh) and its operation is divided into 6 sections.

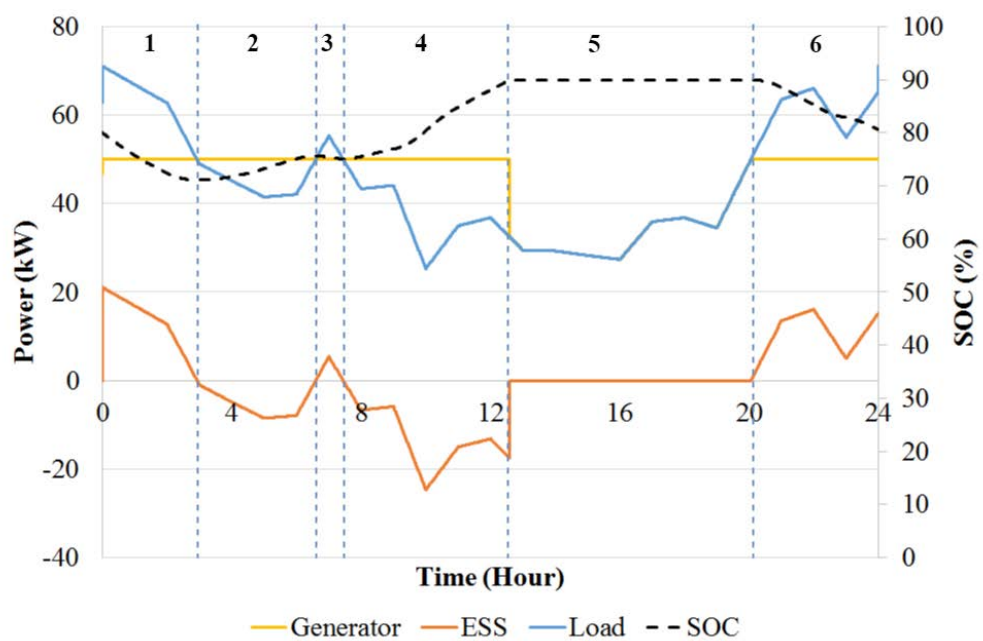


**Figure 5.4: Generator-ESS system with large ESS size**

In this case, the operation from section 1 to 6 is the same as that in case 3. However, one distinct difference is that the section 4 in this case is prolonged as more energy is needed to charge the ESS to 90%. It can be seen that the utilisation of ESS in this case is lower than that in case 3 due to a lower SOC range in this case. It will be presented in the later part of this study where a generator-ESS system with a smaller ESS size will have a lower COE compared to that with a larger ESS size. The larger ESS size in case 4 is redundant.

### 5.2.3 PV-ESS System

This section describes the operation of the PV-ESS system. There are two scenarios illustrated using the same PV and ESS size, which is the condition during high solar irradiation and condition during low solar irradiation.

#### Case 5: System during High Solar Irradiance

Figure 5.5 shows the PV-ESS system under high solar irradiance and its operation is divided into 6 sections.

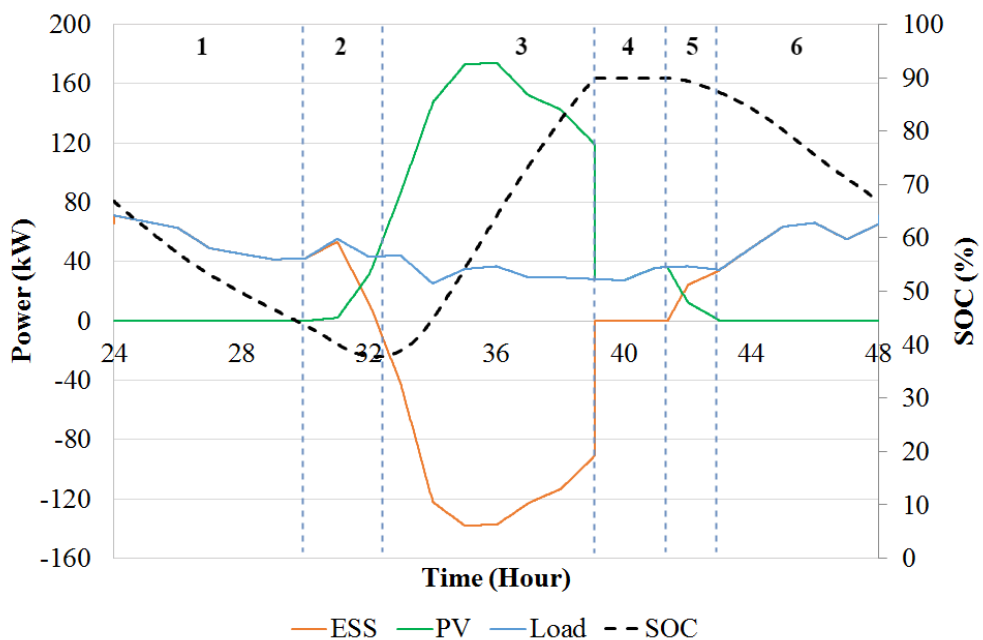


**Figure 5.5: PV-ESS system under high solar irradiance**

In Section 1, load demand is fully served by the ESS. In Section 2 where PV has started producing power, the load is supplied by both the ESS and PV. During both section 1 and 2, it can be observed that SOC decreases as the ESS is being discharged. However, in Section 3,  $P_{PV}$  exceeds  $P_{Load}$  and the excess

$P_{PV}$  is used to charge the ESS, causing SOC to rise. In section 4, SOC has reached the  $SOC_{Max}$  of 90% and PV undergoes deloading operation. In this case, the  $P_{PV}$  value is the same as that of the  $P_{Load}$ . ESS is idle in this section. In Section 5,  $P_{PV}$  is no longer greater than  $P_{Load}$ . Both the ESS and PV supplies the load demand in this condition. In Section 6, the ESS fully meets the load demand as there is no PV power output during that time.

### Case 6: System during Low Solar Irradiance

Figure 5.6 shows the PV-ESS system under low solar irradiance and its operation is divided into 5 sections.

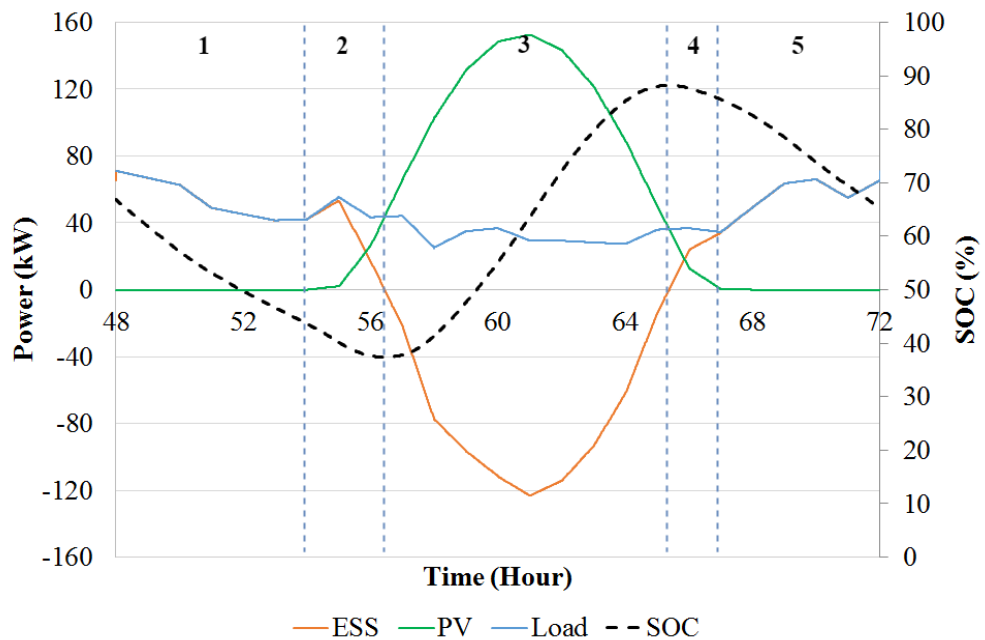


**Figure 5.6: PV-ESS system under low solar irradiance**

For the system during low solar irradiance, one difference in its operation as compared to when it is operated under high solar irradiance is such that there exists no PV deloading operation. It can be seen that in Section 3 where  $P_{PV}$  is

greater than  $P_{Load}$ , excess  $P_{PV}$  is charged into the ESS causing the SOC to rise. However, since it is operating on a day which has a low solar irradiance, the charging of the ESS in Section 3 does not raise the SOC to  $SOC_{Max}$ . Hence, no PV deloading operation is required.

### **5.3 Performance of Generator-PV-ESS System**

#### **5.3.1 Case Study 1: Load Following Operation with Varying ESS Size**

The following case study shows the operation of a system in load following dispatch strategy on a same day with varying ESS sizes, using generator size of 50 kW, PV size of 80 kW. In scenario 1, the system has ESS size of 5 strings (277.6 kWh) while that in scenario 2 has ESS size of 3 strings (166.56 kWh). A quick observation reveals the deloading operation in section 7 scenario 2, due to insufficient ESS capacity to store excess PV power on that particular day. Having a larger ESS size, the system as seen in scenario 1 does not undergo any PV deloading operation on that particular day.

#### **Scenario 1: System with Larger ESS Size**

Figure 5.7 shows the generator-PV-ESS system under load following operation with an ESS size of 5 strings (277.6 kWh). The operation of the system is divided into 8 sections.

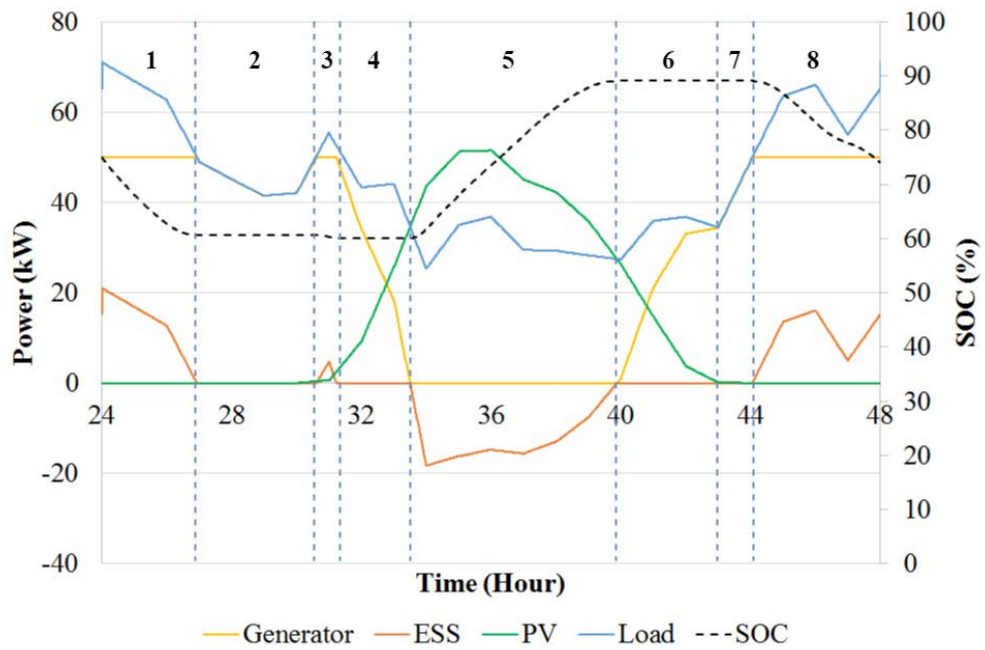


**Figure 5.7: Load following operation of system having 50 kW generator, 80 kW PV (Scenario 1: ESS size of 5 strings)**

In section 1 of Figure 5.7, load demand,  $P_{Load}$  is greater than the generator maximum output,  $P_{GenMax}$ . This causes the ESS to be discharged in order to meet the load demand. In section 2,  $P_{Load}$  is lesser than  $P_{GenMax}$  and generator will supply just enough power to meet the load demand. In section 3, the system is in the same scenario to that of section 1. One minor difference is that PV now starts to output power,  $P_{PV}$ .  $P_{Load}$  is met by the ESS discharge and  $P_{PV}$ . Meanwhile in section 4,  $P_{load}$  is lesser than  $P_{GenMax}$ .  $P_{Load}$  is supplied by  $P_{PV}$  and  $P_{Gen}$ .

In section 5,  $P_{PV}$  exceeds  $P_{Load}$  and generator is switched off. Excess energy from PV is charged into the ESS. By the end of the charging of the ESS, the SOC is still within the limit of  $SOC_{Max}$  (90%). The generator and PV both supplies power to meet the load demand in Section 6. In section 7, generator fully meets

the load demand. Meanwhile in section 8,  $P_{Load}$  is greater than  $P_{GenMax}$ . Generator runs at maximum output of  $P_{GenMax}$  and ESS is discharged in order to meet the load demand.

### Scenario 2: System with Smaller ESS Size

Figure 5.8 illustrates scenario 2 where the generator-PV-ESS system operates under load following operation with an ESS size of 3 strings (166.56 kWh). The operation of the system is divided into 10 sections.

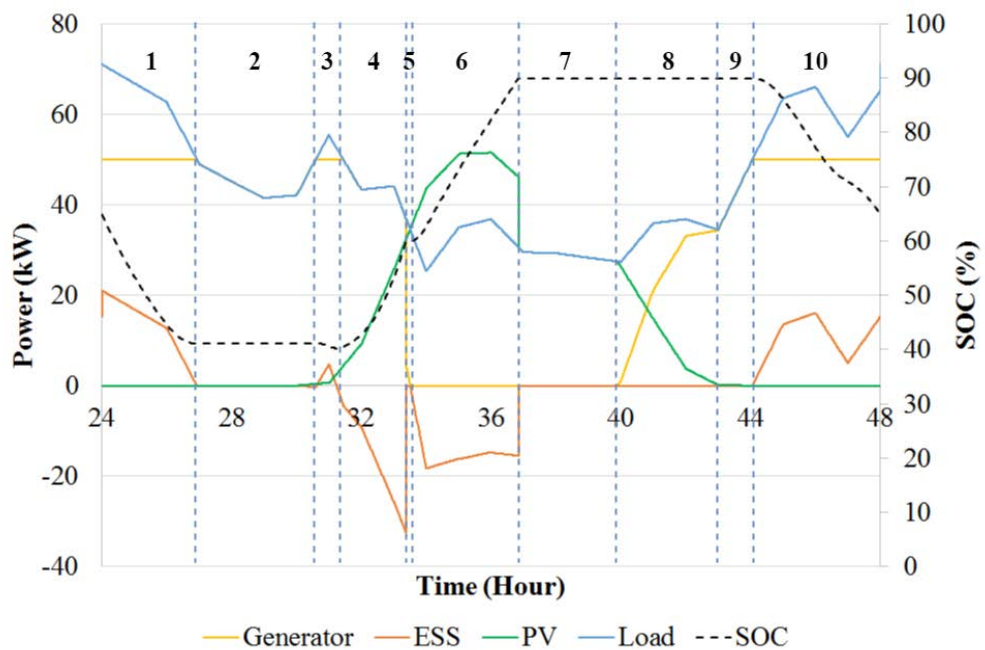


**Figure 5.8: Load following operation of system having 50 kW generator, 80 kW PV (Scenario 2: ESS size of 3 strings)**

The sections 1 to 3 has similar operation to that in scenario 1. However, in section 4,  $P_{PV}$  is charged into the ESS, even while it is not in excess. This happens as the SOC in section is below 60%, which is the  $SOC_{Mid}$  specified in our algorithm. The system will charge the ESS to  $SOC_{Mid}$  before it undergoes a

charging operation during condition of  $P_{PV} > P_{Load}$ . In section 5, generator starts to switch off but not fully so as excess PV condition has not been met.  $P_{PV} > P_{Load}$  condition is met in section 6 and ESS is charged by excess PV power. In section 7, PV undergoes deloading operation as SOC of the ESS has reached  $SOC_{Max}$ . The sections 8,9 and 10 of case 2 basically undergoes the same operation as sections 6,7 and 8 of case 1.

Table 5.1 shows the power flow equation for the system in load following operation with varying ESS size.

**Table 5.1: Power flow equation for the system in load following operation with varying ESS size**

Section	Scenario 1: System with bigger ESS size (5 strings)	Scenario 2: System with smaller ESS size (3 strings)
1.	$P_{Load} = P_{Gen} + P_{ESS}$	$P_{Load} = P_{Gen} + P_{ESS}$
2.	$P_{Load} = P_{Gen}$	$P_{Load} = P_{Gen}$
3.	$P_{Load} = P_{Gen} + P_{ESS} + P_{PV}$	$P_{Load} = P_{Gen} + P_{ESS} + P_{PV}$
4.	$P_{Load} = P_{Gen} + P_{PV}$	$P_{Load} = P_{Gen} - P_{ESS} + P_{PV}$
5.	$P_{Load} = P_{PV} - P_{ESS}$	$P_{Load} = P_{PV}$
6.	$P_{Load} = P_{Gen} + P_{PV}$	$P_{Load} = P_{PV} - P_{ESS}$
7.	$P_{Load} = P_{Gen}$	$P_{Load} = P_{PV}$
8.	$P_{Load} = P_{Gen} + P_{ESS}$	$P_{Load} = P_{Gen} + P_{PV}$
9.		$P_{Load} = P_{Gen}$
10.		$P_{Load} = P_{Gen} + P_{ESS}$

### 5.3.2 Case Study 2: Cycle Charging Operation with Varying Solar Irradiance

The following explains the operation of a system consisting of 50 kW generator, 60 kW PV and ESS size of 3 strings in cycle charging dispatch strategy. Scenario 1 shows the operation of the system in day 1 which has a lower PV output than that in day 9, which is as represented in scenario 2.

## Scenario 1: Operation during Low PV Output

Figure 5.9 shows the generator-PV-ESS system under cycle charging operation on a particular day with a low PV output. The operation of the system is divided into 10 sections.

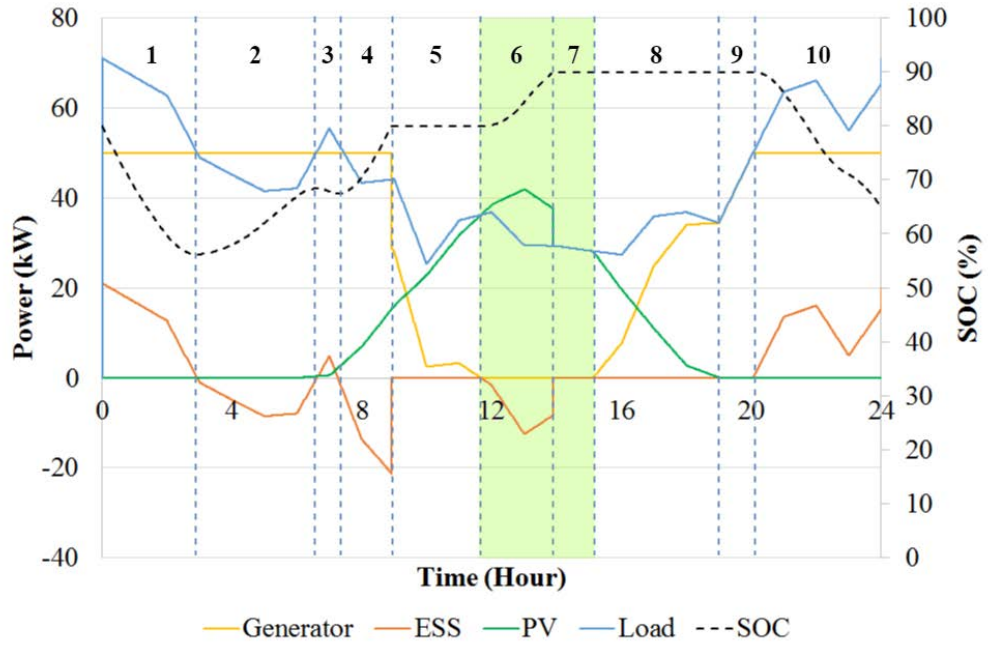


**Figure 5.9: System in cycle charging operation with 50 kW generator, ESS size of 3 strings, PV size of 60 kW at (a) low PV output day**

In section 1, load demand,  $P_{Load}$  is greater than the generator maximum output,  $P_{GenMax}$ . This causes the ESS to be discharged in order to meet the load demand. In section 2,  $P_{Load}$  is lesser than  $P_{GenMax}$ . Since SOC is not at  $SOC_{Max}$ , generator runs at  $P_{GenMax}$  and the surplus energy is charged into the ESS. In section 3, the system is in the same scenario to that of section 1. One minor difference is that PV now starts to produce power,  $P_{PV}$ .  $P_{Load}$  is met by the ESS discharge and  $P_{PV}$ . Meanwhile in section 4,  $P_{load}$  is lesser than  $P_{GenMax}$ .  $P_{Load}$  is supplied by  $P_{PV}$  and  $P_{Gen}$ . The generator runs at  $P_{GenMax}$  and surplus energy is charged into the ESS.

In section 5, both the generator and PV meets the load demand. When the  $P_{PV}$  exceeds  $P_{Load}$  in section 6, generator is switched off and excess energy is charged into the ESS. Generator is still turned off during in section 7. However, since  $SOC_{Max}$  has been reached, PV undergoes deloading operation and PV output is reduced to prevent overcharging of the ESS. Load demand is satisfied by both  $P_{PV}$  and  $P_{Load}$  in section 8. In section 9, generator supplies power to meet the load demand. In section 10, ESS is discharged in order to meet the load demand.

### Scenario 2: Operation during High PV Output

Figure 5.10 shows the generator-PV-ESS system under cycle charging operation on a particular day with a high PV output. The operation of the system is divided into 9 sections.

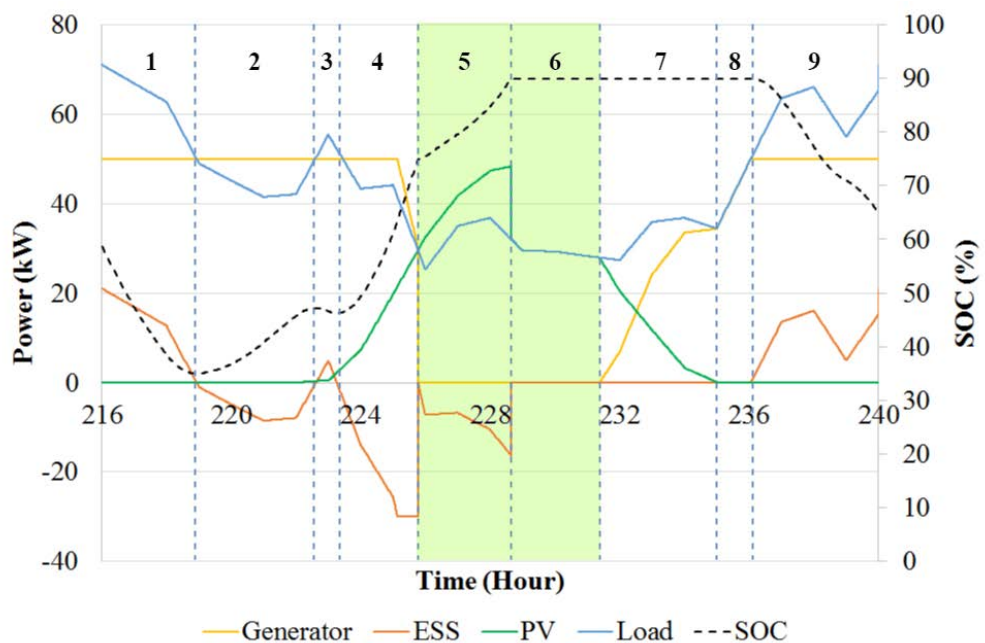


**Figure 5.10: System in cycle charging operation with 50 kW generator, ESS size of 3 strings, PV size of 60 kW at (b) high PV output day**

From Figure 5.10, it can be seen that the condition of excess  $P_{PV}$  ( $P_{PV} > P_{Load}$ ) happens earlier during the day as compared to that in Figure 5.9. This causes the generator to be switched off for a longer period of time compared the one in operation during low PV output. The power flow equation for the operation of the system in low and high PV output is summarized in Table 5.2.

**Table 5.2: Power flow equation for the system in cycle charging operation during low and high PV output**

Section	Cycle Charging during low PV output	Cycle Charging during high PV output
1.	$P_{Load} = P_{Gen} + P_{ESS}$	$P_{Load} = P_{Gen} + P_{ESS}$
2.	$P_{Load} = P_{Gen} - P_{ESS}$	$P_{Load} = P_{Gen} - P_{ESS}$
3.	$P_{Load} = P_{Gen} + P_{ESS} + P_{PV}$	$P_{Load} = P_{Gen} + P_{ESS} + P_{PV}$
4.	$P_{Load} = P_{Gen} - P_{ESS} + P_{PV}$	$P_{Load} = P_{Gen} - P_{ESS} + P_{PV}$
5.	$P_{Load} = P_{Gen} + P_{PV}$	$P_{Load} = P_{PV} - P_{ESS}$
6.	$P_{Load} = P_{PV} - P_{ESS}$	$P_{Load} = P_{PV}$
7.	$P_{Load} = P_{PV}$	$P_{Load} = P_{Gen} + P_{PV}$
8.	$P_{Load} = P_{Gen} + P_{PV}$	$P_{Load} = P_{Gen}$
9.	$P_{Load} = P_{Gen}$	$P_{Load} = P_{Gen} + P_{ESS}$
10.	$P_{Load} = P_{Gen} + P_{ESS}$	

### 5.3.3 Case Study 3: Fuzzy Control Operation

The following section explains the operation of a system consisting of 50 kW generator, 60 kW PV and ESS size of 3 strings in fuzzy control dispatch strategy. Scenario 1 shows the operation of the system in day 3 which has a lower PV output than that in day 5, which is as represented in scenario 2. It should also be noted on the difference in value for  $P_{Fuzzy}$  between the two days, where  $P_{Fuzzy}$  in day 3 is lower than that in day 5. The following section will discuss the operation of the system during both of the days.

### Scenario 1: Operation during Low PV Output

Figure 5.11 shows the generator-PV-ESS system under fuzzy control dispatch strategy on a particular day with a low PV output. The operation of the system is divided into 11 sections.

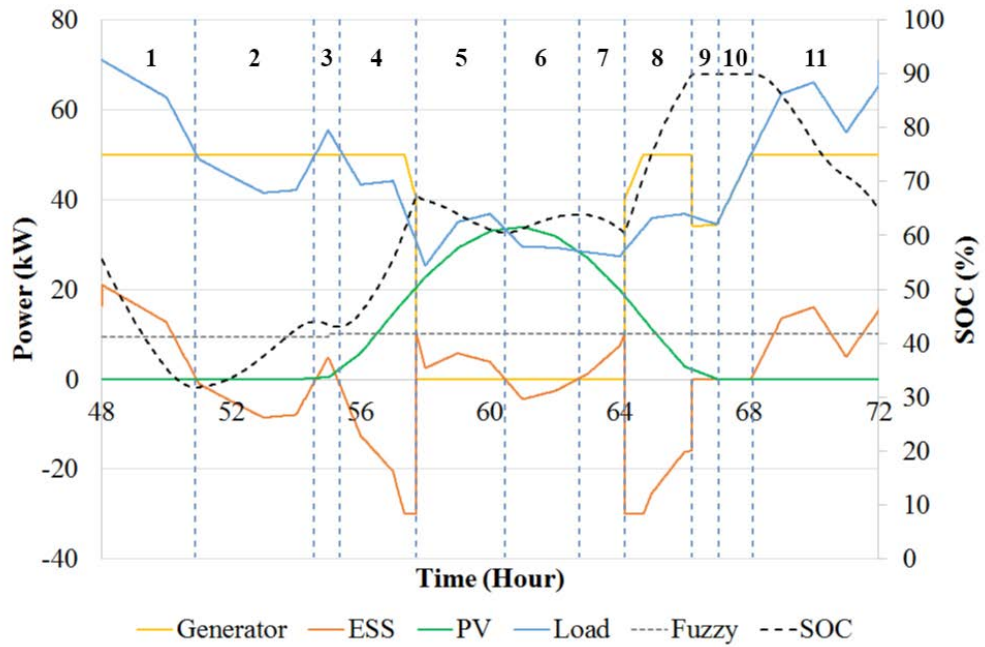


**Figure 5.11: System in fuzzy control operation with 50 kW generator, ESS size of 3 strings, PV size of 60 kW at (a) low PV output day**

The operation of the system from section 1 to 4 is similar to that in the cycle charging dispatch strategy. In section 5 to 7, the condition  $P_{PV} > P_{Load} - P_{Fuzzy}$  is met. Generator is switched off during the whole time period. In section 8, when condition  $P_{PV} > P_{Load} - P_{Fuzzy}$  is no more fulfilled and SOC is below 80%, generator is turned on and outputs excess power in order to charge the ESS. In section 9 and 10,  $SOC_{Max}$  has been reached and generator supply enough power just to

meet the load demand. In section 11, ESS is discharged in order to meet the load demand with the generator supplying power at  $P_{GenMax}$ .

### Scenario 2: Operation during High PV Output

Figure 5.12 shows the generator-PV-ESS system under fuzzy control dispatch strategy operation on a particular day with a high PV output. The operation of the system is divided into 10 sections.

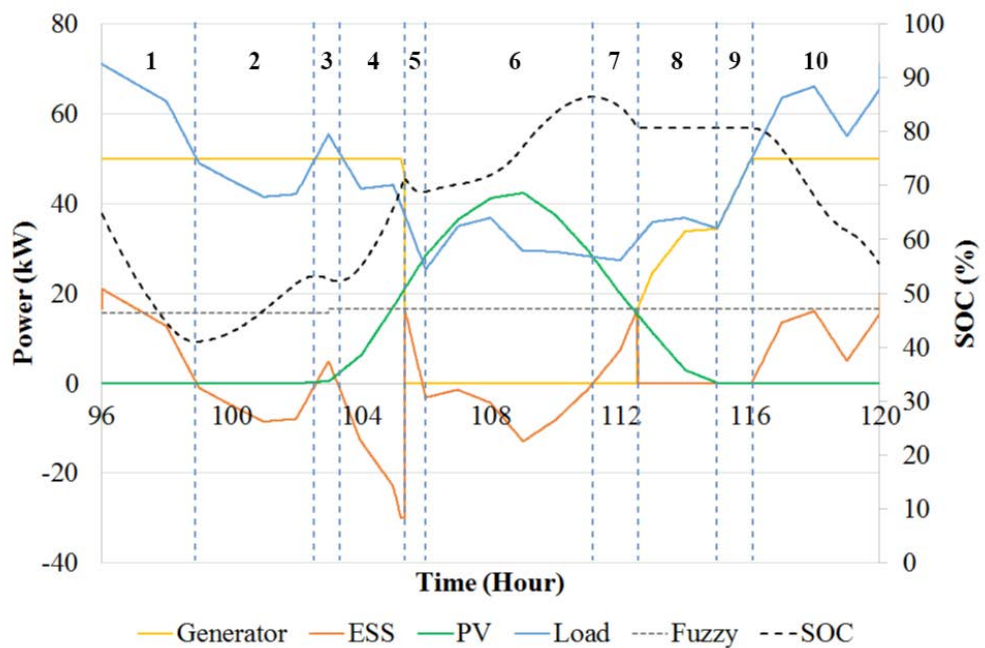


**Figure 5.12: System in fuzzy control operation with 50 kW generator, ESS size of 3 strings, PV size of 60 kW at (b) high PV output day**

As the FLC detects a higher solar irradiance for the day, a higher  $P_{Fuzzy}$  value is generated as compared to that in case 1. This causes the generator to turn off at an earlier time period, which starts at section 5. Other than that, generator switch-off time is extended in section 7, as compared to that in case 1. This

extended generator switch-off time basically reduces the overall generator run time, which will impact the system COE value positively. In section 8, the condition of  $SOC < 80\%$  and  $P_{PV} < P_{Load} - P_{Fuzzy}$  is no more met. Generator is switched on and supplies power in order to meet the load demand. PV power also contributes to meet the load demand in this section. In section 9, load demand is met solely by the generator. Finally, in section 10 the ESS is discharged in order to meet the load demand and generator operates at maximum loading factor. The power flow equation for the operation of the system in low and high PV output is summarized in Table 5.3.

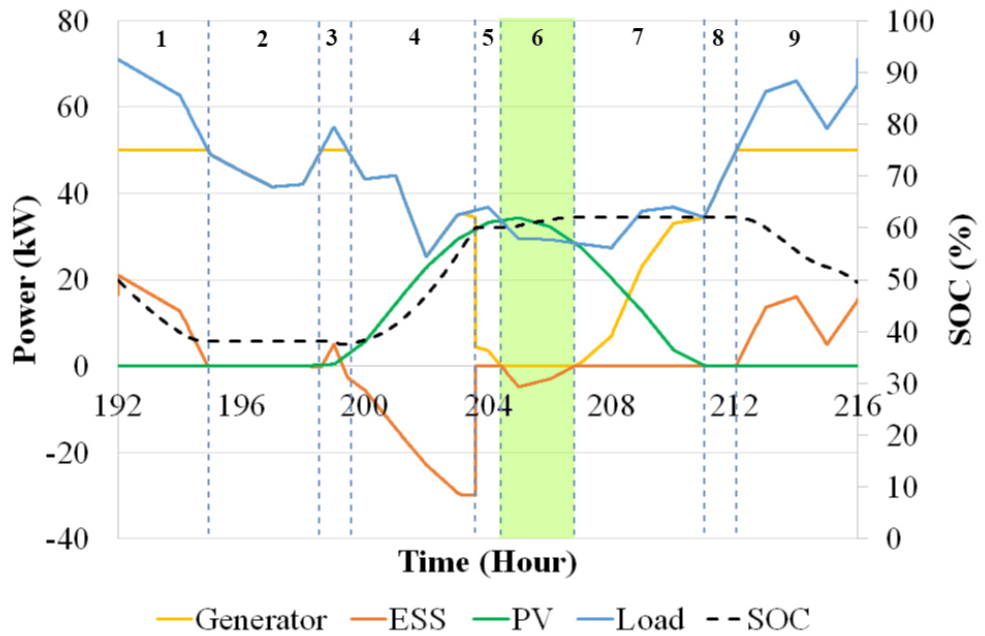
**Table 5.3: Power flow equation for the system in fuzzy control operation during low and high PV output**

Section	FLC strategy during low PV output	FLC strategy during high PV output
1.	$P_{Load} = P_{Gen} + P_{ESS}$	$P_{Load} = P_{Gen} + P_{ESS}$
2.	$P_{Load} = P_{Gen} - P_{ESS}$	$P_{Load} = P_{Gen} - P_{ESS}$
3.	$P_{Load} = P_{Gen} + P_{ESS} + P_{PV}$	$P_{Load} = P_{Gen} + P_{ESS} + P_{PV}$
4.	$P_{Load} = P_{Gen} - P_{ESS} + P_{PV}$	$P_{Load} = P_{Gen} - P_{ESS} + P_{PV}$
5.	$P_{Load} = P_{PV} + P_{ESS}$	$P_{Load} = P_{PV} + P_{ESS}$
6.	$P_{Load} = P_{PV} - P_{ESS}$	$P_{Load} = P_{PV} - P_{ESS}$
7.	$P_{Load} = P_{PV} + P_{ESS}$	$P_{Load} = P_{PV} + P_{ESS}$
8.	$P_{Load} = P_{Gen} + P_{PV} - P_{ESS}$	$P_{Load} = P_{Gen} + P_{PV}$
9.	$P_{Load} = P_{Gen} + P_{PV}$	$P_{Load} = P_{Gen}$
10.	$P_{Load} = P_{Gen}$	$P_{Load} = P_{Gen} + P_{ESS}$
11.	$P_{Load} = P_{Gen} + P_{ESS}$	

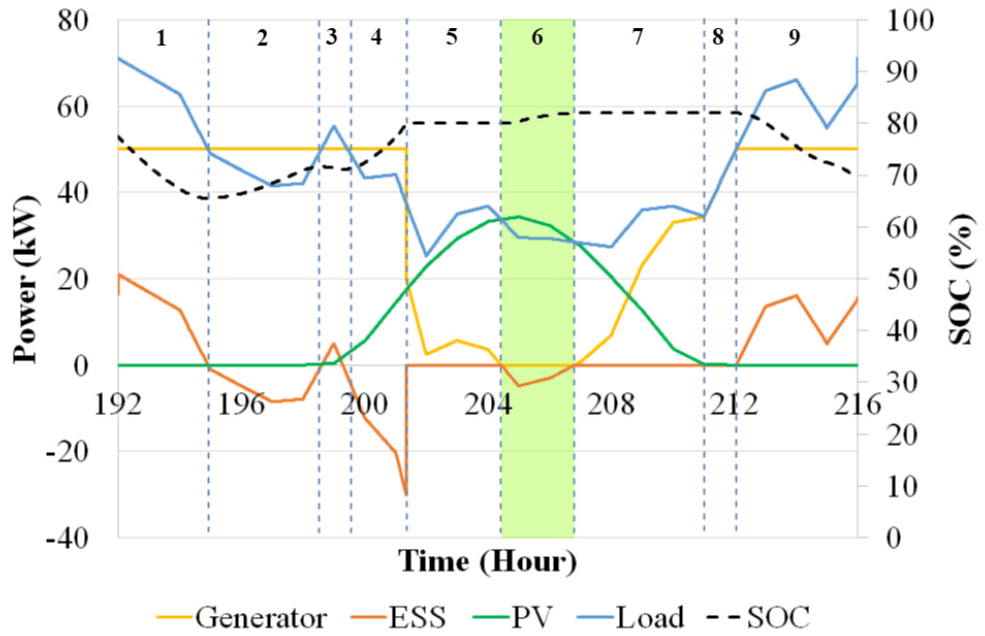
#### **5.3.4 Case Study 4: Comparison of the Fuzzy Control Dispatch Strategy with the Load Following and Cycle Charging Strategies under Various Solar Irradiance**

This case study is to show the effects of solar irradiance on the switch-off time of the generator under different control strategies. In this case study, 50 kW

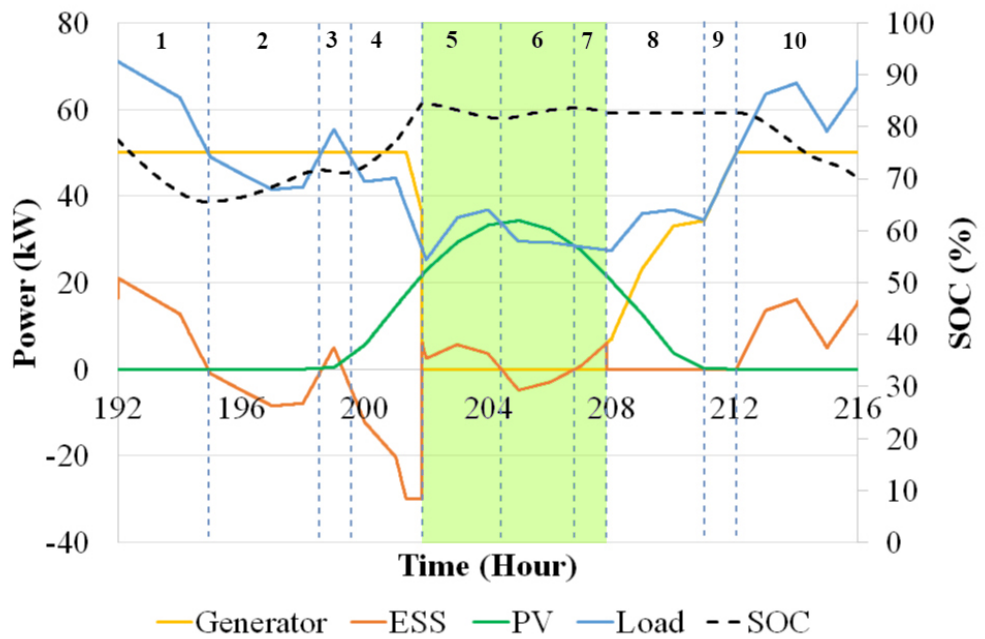
generator, 60 kW PV, ESS size of 6 strings (333.12 kWh) and 30 kW bi-directional converter are used. Figure 5.13 (a), (b) and (c) shows the effects of the low solar irradiance on the switch-off time of the generator under the fuzzy control, load following and cycle charging dispatch strategies respectively. Figure 5.14 (a), (b) and (c) shows the effect of the high solar irradiance on the switch-off time with the three dispatch strategies.



(a)

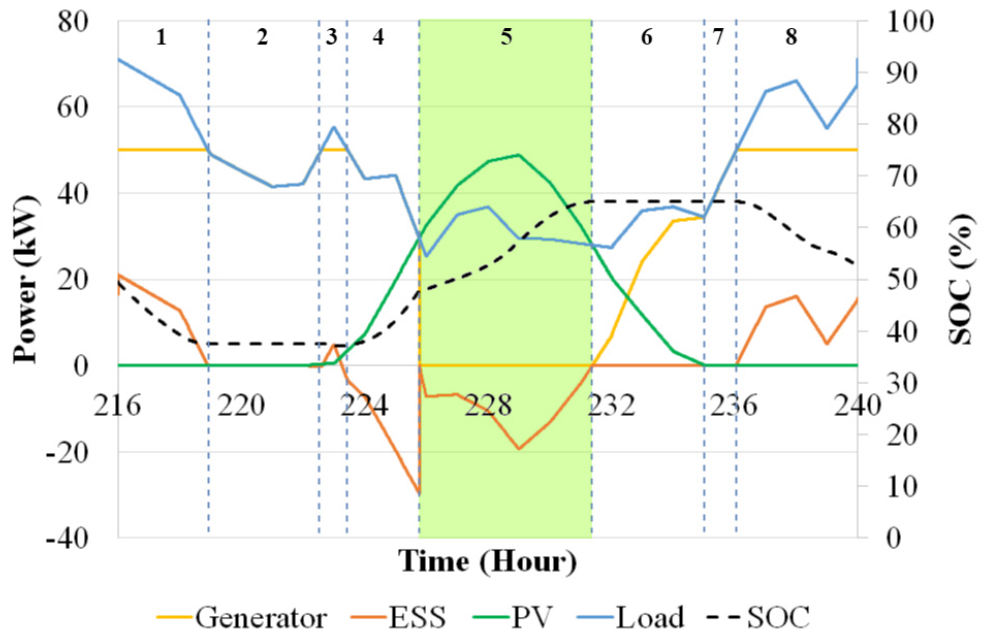


(b)

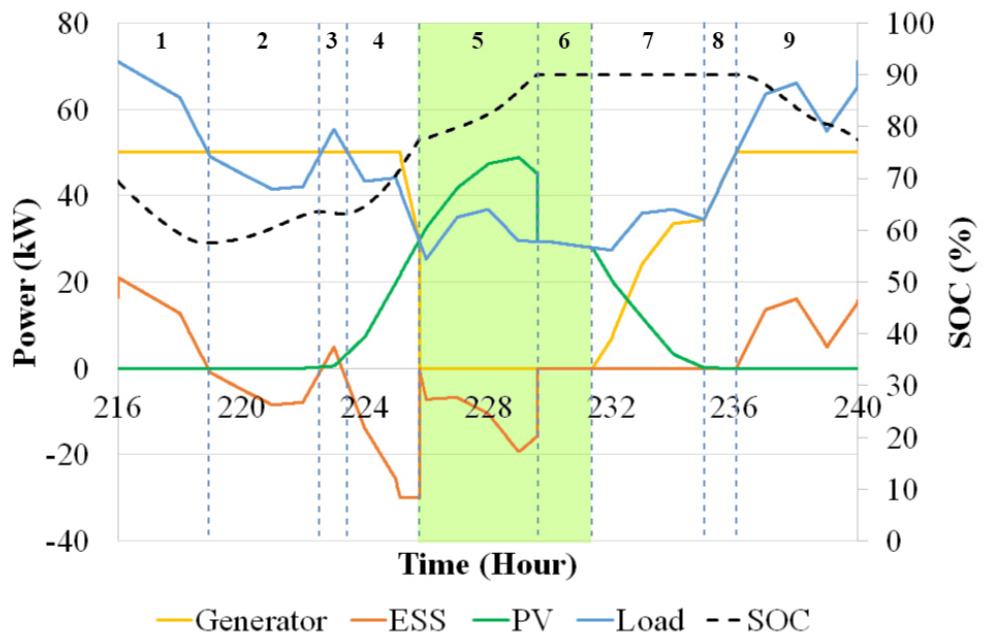


(c)

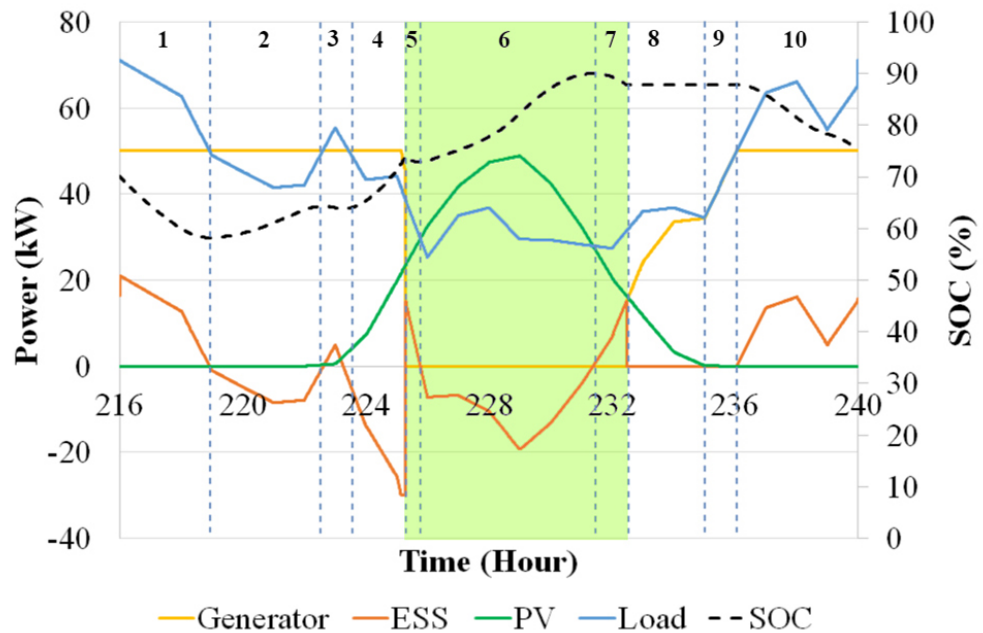
**Figure 5.13: Low solar irradiance operation in (a) load following (b) cycle charging (c) fuzzy control**



(a)



(b)



(c)

**Figure 5.14: High solar irradiance operation in (a) load following (b) cycle charging (c) fuzzy control**

It is shown that the switch-off time of the generator is prolonged by the fuzzy control dispatch strategy as compared to that by the load following and cycle charging dispatch strategy. Although the switch-off time is prolonged, the SOC of ESS is sustained at the correct level by the generator and the PV system such that the balance between the power supply and load demand is maintained at all times. With the prolonged switch-off time of the generator, the amount of diesel fuel and generator replacement units required are reduced. This causes the cost COE to be lower than that of the load following and cycle charging dispatch strategies.

## **5.4. Economic Considerations**

This section aims to provide an in depth analysis of the economic parameters considered for all the systems simulated. The economic parameters include the NPC, COE, payback period, as well as the ROI. Other than that, the costs associated with different systems will be investigated and analysed. Although the COE is used as a metric for the feasibility of the system, it is beneficial to also consider other economic parameters involved as they highly influence the value of the COE produced.

An analysis of the economic performance of all the systems simulated are provided in this section. They include the generator-PV, generator-ES, PV-ESS, as well as the generator-PV-ESS system in various dispatch strategies.

### **5.4.1. Economic Analysis of Generator-PV System**

In the generator-PV system, the generator size is fixed at 80 kW, as it needs to meet the peak load demand entirely. This is because the PV peak power output happens on a different time period than that of the peak load demand. Hence, the generator needs to be sized to fully meet the peak load demand.

Table 5.4 shows the summary of the economic parameters of the generator-PV system. In the table, the various parameters included covers the COE, fuel cost

per year, generator runtime per year, as well as generator replacement required within the whole project lifetime.

**Table 5.4: Economic analysis for generator-PV system**

PV size (kW)	COE (\$/kWh)	Fuel cost (\$/year)	Generator runtime (hour/year)	Generator replacement (unit/lifetime)
10	0.2219	58412	8640	14
20	0.2207	56156	8640	14
30	0.2203	53886	8640	14
40	0.2199	51614	8626	14
50	0.2194	49489	8316	13
60	0.2170	47965	7369	12
70	0.2111	47015	6665	11
80	0.2098	46487	6367	10
90	0.2120	46036	6266	10
100	0.2158	45632	6178	10
110	0.2196	45268	6100	10
120	0.2236	44936	6031	10

Figure 5.15 shows the plotted COE values when the PV size of the system is varied in a generator-PV system.

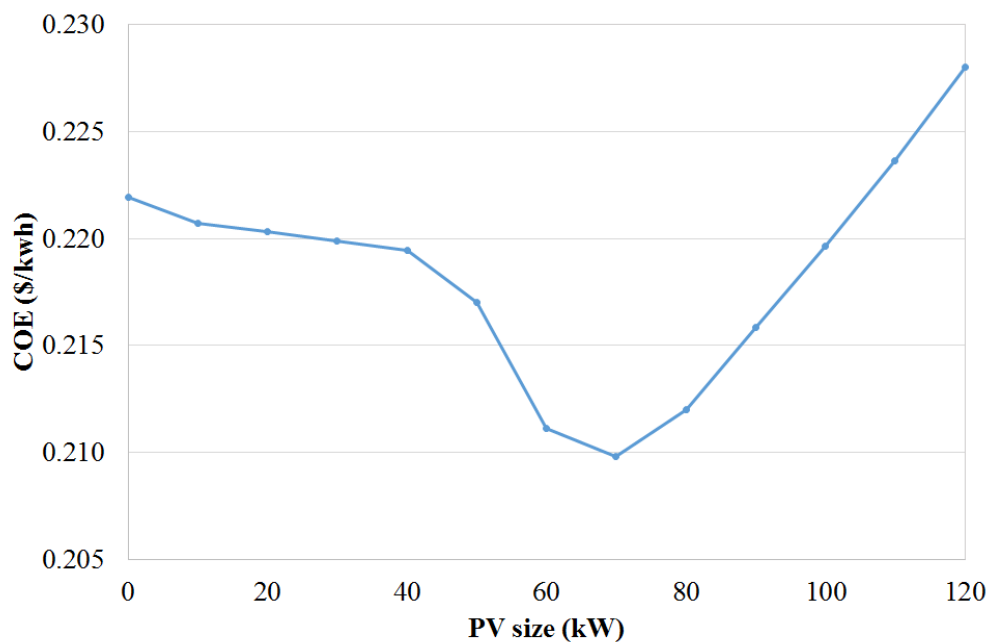


**Figure 5.15: COE of generator-PV system**

The trend is such that when PV size increase up to 70 kW, COE of the system decreases. This scenario happens because as PV size increases, the generator runtime decreases, causing a decrease in the number of generator replacements needed as well as the decrease in fuel cost incurred.

However, when PV size is past 70 kW, COE values increase steadily. The increase in COE values past the PV size of 70 kW can be explained using Figure 5.16, where the relationship between the generator runtime and generator replacement is outlined.

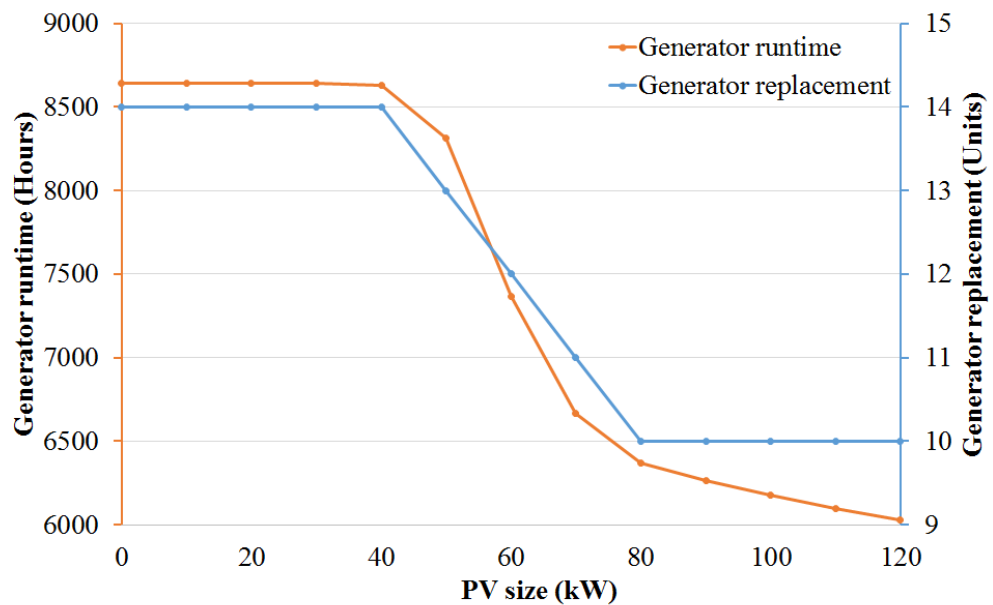


**Figure 5.16: Generator runtime vs generator replacement**

As it can be seen, as generator runtime decreases from PV of 40 kW onwards, the generator replacement units decrease as well. However, from PV of 70 kW to 120 kW, the decrease in generator runtime is not significant enough to warrant a lower number of generator replacement units. It can be seen that for PV size of 80 to 120 kW, generator replacement units remain at 10 units.

#### 5.4.2. Economic Analysis of Generator-ESS System

In the generator-ESS system, various ESS and generator sizes are simulated. The ESS size ranges from 1 to 15 strings while generator sizes simulated are 40 to 70 kW. Based on simulation, it is found that the systems using generator size of 40 kW could not meet the load demand. Only generators with the size of 50, 60 and 70 kW are technically feasible to meet the load demand. The COE values for the generator-ESS system is shown in Table 5.5.

**Table 5.5: COE values for generator-ESS system**

ESS Size (strings)	Generator Size (kW)		
	50	60	70
1	-	0.1997	0.2114
2	-	0.2026	0.2143
3	0.2022	0.2055	0.2173
4	0.2051	0.2085	0.2202
5	0.2080	0.2114	0.2231
6	0.2110	0.2143	0.2260
7	0.2139	0.2172	0.2290
8	0.2168	0.2201	0.2319
9	0.2197	0.2231	0.2348
10	0.2227	0.2260	0.2377
11	0.2256	0.2289	0.2406
12	0.2285	0.2318	0.2436

The empty COE values for generator size of 50 kW when ESS size of 1 and 2 strings are used and it indicates that they are technically not feasible to meet the load demand.

### 5.4.3. Economic Analysis PV-ESS System

In the PV-ESS system, various PV and ESS string sizes are simulated. Table 5.6 shows the COE values for the PV-ESS system.

**Table 5.6: COE values for PV-ESS system**

ESS Size (strings)	PV Size (kW)							
	260	270	280	290	300	310	320	330
25		0.2558	0.2612	0.2684	0.2757	0.2829	0.2901	0.2956
26		0.2587	0.2641	0.2714	0.2786	0.2858	0.2930	0.2985
27		0.2616	0.2671	0.2743	0.2815	0.2887	0.2959	0.3014
28		0.2645	0.2700	0.2772	0.2844	0.2916	0.2988	0.3043
29		0.2674	0.2729	0.2801	0.2873	0.2945	0.3017	0.3072
30		0.2703	0.2758	0.2830	0.2902	0.2974	0.3046	0.3101
31		0.2732	0.2787	0.2859	0.2931	0.3003	0.3075	0.3130
32	0.2690	0.2762	0.2817	0.2889	0.2961	0.3033	0.3105	0.3160
33	0.2719	0.2791	0.2846	0.2918	0.2990	0.3062	0.3134	0.3189
34	0.2748	0.2820	0.2875	0.2947	0.3019	0.3091	0.3163	0.3218
35	0.2777	0.2849	0.2904	0.2976	0.3048	0.3120	0.3192	0.3247
36	0.2806	0.2878	0.2933	0.3005	0.3077	0.3149	0.3221	0.3276
37	0.2835	0.2907	0.2962	0.3034	0.3106	0.3178	0.3250	0.3305
38	0.2864	0.2936	0.2991	0.3063	0.3135	0.3207	0.3279	0.3334
39	0.2893	0.2965	0.3020	0.3092	0.3164	0.3236	0.3308	0.3363
40	0.2922	0.2994	0.3049	0.3121	0.3193	0.3265	0.3337	0.3392

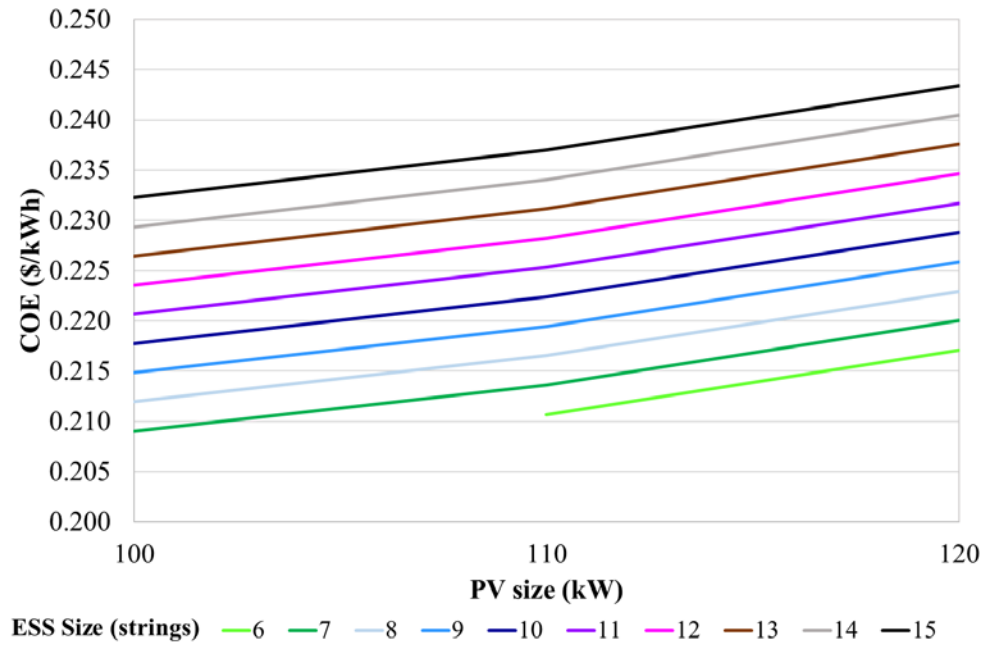
The minimum ESS size required at a PV size of 260 kW is at 32 strings. Meanwhile, for PV size of 270 kW onwards the minimum ESS size required is at 25 strings. It can be observed that PV and ESS size requirement in this system is higher compared to all the previous systems. This is because PV outputs power only during a certain period of time during the day. On periods without PV output, the ESS solely supplies to meet the load demand. This also means that there has to be enough excess PV output which can be charged into the ESS, and can be further discharged to meet the load demand when PV is not supplying power. The PV-ESS system which has the lowest COE is the system having a PV of 270 kW and ESS size of 25 strings, at a COE of 0.2558 \$/kWh.

### **5.5. Economic Analysis of Generator-PV-ESS System**

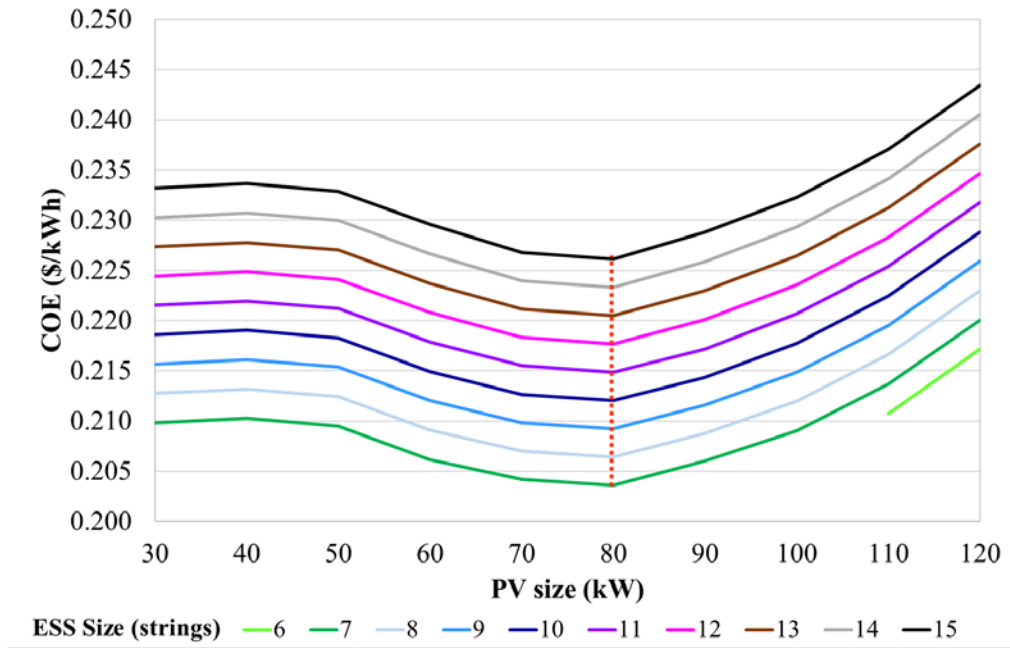
The results for the generator-PV-ESS system using load following and cycle charging dispatch strategies are presented in this section. The results using generator sizes of 40, 50, 60 kW were presented. The PV sizes considered are from 30-120 kW with 10 kW step size, while the ESS sizes considered are 3-15 strings with 1 string step size in between.

### 5.5.1. Generator Size at 40 kW

Figure 5.17 (a) and (b) shows the COE values for a generator-PV-ESS system with generator size of 40 kW, under the load following and cycle charging dispatch strategies.



(a)



(b)

**Figure 5.17: COE values for 40 kW generator (a) load following (b) cycle charging**

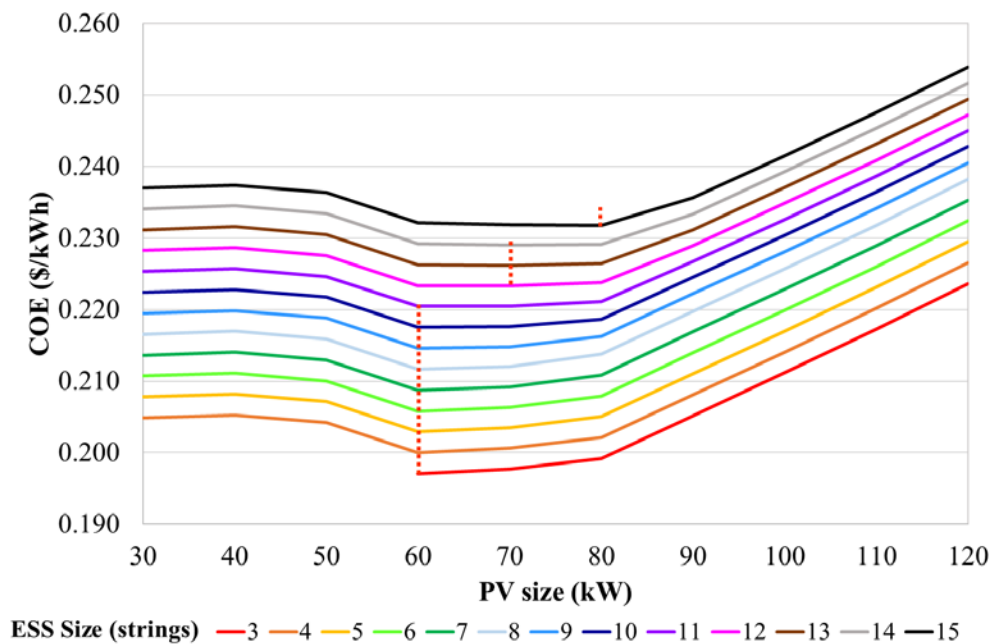
In Figure 5.17 (a), with the load following strategy operation at 40 kW generator size, the minimum ESS size required to meet the load demand is 7 strings at 100 kW PV size. At PV size of 110 kW and 120 kW, minimum ESS size is at 6 strings. There are a total of 29 PV- ESS string size combinations which are able to meet the load demand. The lowest COE attained by this system is at 0.2091 \$/kWh, which is achieved by having ESS size of 7 strings and PV size of 100 kW. The highest COE attained is 0.2434 \$/kWh when ESS size of 15 strings and PV size of 120 kW is used.

Meanwhile in Figure 5.17 (b), for the system in cycle charging strategy at minimum ESS size of 6 strings, only PV size of 110 kW and 120 kW are able to meet the load demand. At ESS size of 7 strings and above, all the PV sizes

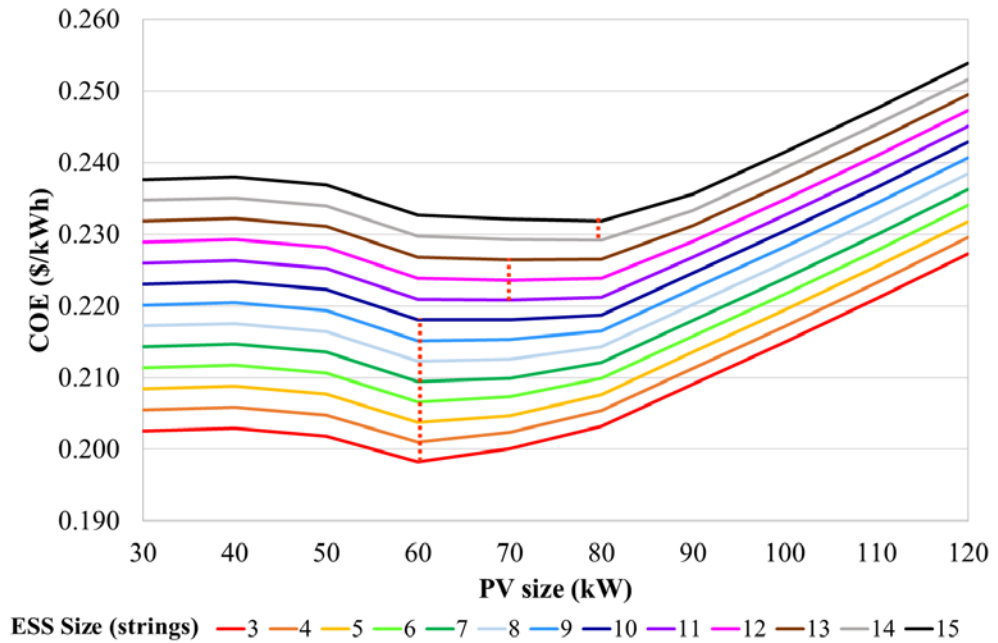
from 30-120 kW are able to meet the load demand. In total, there are 58 PV-ESS string size combinations which could not meet the load demand. The lowest COE attained by this system is at 0.2036 \$/kWh, which is achieved by having ESS size of 7 strings and PV size of 80 kW. The highest COE attained is 0.2435 \$/kWh when ESS size of 15 strings and PV size of 120 kW is used. Across the ESS size from 7- 15 strings, it is found that the lowest COE achieved at any ESS string size happens when PV size is at 80 kW. Above PV size of 80kW, COE increases across all ESS string size.

### 5.5.2. Generator Size at 50 kW

Figure 5.18 (a) and (b) shows the COE values for a generator-PV-ESS system with generator size of 50 kW, under the load following and cycle charging dispatch strategies.



(a)



(b)

**Figure 5.18: COE values for 50 kW generator (a) load following (b) cycle charging**

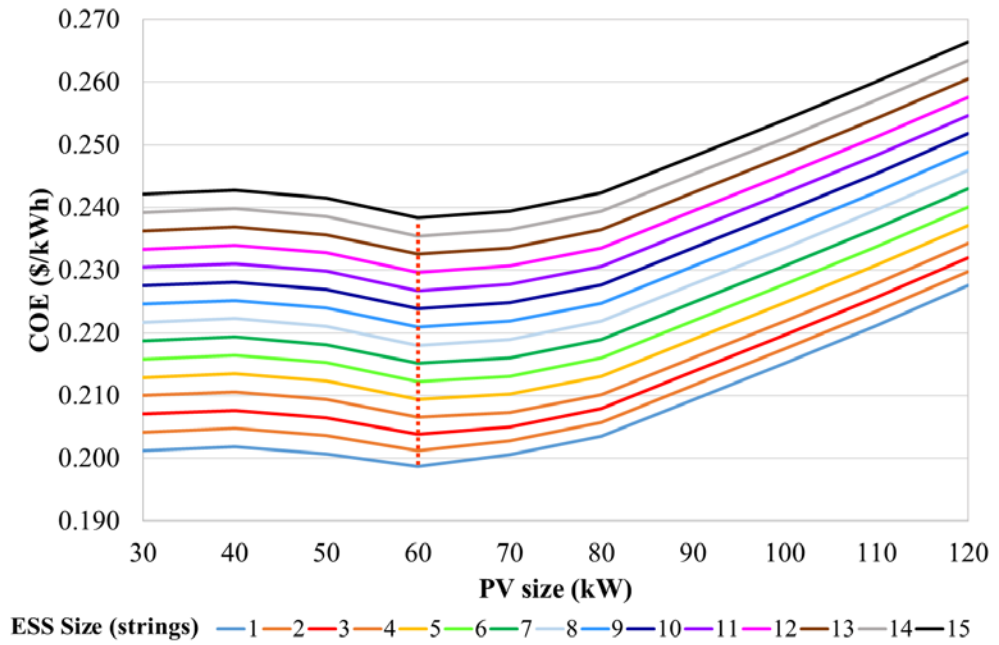
When generator size of 50 kW is used, the system in either load following or cycle charging strategy has a minimum ESS string size of 3 strings. ESS size of 1 and 2 strings are not able to meet the load demand. As shown in Figure 5.18 (a), using the load following strategy at ESS size of 3 strings, the minimum PV size is at 60 kW. For ESS size of 4 strings onwards, PV size of 30- 120 kW are able to meet the load demand. There are a total of 127 PV-ESS string size combinations which are able to meet the load demand. The lowest COE attained by this system is at 0.1971 \$/kWh, which is achieved by having ESS size of 3 strings and PV size of 60 kW. The highest COE attained is 0.2539 \$/kWh when ESS size of 15 strings and PV size of 120kW is used. For ESS size of 3 to 11 strings, the lowest COE achieved is at PV size is at 60 kW. From ESS size of

12 to 14 strings, lowest COE achieved is when PV of 70 kW is used. At ESS size of 15 strings, lowest COE is achieved at PV size of 80 kW.

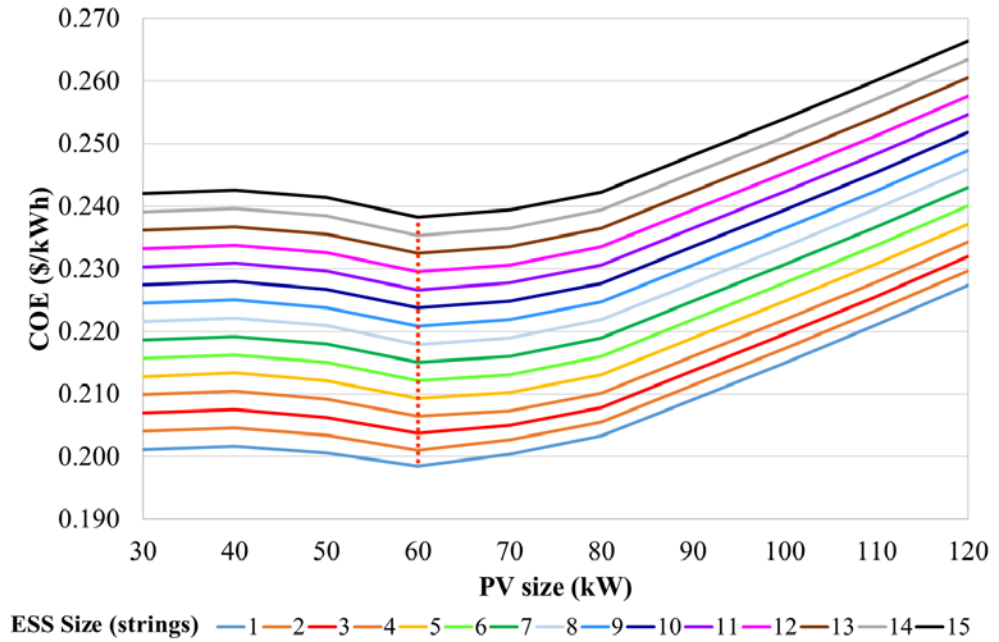
For the system in cycle charging strategy as shown in Figure 5.18 (b), the lowest COE attained by this system is at 0.1983 \$/kWh, which is achieved by having ESS size of 3 strings and PV size of 60 kW. The highest COE attained is 0.2539 \$/kWh when ESS size of 15 strings and PV size of 120 kW is used. Across the ESS size from 3 to 10 strings, it is found that the lowest COE achieved at any ESS string size happens when PV size is at 60 kW. From ESS size of 11- 13 strings, lowest COE achieved is when PV of 70 kW is used. At ESS size of 14 and 15 strings, lowest COE is achieved at PV size of 80 kW. There are a total of 130 PV-ESS string size combinations which are able to meet the load demand, with 3 more extra feasible combinations compared to that in load following strategy.

### **5.5.3. Generator Size at 60 kW**

Figure 5.19 (a) and (b) shows the COE values for a generator-PV-ESS system with generator size of 60kW under the load following and cycle charging dispatch strategies.



(a)



(b)

**Figure 5.19: COE values for 60 kW generator (a) load following (b) cycle charging**

When generator with a size of 60 kW is used, all the ESS and PV size combinations are able to fully meet the load demand. When the system is

operated in load following strategy, the lowest COE attained by this system is at 0.1987 \$/kWh, which is achieved by having ESS size of 1 string and PV size of 60 kW. The highest COE attained is 0.2664 \$/kWh when ESS size of 15 strings and PV size of 120 kW is used. Across the ESS size from 1- 15 strings, it is found that the lowest COE achieved at any ESS string size happens when PV size is at 60 kW. Above PV size of 60 kW, COE increases across all ESS string size.

With the system in cycle charging strategy, the lowest COE attained by this system is at 0.1985 \$/kWh, which is achieved by having ESS size of 1 string and PV size of 60 kW. The highest COE attained is 0.2664 \$/kWh when ESS string size of 15 and PV size of 120 kW is used. Across the ESS size from 1 to 15 strings, it is found that the lowest COE achieved at any ESS string size happens when PV size is at 60 kW. Above PV size of 60 kW, COE increases across all ESS string size.

#### **5.5.4 Economic Comparison for Load Following and Cycle Charging**

The following section summarizes the performance of the load following and cycle charging strategy under generator size of 40, 50 and 60 kW. Table 5.7 and Table 5.8 summarizes various parameters for the load following and cycle charging dispatch strategies respectively, taking into account the system with the PV-ESS combination which produces the lowest COE under each generator size.

**Table 5.7: Economic summary for load following dispatch strategy**

	Standalone Generator	Load Following		
Generator Size (kW)	80	40	50	60
PV size (kW)	-	100	60	60
ESS size (strings)	-	7	3	1
Generator runtime (Hour/ Year)	8760	6193	7370	7370
Generator replacement (units)	14	10	12	12
Payback (year)	0	10.66	8.39	8.62
Fuel Cost (\$/ Year)	60,658	38,520	44,879	45,178
NPC (\$)	1,106,217	1,042,129	982,455	990,431
COE (\$/kWh)	0.2219	0.2091	0.1971	0.1987
% cost reduction	0	5.07	11.18	10.46

**Table 5.8: Economic summary for cycle charging dispatch strategy**

	Standalone Generator	Cycle Charging		
Generator Size (kW)	80	40	50	60
PV size (kW)	-	80	60	60
ESS size (strings)	-	7	3	1
Generator runtime (Hour/ Year)	8760	6368	7369	7369
Generator replacement (units)	14	10	12	12
Payback (year)	0	10.14	8.5	8.6
Fuel Cost (\$/ Year)	60,658	41,769	45,336	45,094
NPC (\$)	1,106,217	1,014,847	988,354	989,338

COE (\$/kWh)	0.2219	0.2036	0.1983	0.1985
% cost reduction	0	8.25	10.64	10.55

Among the parameters compared are the generator runtime, the corresponding generator replacement units, fuel cost incurred, payback period of the project, net present cost (NPC) and COE, as well as the percentage of cost reduction of each system against the standalone generator system.

As it can be seen, the standalone generator system has the highest NPC and COE values compared to that of the generator-PV-ESS system in load following and cycle charging dispatch strategies. With the generator running continuously, generator replacement units required throughout the project is the highest at 14 units. Comparing the various generator sizes for the system operating in load following strategy, the system which utilizes generator 50 kW has the lowest NPC and COE. This translates into the highest percentage cost reduction over the standalone generator system, which is at 11.18%. Although this configuration requires more generator replacement units and has a higher fuel cost compared to the configuration with 40 kW generator, the configuration at 50 kW still has a lower NPC and COE due to a smaller PV size required. The configuration at 50 kW generator requires a PV of 60 kW while that of the 40 kW requires a significantly larger PV size of 100 kW. It can also be noted that generator size increases, ESS size requirement decreases.

For the generator-PV-ESS system in cycle charging operation, the configuration with 50 kW generator also has the lowest NPC and COE compared to the

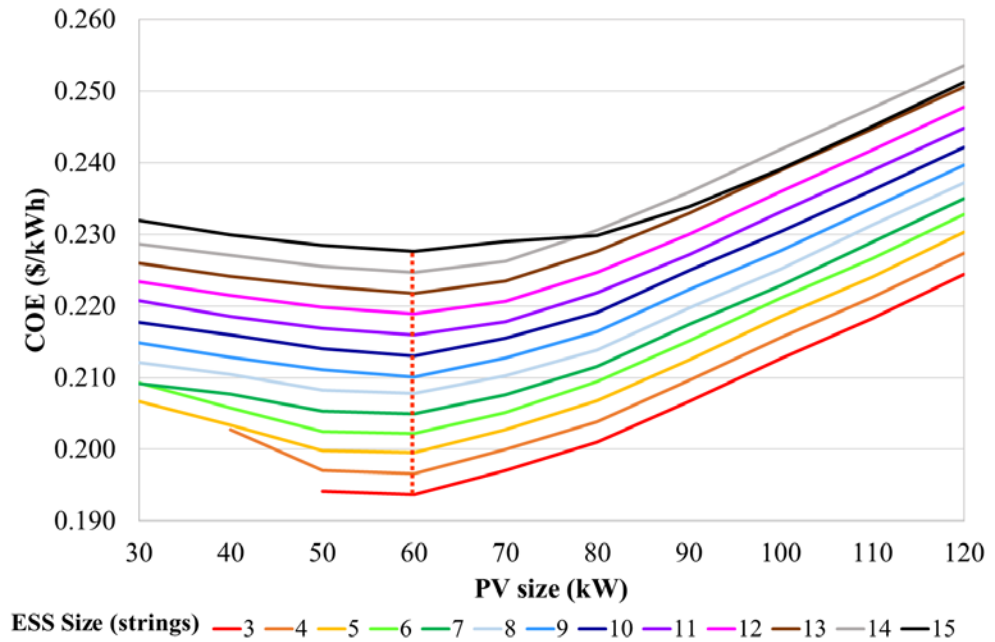
configuration with other generator sizes. Other than that, the configuration with 40 kW generator requires a lower PV size, which is at 80 kW compared to 100 kW PV size when load following operation is used. One explanation for this is that in cycle charging, ESS is charged by both the generator and PV, compared to ESS charging by PV only in load following dispatch strategy.

## **5.6 Fuzzy Control Dispatch Strategy**

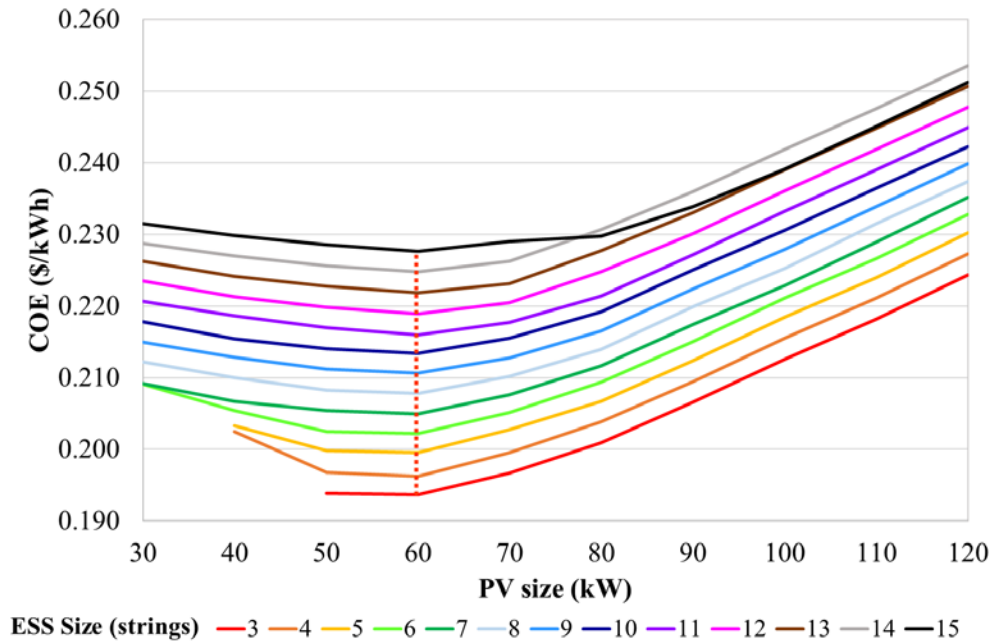
The following presents the economic results for the system in fuzzy control dispatch strategy. Instead of considering generator size of 40, 50, 60 kW for this dispatch strategy, only generator size of 50 kW is considered. This is because it has been found that generator of 50 kW produces the lowest COE compared to other sizes, in either load following or cycle charging dispatch strategy. The following section shows four different results when different combinations of membership functions and fuzzy rules are used. In this study, the two membership functions MF1 and MF2 are evaluated alongside with two fuzzy rules Rule 1 and Rule 2. Fuzzy 1: Rule 1-MF 1, Fuzzy 2: Rule 1-MF 2, Fuzzy 3: Rule 2-MF 1, Fuzzy 4: Rule 2-MF 2.

### 5.6.1 Economic Analysis of Fuzzy Control Dispatch Strategy

Figure 5.20 (a) and (b) shows the COE values for a generator-PV-ESS system in the fuzzy logic control dispatch strategy, under the Rule 1- MF 1 and Rule 1- MF 2 configuration respectively.



(a)



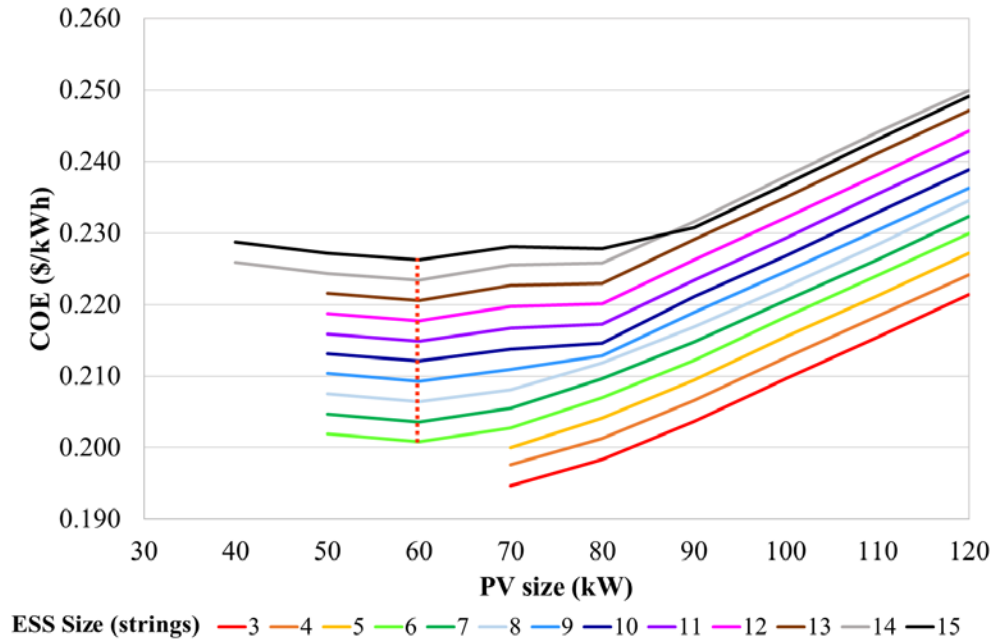
(b)

**Figure 5.20: Fuzzy control dispatch strategy (a) Rule 1- MF 1 (b) Rule 1- MF 2**

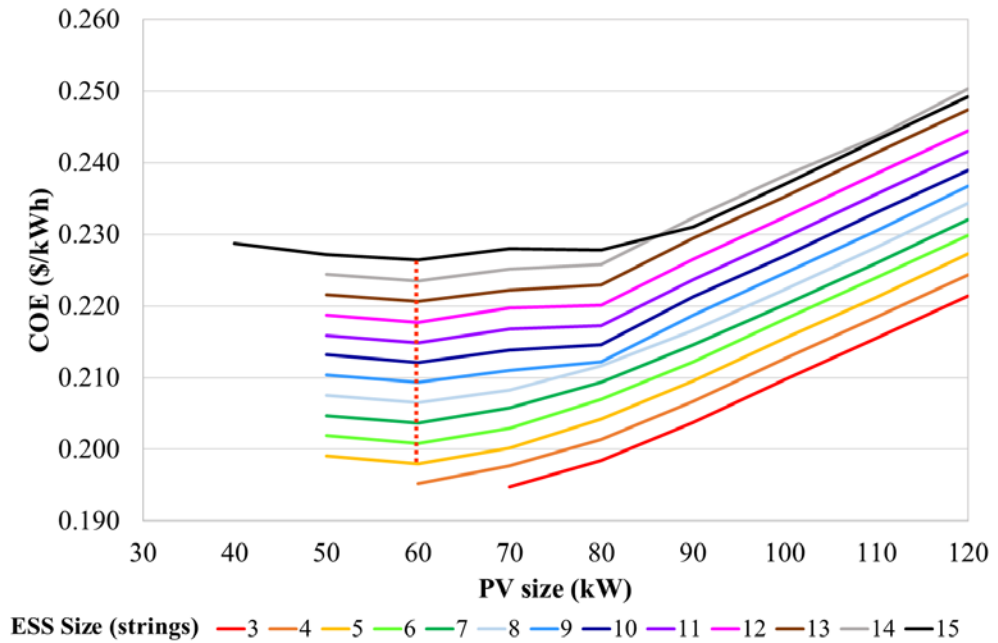
In the Rule 1- MF 1 configuration as shown in Figure 5.20 (a), it can be seen that the minimum COE obtained is at 0.1936 \$/kWh. It is obtained at PV size of 60 kW and ESS size of 3 strings. The COE value achieved is lower than that using the load following or cycle charging dispatch strategy. As it can be observed, the best PV size across all ESS string size is at 60 kW, where minimum COE is achieved at their respective ESS sizes.

Meanwhile in the Rule 1- MF 2 configuration shown in Figure 5.20 (b), the lowest COE achieved is at 0.1937 \$/kWh. It is also achieved when PV size is at 60 kW and ESS size at 3 strings. The lowest COE is achieved at PV size of 60 kW across all ESS string sizes. One observation which can be made is that there are 127 feasible combinations of PV-ESS in the Rule 1- MF 1 configuration,

compared to 126 feasible combinations in Rule 1- MF 2 configuration. Figure 5.21 (a) and (b) shows the COE values for a generator-PV-ESS system in the fuzzy control dispatch strategy under the Rule 2- MF 1 and Rule 2-MF 2 configuration respectively.



(a)



(b)

**Figure 5.21: Fuzzy control dispatch strategy (a) Rule 2- MF 1 (b) Rule 2- MF 2**

In the Rule 2- MF 1 and Rule 2- MF 2 configuration as shown in Figure 5.21 (a) and (b) respectively, it can be seen that the minimum COE obtained for both the fuzzy configuration is at 0.1947 \$/kWh. It is obtained at PV size of 70 kW and ESS size of 3 strings. The COE value achieved is lower than that using the load following or cycle charging strategy. In the Rule 2- MF 1 configuration, at ESS size of 6 strings onwards, the best PV size across all ESS string size is at 60 kW, where minimum COE is achieved at their respective ESS sizes.

Meanwhile for that of the Rule 2- MF 2 configuration, PV size of 60 kW produces the lowest COE at ESS size of 5 strings onwards. One observation which can be made is that there are 100 feasible combinations of PV-ESS in the Rule 2- MF 1 configuration, compared to 102 feasible combinations in Rule 2- MF 2 configuration. Comparing configurations using Rule 1 and Rule 2, fuzzy

configurations which uses Rule 1 tend to have more feasible combinations of PV-ESS as compared to that which uses Rule 2.

### 5.6.2 Economic Comparison for Fuzzy Control Dispatch Strategy

The following section summarizes the performance of all the fuzzy control dispatch strategy configuration used. There are a total of four different fuzzy control configurations, which is formed from two different fuzzy rules and membership functions respectively. The comparison is summarized in Table 5.9 where the PV-ESS combinations under different fuzzy control configurations which produce the lowest COE is compared.

**Table 5.9: Economic summary of fuzzy control dispatch strategy**

	Standalone Generator	Rule 1- MF 1	Rule 1- MF 2	Rule 2- MF 1	Rule 2- MF 2
Generator size (kW)	80	50	50	50	50
PV size (kW)	-	60	60	70	70
ESS size (strings)	-	3	3	3	3
ESS size (kWh)	-	166.56	166.56	166.56	166.56
Converter size (kW)	-	30	30	40	40
Payback (year)	0	8.27	8.27	8.56	8.56
Fuel Cost (\$ USD/year)	60,658	45,283	45,303	43,419	43,437
Generator runtime (Hours/year)	8760	6235	6223	5945	5954
Generator replacement (units)	14	10	10	9	9
NPC (\$USD)	1,106,217	965,261	965,395	970,368	970,694

COE (\$ USD/kWh)	0.2219	0.1936	0.1937	0.1947	0.1947
CO <sub>2</sub> emission (kg)	461,528	344,545	344,697	330,362	330,499
COE reduction (%)	0	12.74	12.71	12.28	12.25
CO <sub>2</sub> reduction (%)	0	25.35	25.31	28.42	28.39

As it can be seen, configurations which utilizes the Rule 1 has a lower PV size requirement at 60 kW, compared to those of Rule 2 which has a PV size requirement of 70 kW. All four fuzzy configurations have a ESS size requirement of 3 strings. Other than that, configurations which utilizes Rule 2 have lower generator runtime hours, which leads to a lower number of generator replacement units required over the project lifetime. It can also be seen that the configurations with Rule 2 has a lower fuel consumption cost over that of Rule 1. Among all the four fuzzy control strategy configurations, the Rule 1- MF 1 configuration produces a system with the lowest NPC and COE. With a NPC of \$965,261 and a COE of \$ 0.1936/kWh, it represents a 12.74% of cost reduction over that of the standalone generator system. In terms of payback period for the system, the configuration which utilizes Rule 1 has a payback period of 8.3 years, versus 8.6 years of the configurations utilising Rule 2.

Although configurations based on Rule 2 compared here has a lower fuel cost and lower number of generator replacement units required, they still fail to produce a lower NPC and COE than the configurations based on Rule 1. This is due to the fact that configurations using Rule 2 require a PV size of 70 kW compared to that of Rule 1, which is at PV size of 60 kW. With the PV being

the most expensive component in the system, any increase in PV size requirement will significantly increase the NPC and COE of the system.

## **5.7 Fuzzy Control Dispatch Strategy Using Different Load Profiles**

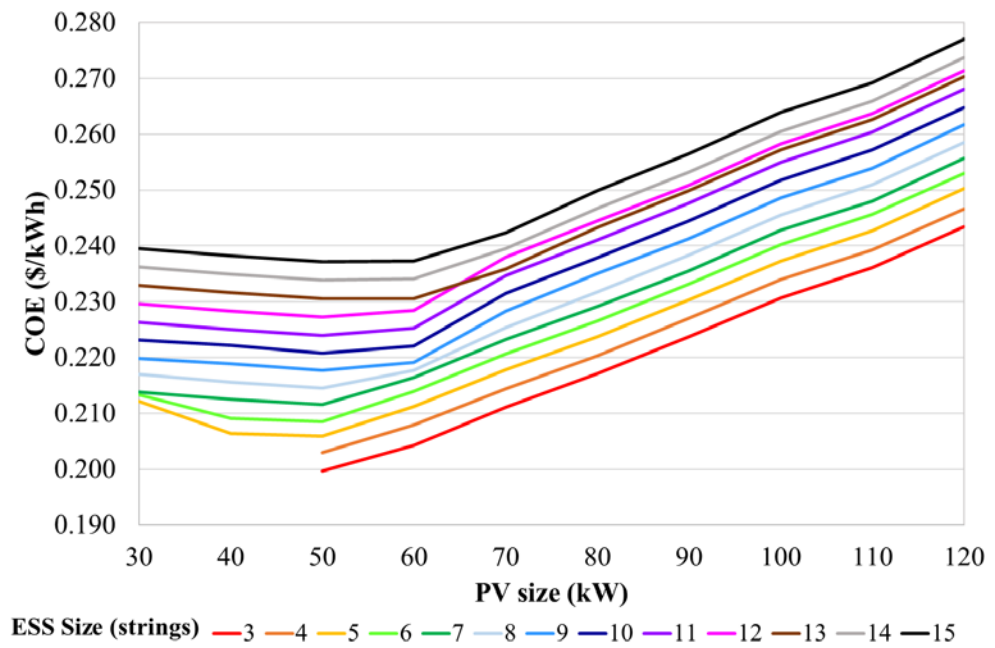
Using the other two extra load profiles defined in Chapter 3, the generator-PV-ESS is implemented using the fuzzy control dispatch strategy. The two extra load profiles are the load profile 2 and load profile 3. Both of these load profiles are used to validate and compare the initial findings obtained when using load profile 1 in the fuzzy control dispatch strategy. It is also important that the fuzzy control dispatch strategy developed will also work in other types of load profile and must be proven to be able to work in different kinds of scenarios.

### **5.7.1 Fuzzy Control Dispatch Strategy in Load Profile 2**

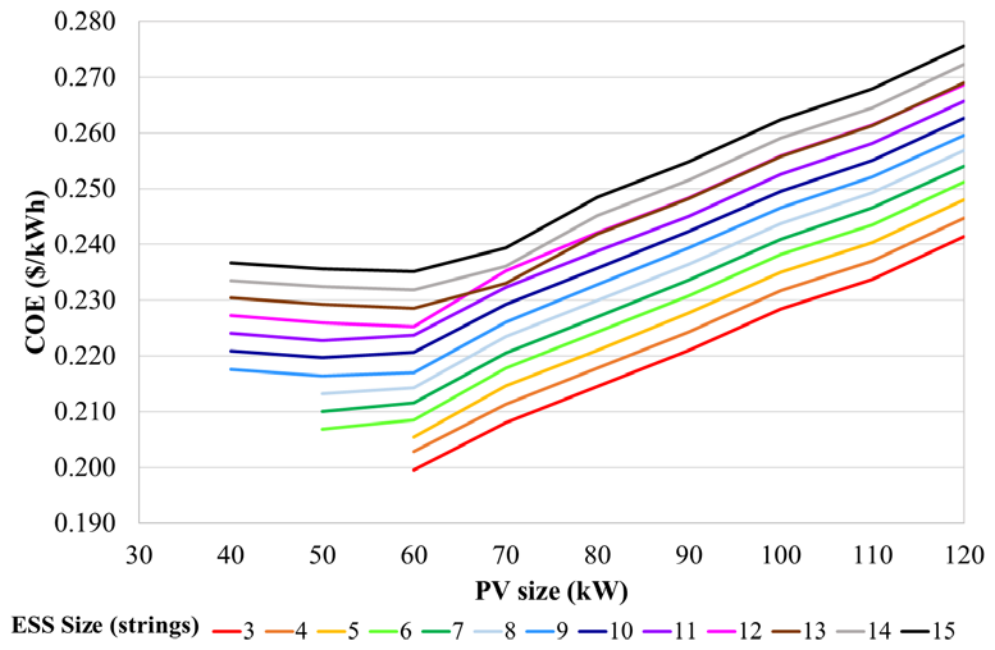
Table 5.10 shows the economic performance of the generator-PV-ESS system under fuzzy control dispatch strategy when compared to the standalone generator system, under load profile 2. It can be seen that the Rule 2- MF 1 fuzzy configuration produced the lowest percentage cost reduction of 13.9% compared to standalone generator system. Figure 5.22 shows all the COE values at different size of PV and ESS.

**Table 5.10: Economic comparison between standalone diesel generator system and generator-PV-ESS system using fuzzy control dispatch strategy for load profile 2**

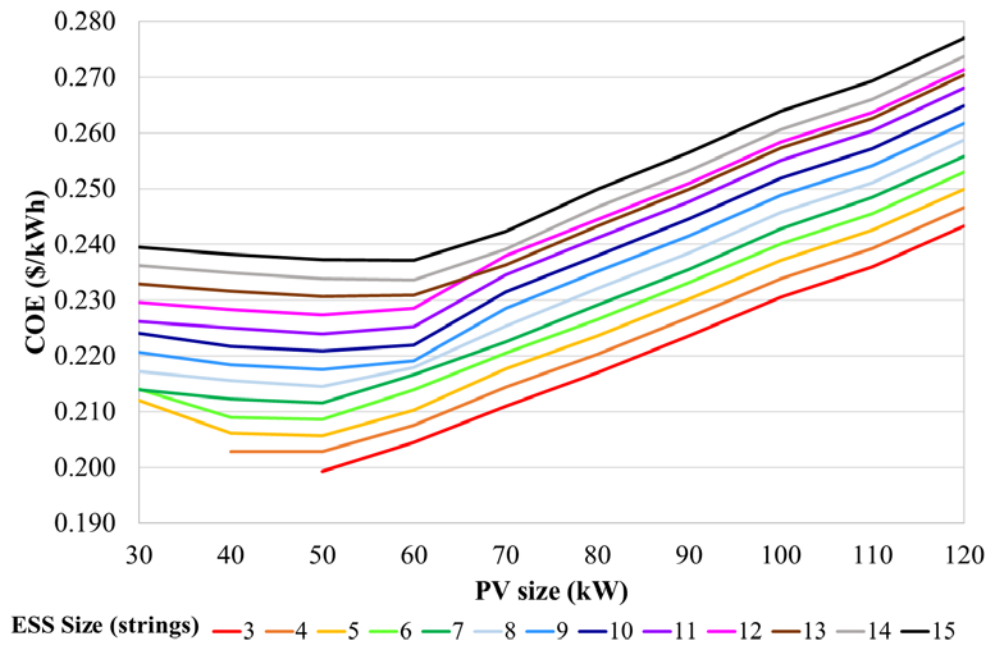
	Standalone Generator	Rule 1- MF 1	Rule 1- MF 2	Rule 2- MF 1	Rule 2- MF 2
PV size (kW)	-	50	60	50	60
ESS size (strings)	-	3	3	3	3
COE (\$/kWh)	0.2316	0.1997	0.1996	0.1994	0.1997
Fuel Cost (\$)	54045	41209	39590	41213	39601
% cost reduction	-	13.77	13.82	13.90	13.77



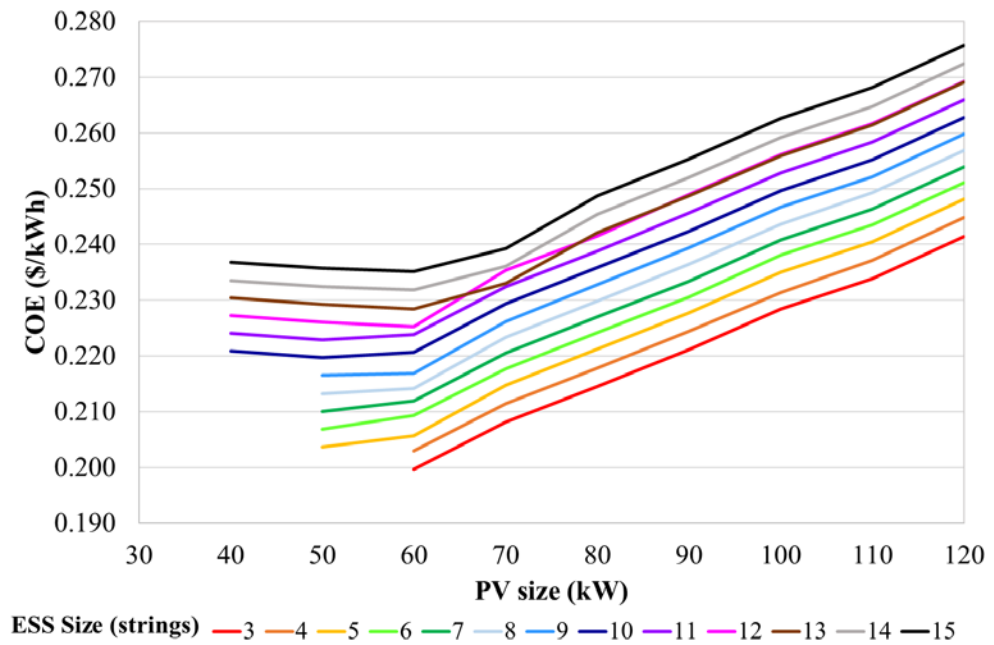
(a)



(b)



(c)



(d)

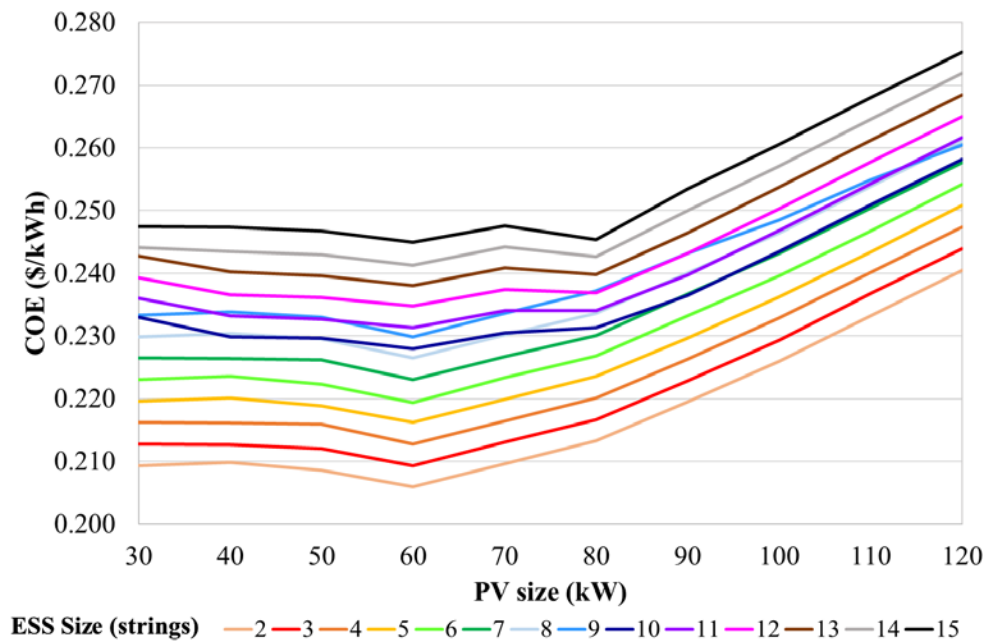
**Figure 5.22: COE values obtained with fuzzy control dispatch strategy in load profile 2 (a) Rule 1-MF 1 (b) Rule 1-MF 2 (c) Rule 2-MF 1 (d) Rule 2-MF 2**

### 5.7.2 Fuzzy Control Dispatch Strategy in Load Profile 3

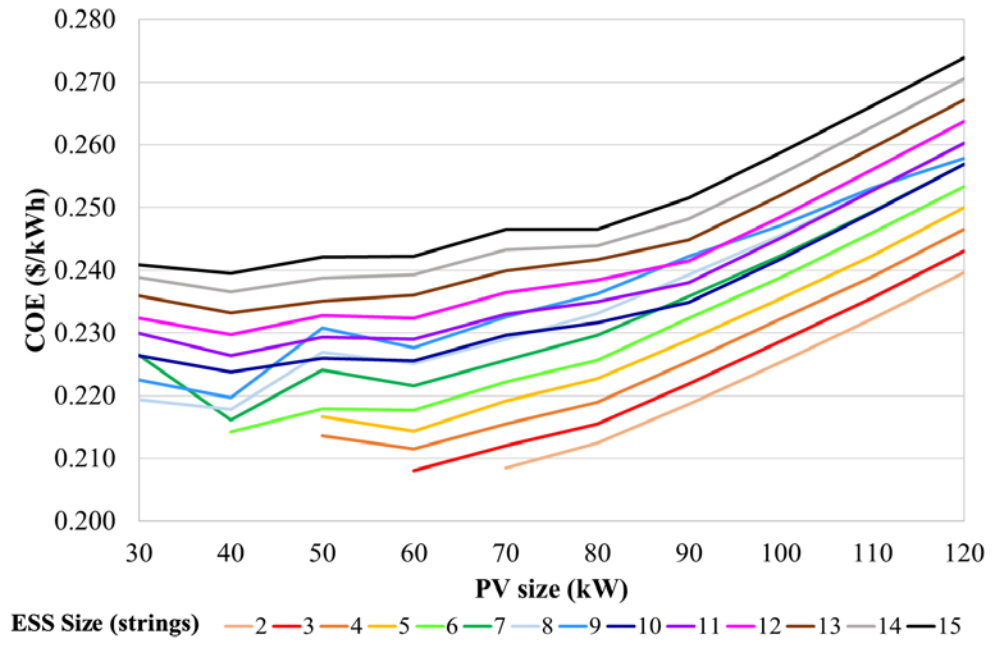
Table 5.11 shows the economic performance of the generator-PV-ESS system under fuzzy control dispatch strategy when compared to the standalone generator system, under load profile 3. It can be seen that the Rule 2- MF 2 fuzzy configuration produced the lowest percentage cost reduction of 13.06 % compared to standalone generator system. Figure 5.23 shows all the COE values at different size of PV and ESS.

**Table 5.11: Economic comparison between standalone diesel generator system and generator-PV-ESS system using fuzzy control dispatch strategy for load profile 3**

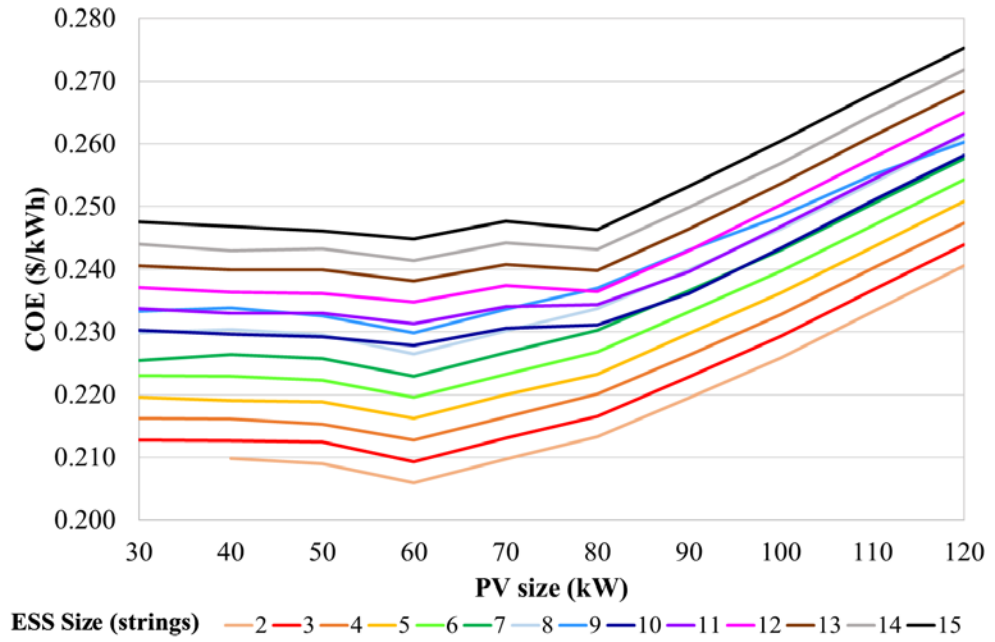
	Standalone Generator	Rule 1- MF 1	Rule 1- MF 2	Rule 2- MF 1	Rule 2- MF 2
PV size (kW)	-	60	70	60	60
ESS size (strings)	-	2	2	2	3
COE (\$/kWh)	0.2359	0.2059	0.2085	0.2059	0.2051
Fuel Cost (\$)	53706	38548	37669	38548	38417
% cost reduction	-	12.72	11.62	12.72	13.06



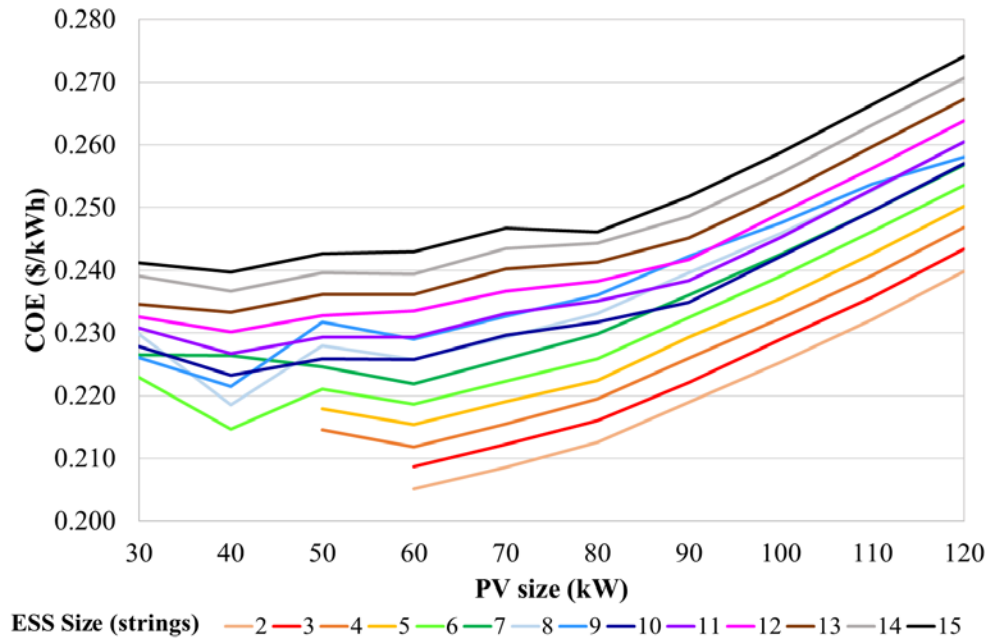
(a)



(b)



(c)



(d)

**Figure 5.23: COE values obtained with fuzzy control dispatch strategy in load profile 3 (a) Rule 1-MF 1 (b) Rule 1-MF 2 (c) Rule 2-MF 1 (d) Rule 2-MF 2**

## 5.8 Summary

Various types of HES systems have been developed in this study. They are the generator-PV, generator-ESS, PV-ESS, and the generator-PV-ESS system. All the different types of HES were compared in terms of its operation, as well as the COE value of each system.

Two dispatch strategies were developed for the generator-PV-ESS system and they are the load following and cycle charging dispatch strategies. Between the load following and cycle charging dispatch strategy, it can be seen that the

system with generator size of 50 kW in cycle charging dispatch strategy has the lowest COE and shows a 10.65% COE reduction over the standalone generator system. Using the fuzzy control dispatch strategy, further improvements in COE reduction is observed. A total of four fuzzy configurations were developed using two different fuzzy rule and output membership function respectively. It is shown that the Rule 1- MF 1 fuzzy configuration produced the lowest COE and shows a 12.74% COE reduction compared to the standalone generator system. As a conclusion, the fuzzy control dispatch strategy is better than the load following and cycle charging dispatch strategies. Furthermore, the developed fuzzy control dispatch strategy has been tested on another two different load profiles. Results obtained is promising, showing a COE reduction of 13.77% and 13.06% for load profile 2 and load profile 3 respectively.

## CHAPTER 6

### CONCLUSION AND FUTURE WORKS

#### 6.1 Conclusion

A novel fuzzy control dispatch strategy has been developed for the generator-PV-ESS system. The fuzzy control dispatch strategy is effective in reducing generator runtime, which contributes to a lower COE being produced. Prior to designing the fuzzy control dispatch strategy, various HES types were designed and evaluated and they include the generator-PV, generator-ESS, PV-ESS and generator-PV-ESS system. The generator-PV-ESS system produced the lowest COE among all the HES evaluated. The generator-PV-ESS system was initially simulated using the default load following and cycle charging strategy. Although it produces a good COE reduction compared to other HES types, the novel fuzzy control dispatch strategy developed in this study produced an even greater COE reduction over that of load following and cycle charging strategy.

In the fuzzy control dispatch strategy, the charging of the ESS can happen even before the PV power is in excess. During this condition, generator will be switched off. This in turn reduces the generator runtime and results in lesser generator replacement units needed. Other than that, another feature of the fuzzy control dispatch strategy is such that it is able to utilise forecasted PV output

and ensure ESS has enough capacity to store excess PV. This reduces the wastage of PV output due to deloading operation.

These are the conclusion which can be drawn:

*1. To determine the optimal size for each component in the HES*

In this study, a wide range of component sizes are first defined. The simulation performed will use these values of component sizes and COE will be calculated based on output data obtained from each of the simulation such as generator runtime, fuel consumption, and ESS throughput. If by any chance that a particular size combination of components results in an unmet load, that particular combination will be considered as not feasible and COE will not be calculated for that particular combination. Optimal size of components has been determined for all HES types.

*2. To develop control strategies for the operation of HES to achieve a minimal cost of energy*

Control strategies for different types of HES has been developed, and these HES include the generator-PV, generator-ESS, PV-ESS and the generator-PV-ESS system. All the HES was developed and modelled in Matlab Simulink, alongside their respective control strategies. HES with two energy sources such as the generator-PV, generator-ESS and PV-ESS has a relatively low complexity in terms of its control strategy. However, in HES which has more than two energy sources such as the generator-PV-ESS system, the control strategy is generally more complex. The widely used load following and cycle

charging dispatch strategy is developed for the generator-PV-ESS system. Other than that, a novel fuzzy control dispatch strategy is developed for the generator-PV-ESS system. The fuzzy control dispatch strategy is effective in reducing the generator switch-on time and hence produces a lower COE. In designing the optimal fuzzy control dispatch strategy, two different fuzzy rules and output membership functions were used respectively, giving a total of four different fuzzy control configurations. The resultant COE of using these different fuzzy control configurations were further compared in order to obtain the system with the lowest COE.

*3. To evaluate the performance of the control strategies developed for the HES*

The control strategies were evaluated based on its technical feasibility and economic feasibility. In evaluating the technical feasibility of the control strategies, various operating condition and scenarios were used to analyse the operation of the system. For example, the operation of the HES were analysed in different operating conditions, such as conditions with varying levels of solar irradiance, and varying component sizes such as the PV and ESS.

Meanwhile, in evaluating the economic feasibility of HES, the COE obtained of each types of HES under various component sizes and dispatch strategies were compared. It is found that the generator-PV-ESS system produces the lowest COE compared to other HES such as the generator-PV, generator-ESS and PV-ESS system. A further evaluation on the generator-PV-ESS shows that the novel fuzzy control dispatch strategy developed in this study outperforms

the widely used dispatch strategies such as the load following and cycle charging dispatch strategy.

## **6.2 Limitation and Future Work**

Compared to the load following and cycle charging strategy, the fuzzy control dispatch strategy shows a better performance in terms of producing a system with a lower COE. However, there are improvements which can be done on the fuzzy controller in terms of the tuning of fuzzy parameters. In this study, a total of four different fuzzy configurations are used and their performance is compared against each other. Using more sophisticated fuzzy tuning methods, it is believed that the COE achieved could be even lower.

In this study, an ideal battery model is used where energy losses are not considered during charging and discharging operation of the ESS. If a more realistic battery model is used, a more accurate ESS lifetime can be obtained, which in turn produces a more accurate COE value. Energy losses were also not considered for components such as the bi-directional converter and PV inverter. In the future, energy losses in these components can be considered to obtain a more accurate COE calculation. Other than that, the simulation employed in this study has a simulation time of 30 days. In order to calculate COE of each system, the simulation results from the 30 day simulation is extrapolated to 365 days. The reason behind this is due to the long simulation time needed when simulation is run on a low specification computer.

While PV output forecasting is beyond the scope of this study, future works can include elements of PV output forecasting. A good PV forecasting feature will enable a more accurate COE to be obtained. Other than that, sensitivity analysis can be performed on parameters vital to the calculation of the COE, such as the diesel fuel price or the component price. These parameters can be varied in order to see how uncertainties can impact the COE of the system.

Other than that, the study deals with energy supply in rural residential areas and the fuzzy control dispatch strategy developed might not be optimal when used on a commercial type of load profile.

## LIST OF REFERENCES

- Abadlia, I., Bahi, T., Bouzeria, H., 2016. Energy management strategy based on fuzzy logic for compound RES/ESS used in stand-alone application. *Int. J. Hydrog. Energy* 41, 16705–16717. doi:10.1016/j.ijhydene.2016.07.120
- Abedi, S., Alimardani, A., Gharehpetian, G.B., Riahy, G.H., Hosseinian, S.H., 2012. A comprehensive method for optimal power management and design of hybrid RES-based autonomous energy systems. *Renew. Sustain. Energy Rev.* 16, 1577–1587. doi:10.1016/j.rser.2011.11.030
- Achievement & Awards [WWW Document], n.d. . TNB Energy Serv. URL <http://tnbes.com.my/achievement-awards/> (accessed 10.16.16).
- Adaramola, M.S., Paul, S.S., Oyewola, O.M., 2014. Assessment of decentralized hybrid PV solar-diesel power system for applications in Northern part of Nigeria. *Energy Sustain. Dev.* 19, 72–82. doi:10.1016/j.esd.2013.12.007
- Ajan, C.W., Ahmed, S.S., Ahmad, H.B., Taha, F., Mohd Zin, A.A.B., 2003. On the policy of photovoltaic and diesel generation mix for an off-grid site: East Malaysian perspectives. *Sol. Energy* 74, 453–467. doi:10.1016/S0038-092X(03)00228-7
- Al Busaidi, A.S., Kazem, H.A., Al-Badi, A.H., Farooq Khan, M., 2016. A review of optimum sizing of hybrid PV–Wind renewable energy systems in oman. *Renew. Sustain. Energy Rev.* 53, 185–193. doi:10.1016/j.rser.2015.08.039
- Al-Alawi, A., M Al-Alawi, S., M Islam, S., 2007. Predictive control of an integrated PV-diesel water and power supply system using an artificial neural network. *Renew. Energy* 32, 1426–1439. doi:10.1016/j.renene.2006.05.003
- Ameen, A.M., Pasupuleti, J., Khatib, T., 2015. Simplified performance models of photovoltaic/diesel generator/battery system considering typical control strategies. *Energy Convers. Manag.* 99, 313–325. doi:10.1016/j.enconman.2015.04.024
- Arun, P., Banerjee, R., Bandyopadhyay, S., 2008. Optimum sizing of battery-integrated diesel generator for remote electrification through design-space approach. *Energy* 33, 1155–1168. doi:10.1016/j.energy.2008.02.008
- Ashourian, M.H., Cherati, S.M., Mohd Zin, A.A., Niknam, N., Mokhtar, A.S., Anwari, M., 2013. Optimal green energy management for island resorts in Malaysia. *Energy* 51, 36–45. doi:10.1016/j.renene.2012.08.056
- Aziz, K.A., Shamsudin, K.N., 2013. TNB Experience in Developing Solar Hybrid Station at RPS Kemar, Gerik, Perak Darul Ridzuan. *IOP Conf. Ser. Earth Environ. Sci.* 16, 012145. doi:10.1088/1755-1315/16/1/012145
- Bala, B., Siddique, S.A., 2009. Optimal design of a PV-diesel hybrid system for electrification of an isolated island—Sandwip in Bangladesh using genetic algorithm. *Energy Sustain. Dev.* 13, 137–142. doi:10.1016/j.esd.2009.07.002

- Basir Khan, M.R., Jidin, R., Pasupuleti, J., Shaaya, S.A., 2015. Optimal combination of solar, wind, micro-hydro and diesel systems based on actual seasonal load profiles for a resort island in the South China Sea. *Energy* 82, 80–97. doi:10.1016/j.energy.2014.12.072
- Bernal-Agustín, J.L., Dufo-López, R., 2009. Simulation and optimization of stand-alone hybrid renewable energy systems. *Renew. Sustain. Energy Rev.* 13, 2111–2118. doi:10.1016/j.rser.2009.01.010
- Borhanazad, H., Mekhilef, S., Saidur, R., Boroumandjazi, G., 2013. Potential application of renewable energy for rural electrification in Malaysia. *Renew. Energy* 59, 210–219. doi:10.1016/j.renene.2013.03.039
- Borowy, B.S., Salameh, Z.M., 1996. Methodology for optimally sizing the combination of a battery bank and PV array in a wind/PV hybrid system. *IEEE Trans. Energy Convers.* 11, 367–375. doi:10.1109/60.507648
- Branker, K., Pathak, M.J.M., Pearce, J.M., 2011. A review of solar photovoltaic levelized cost of electricity. *Renew. Sustain. Energy Rev.* 15, 4470–4482. doi:10.1016/j.rser.2011.07.104
- C.D. Barley, 1996. Modeling and optimization of dispatch strategies for remote hybrid power systems. PhD Thesis.
- C.D. Barley, L.F.B.C.D., C.B. Winn, H.J.G., 1995. Optimal Control of Remote Hybrid Power Systems Part 1: Simplified Model, in: *Optimal Control of Remote Hybrid Power System Part 1: Simplified Model*. Presented at the Windpower 1995.
- Chedid, R., Rahman, S., 1997. Unit sizing and control of hybrid wind-solar power systems. *IEEE Trans. Energy Convers.* 12, 79–85. doi:10.1109/60.577284
- Chong, L.W., Wong, Y.W., Rajkumar, R.K., Isa, D., 2016. An optimal control strategy for standalone PV system with Battery-Supercapacitor Hybrid Energy Storage System. *J. Power Sources* 331, 553–565. doi:10.1016/j.jpowsour.2016.09.061
- Diaf, S., Diaf, D., Belhamel, M., Haddadi, M., Louche, A., 2007. A methodology for optimal sizing of autonomous hybrid PV/wind system. *Energy Policy* 35, 5708–5718. doi:10.1016/j.enpol.2007.06.020
- Dufo-López, R., Bernal-Agustín, J.L., 2005. Design and control strategies of PV-Diesel systems using genetic algorithms. *Sol. Energy* 79, 33–46. doi:10.1016/j.solener.2004.10.004
- Dufo-López, R., Bernal-Agustín, J.L., Yusta-Loyo, J.M., Domínguez-Navarro, J.A., Ramírez-Rosado, I.J., Lujano, J., Asó, I., 2011. Multi-objective optimization minimizing cost and life cycle emissions of stand-alone PV–wind–diesel systems with batteries storage. *Appl. Energy* 88, 4033–4041. doi:10.1016/j.apenergy.2011.04.019
- Fadaeenejad, M., Radzi, M.A.M., AbKadir, M.Z.A., Hizam, H., 2014. Assessment of hybrid renewable power sources for rural electrification in Malaysia. *Renew. Sustain. Energy Rev.* 30, 299–305. doi:10.1016/j.rser.2013.10.003
- Fossati, J.P., Galarza, A., Martín-Villate, A., Echeverría, J.M., Fontán, L., 2015. Optimal scheduling of a microgrid with a fuzzy logic controlled storage system. *Int. J. Electr. Power Energy Syst.* 68, 61–70. doi:10.1016/j.ijepes.2014.12.032

- Gallo, A.B., Simões-Moreira, J.R., Costa, H.K.M., Santos, M.M., Moutinho dos Santos, E., 2016. Energy storage in the energy transition context: A technology review. *Renew. Sustain. Energy Rev.* 65, 800–822. doi:10.1016/j.rser.2016.07.028
- Gan, L.K., Shek, J.K.H., Mueller, M.A., 2016. Optimised operation of an off-grid hybrid wind-diesel-battery system using genetic algorithm. *Energy Convers. Manag.* 126, 446–462. doi:10.1016/j.enconman.2016.07.062
- Gupta, A., Saini, R.P., Sharma, M.P., 2011. Modelling of hybrid energy system—Part II: Combined dispatch strategies and solution algorithm. *Renew. Energy* 36, 466–473. doi:10.1016/j.renene.2009.04.035
- Ismail, M.S., Moghavvemi, M., Mahlia, T.M.I., 2014. Genetic algorithm based optimization on modeling and design of hybrid renewable energy systems. *Energy Convers. Manag.* 85, 120–130. doi:10.1016/j.enconman.2014.05.064
- Jakhrani, A.Q., Rigit, A.R.H., Othman, A.K., Samo, S.R., Kamboh, S.A., 2012. Life cycle cost analysis of a standalone PV system, in: 2012 International Conference on Green and Ubiquitous Technology (GUT). Presented at the 2012 International Conference on Green and Ubiquitous Technology (GUT), pp. 82–85. doi:10.1109/GUT.2012.6344195
- Kaabeche, A., Ibtouen, R., 2014. Techno-economic optimization of hybrid photovoltaic/wind/diesel/battery generation in a stand-alone power system. *Sol. Energy* 103, 171–182. doi:10.1016/j.solener.2014.02.017
- Khalilpour, R., Vassallo, A., 2016. Planning and operation scheduling of PV-battery systems: A novel methodology. *Renew. Sustain. Energy Rev.* 53, 194–208. doi:10.1016/j.rser.2015.08.015
- Khatib, T., Mohamed, A., Sopian, K., 2013. A review of photovoltaic systems size optimization techniques. *Renew. Sustain. Energy Rev.* 22, 454–465. doi:10.1016/j.rser.2013.02.023
- Khatib, T., Mohamed, A., Sopian, K., Mahmoud, M., 2012. A New Approach for Optimal Sizing of Standalone Photovoltaic Systems. *Int. J. Photoenergy* 2012, e391213. doi:10.1155/2012/391213
- Kolhe, M.L., Ranaweera, K.M.I.U., Gunawardana, A.G.B.S., 2015. Techno-economic sizing of off-grid hybrid renewable energy system for rural electrification in Sri Lanka. *Sustain. Energy Technol. Assess.* 11, 53–64. doi:10.1016/j.seta.2015.03.008
- Lau, K.Y., Tan, C.W., Yatim, A.H.M., 2015. Photovoltaic systems for Malaysian islands: Effects of interest rates, diesel prices and load sizes. *Energy* 83, 204–216. doi:10.1016/j.energy.2015.02.015
- Lau, K.Y., Yousof, M.F.M., Arshad, S.N.M., Anwari, M., Yatim, A.H.M., 2010. Performance analysis of hybrid photovoltaic/diesel energy system under Malaysian conditions. *Energy* 35, 3245–3255. doi:10.1016/j.energy.2010.04.008
- Ma, T., Yang, H., Lu, L., 2015. Study on stand-alone power supply options for an isolated community. *Int. J. Electr. Power Energy Syst.* 65, 1–11. doi:10.1016/j.ijepes.2014.09.023
- Mahmud, A.M., 2010. Evaluation of the solar hybrid system for rural schools in Sabah, Malaysia, in: 2010 IEEE International Conference on Power and Energy (PECon). Presented at the 2010 IEEE International

- Conference on Power and Energy (PECon), pp. 628–633.  
doi:10.1109/PECON.2010.5697657
- Maleki, A., Pourfayaz, F., 2015. Optimal sizing of autonomous hybrid photovoltaic/wind/battery power system with LPSP technology by using evolutionary algorithms. *Sol. Energy* 115, 471–483.  
doi:10.1016/j.solener.2015.03.004
- Mandelli, S., Brivio, C., Colombo, E., Merlo, M., 2016. Effect of load profile uncertainty on the optimum sizing of off-grid PV systems for rural electrification. *Sustain. Energy Technol. Assess.* 18, 34–47.  
doi:10.1016/j.seta.2016.09.010
- Markvart, T., 1996. Sizing of hybrid photovoltaic-wind energy systems. *Sol. Energy* 57, 277–281. doi:10.1016/S0038-092X(96)00106-5
- Merei, G., Berger, C., Sauer, D.U., 2013. Optimization of an off-grid hybrid PV–Wind–Diesel system with different battery technologies using genetic algorithm. *Sol. Energy* 97, 460–473.  
doi:10.1016/j.solener.2013.08.016
- Ngan, M.S., Tan, C.W., 2012. Assessment of economic viability for PV/wind/diesel hybrid energy system in southern Peninsular Malaysia. *Renew. Sustain. Energy Rev.* 16, 634–647.  
doi:10.1016/j.rser.2011.08.028
- Nogueira, C.E.C., Vidotto, M.L., Niedzialkoski, R.K., de Souza, S.N.M., Chaves, L.I., Edwiges, T., Santos, D.B. dos, Werncke, I., 2014. Sizing and simulation of a photovoltaic-wind energy system using batteries, applied for a small rural property located in the south of Brazil. *Renew. Sustain. Energy Rev.* 29, 151–157. doi:10.1016/j.rser.2013.08.071
- PVWatts Calculator [WWW Document], n.d. URL <http://pvwatts.nrel.gov/> (accessed 1.17.17).
- Rich, E., Knight, K., 1990. *Artificial Intelligence*, 2 Sub edition. ed. McGraw-Hill Science/Engineering/Math, New York.
- Shaahid, S.M., El-Amin, I., 2009. Techno-economic evaluation of off-grid hybrid photovoltaic–diesel–battery power systems for rural electrification in Saudi Arabia—A way forward for sustainable development. *Renew. Sustain. Energy Rev.* 13, 625–633.  
doi:10.1016/j.rser.2007.11.017
- Shen, W.X., 2009. Optimally sizing of solar array and battery in a standalone photovoltaic system in Malaysia. *Renew. Energy* 34, 348–352.  
doi:10.1016/j.renene.2008.03.015
- Sidrach-de-Cardona, M., Mora López, L., 1998. A simple model for sizing stand alone photovoltaic systems. *Sol. Energy Mater. Sol. Cells* 55, 199–214. doi:10.1016/S0927-0248(98)00093-2
- Sinha, S., Chandel, S.S., 2015. Review of recent trends in optimization techniques for solar photovoltaic–wind based hybrid energy systems. *Renew. Sustain. Energy Rev.* 50, 755–769.  
doi:10.1016/j.rser.2015.05.040
- Sinha, S., Chandel, S.S., 2014. Review of software tools for hybrid renewable energy systems. *Renew. Sustain. Energy Rev.* 32, 192–205.  
doi:10.1016/j.rser.2014.01.035
- T. Givler, P. Lilienthal, 2005. Using HOMER® Software, NREL’s Micropower Optimization Model, to Explore the Role of Gen-sets in Small Solar Power Systems Case Study: Sri Lanka.

- Tazvinga, H., Xia, X., Zhang, J., 2013. Minimum cost solution of photovoltaic–diesel–battery hybrid power systems for remote consumers. *Sol. Energy* 96, 292–299. doi:10.1016/j.solener.2013.07.030
- Tina, G., Gagliano, S., Raiti, S., 2006. Hybrid solar/wind power system probabilistic modelling for long-term performance assessment. *Sol. Energy* 80, 578–588. doi:10.1016/j.solener.2005.03.013
- Torreglosa, J.P., García, P., Fernández, L.M., Jurado, F., 2015. Energy dispatching based on predictive controller of an off-grid wind turbine/photovoltaic/hydrogen/battery hybrid system. *Renew. Energy* 74, 326–336. doi:10.1016/j.renene.2014.08.010
- Upadhyay, S., Sharma, M.P., 2016. Selection of a suitable energy management strategy for a hybrid energy system in a remote rural area of India. *Energy* 94, 352–366. doi:10.1016/j.energy.2015.10.134
- Veldhuis, A.J., Reinders, A.H.M.E., 2015. Reviewing the potential and cost-effectiveness of off-grid PV systems in Indonesia on a provincial level. *Renew. Sustain. Energy Rev.* 52, 757–769. doi:10.1016/j.rser.2015.07.126
- Yahyaoui, I., Sallem, S., Kamoun, M.B.A., Tadeo, F., 2014. A proposal for off-grid photovoltaic systems with non-controllable loads using fuzzy logic. *Energy Convers. Manag.* 78, 835–842. doi:10.1016/j.enconman.2013.07.091
- Yang, H., Zhou, W., Lu, L., Fang, Z., 2008. Optimal sizing method for stand-alone hybrid solar–wind system with LPSP technology by using genetic algorithm. *Sol. Energy* 82, 354–367. doi:10.1016/j.solener.2007.08.005
- Yap, W.K., Karri, V., 2015. An off-grid hybrid PV/diesel model as a planning and design tool, incorporating dynamic and ANN modelling techniques. *Renew. Energy* 78, 42–50. doi:10.1016/j.renene.2014.12.065
- Zarina, P.P., Mishra, S., Sekhar, P.C., 2014. Exploring frequency control capability of a PV system in a hybrid PV-rotating machine-without storage system. *Int. J. Electr. Power Energy Syst.* 60, 258–267. doi:10.1016/j.ijepes.2014.02.033

## APPENDIX A: Matlab script to fetch component sizes and start simulation

```
for i = 1:150
i=i+1;

s1 = 'A';
s2 = i;
s3 = strcat(s1,num2str(s2)); % get gen value

s4 = 'B';

s5= strcat(s4,num2str(s2)); % get PV value

s6 = 'D';
s7= strcat(s6,num2str(s2)); % get battery value

s8 = 'E';
s9= strcat(s8,num2str(s2)); % get converter value

s10 = 'C';
s11= strcat(s10,num2str(s2)); % get battery string value

t1 = 'F';
write1 = strcat(t1,num2str(s2)); % column to log results

filename = 'FuzNov16.xlsx';
sheet = 'L4';
xlRange = s3;
GenP = xlsread(filename,sheet,xlRange);% gen size
xlRange = s5;
PvP = xlsread(filename,sheet,xlRange);% PV size
xlRange = s7;
BattP = xlsread(filename,sheet,xlRange);% batt size
xlRange = s9;
Converter = xlsread(filename,sheet,xlRange);% converter size

set_param('ESSOneYearInOneMinute_R2015a_fuzzy_July27a/Energy
Storage System', 'Pmax_Grid', 'GenP');
set_param('ESSOneYearInOneMinute_R2015a_fuzzy_July27a/TMY3 Data',
'TotalArea', 'PvP');
set_param('ESSOneYearInOneMinute_R2015a_fuzzy_July27a/Energy
Storage System', 'kWh_Rated', 'BattP');
set_param('ESSOneYearInOneMinute_R2015a_fuzzy_July27a/Energy
Storage System', 'ConvPower', 'Converter');
set_param('ESSOneYearInOneMinute_R2015a_fuzzy_July27a/TMY3 Data',
'Conv', 'Converter');

SimOut = sim('ESSOneYearInOneMinute_R2015a_fuzzy_July27a')
```

```
A=sum(liter_minute2)
a=A(1,1);
a=a*12*0.46;
b=sum(gen_hour2);
b=b*12;
c=battery2(43201,1);
c=(c/2)*12;
D=sum(gen_over)
d=D(1,1);
e=PV_kwh2(43201,1);
f=gen_kwh2(43201,1);
g={a,b,c,d,e,f}; %all variable logged into workspace from Simulink must be in
array form, not time series
```

```
xlRange = write1;
xlswrite(filename,g,sheet,xlRange)
```

```
end
```

```
i = msgbox('Operation Completed');
WarnWave = [sin(1:.6:400), sin(1:.7:400), sin(1:.4:400)];
Audio = audioplayer(WarnWave, 22050);
play(Audio);
```

## APPENDIX B: Matlab script for data logging and importing parameters into Excel for COE calculation

```
for i = 1:1
i=i+1;

s1 = 'B';
s2 = i;
s3 = strcat(s1,num2str(s2)); % get PV value

s4 = 'D';
s5 = i;
s6= strcat(s4,num2str(s5)); % get Fuel $ value

s7 = 'E';
s8 = i;
s9= strcat(s7,num2str(s8)); % get GenHour value

s10 = 'F';
s11 = i;
s12 = strcat(s10,num2str(s11)); % get batt throughput value

s13 = 'J';
s14 = i;
s15= strcat(s13,num2str(s14)); % get battery srtring value

s16 = 'K';
s17 = i;
s18= strcat(s16,num2str(s17)); % get converter value

s19 = 'A';
s20 = i;
s21= strcat(s19,num2str(s20)); % get gensize value

t1 = 'L';
write1 = strcat(t1,num2str(s2)); % column to log results

t2 = 'H';
write2 = strcat(t2,num2str(s2)); % column to log results

filename = 'April22.xlsx';
sheet = 'GenBatt';

xlRange = s3;
PV = xlsread(filename,sheet,xlRange);% PV size
xlRange = s6;
Fuel = xlsread(filename,sheet,xlRange);% Fuel Cost
xlRange = s9;
GenHour = xlsread(filename,sheet,xlRange);% generator hour
xlRange = s12;
```

```

BattThru = xlsread(filename,sheet,xlRange);% batt throughput
xlRange = s15;
BattStr = xlsread(filename,sheet,xlRange);% battery string
xlRange = s18;
Converter = xlsread(filename,sheet,xlRange);% converter size
xlRange = s21;
GenSize = xlsread(filename,sheet,xlRange);% generator size

GenHour = GenHour/60;

```

```

filename = 'COE test2.xlsx';
sheet = 'calc';
xlRange = 'B19';
xlswrite(filename,PV,sheet,xlRange)
xlRange = 'C13';
xlswrite(filename,Fuel,sheet,xlRange)
xlRange = 'B26';
xlswrite(filename,BattStr,sheet,xlRange)
xlRange = 'C44';
xlswrite(filename,GenHour,sheet,xlRange)
xlRange = 'B4';
xlswrite(filename,Converter,sheet,xlRange)
xlRange = 'B11';
xlswrite(filename,GenSize,sheet,xlRange)

```

```

filename = 'COE test2.xlsx';
sheet = 'calc';
xlRange = 'AB37';
COE = xlsread(filename,sheet,xlRange);

```

```

filename = 'April22.xlsx';
sheet = 'GenBatt'; xlRange = write1;
xlswrite(filename,COE,sheet,xlRange)
end

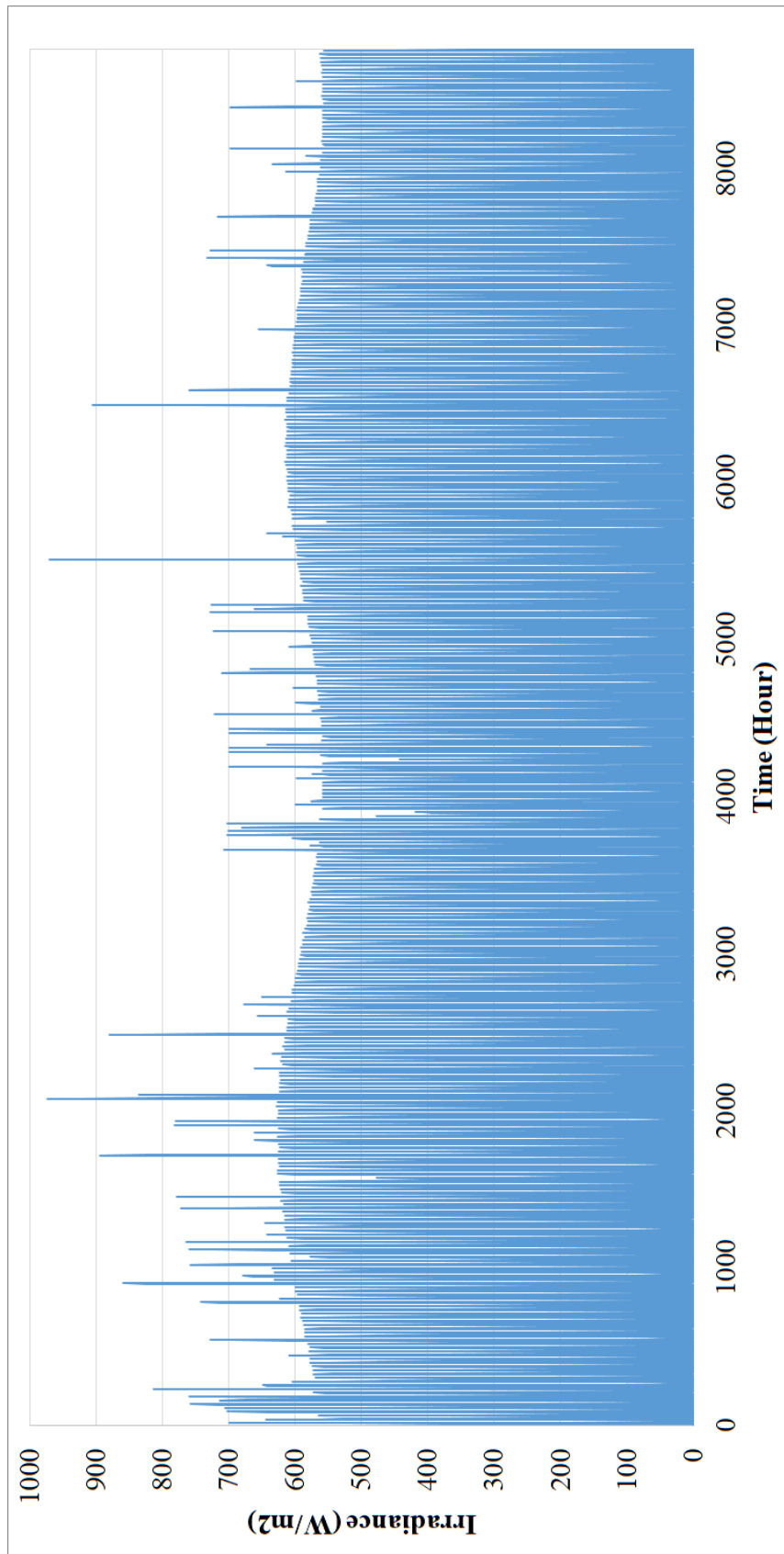
```

```

i = msgbox('Operation Completed');
WarnWave = [sin(1:.6:400), sin(1:.7:400), sin(1:.4:400)];
Audio = audioplayer(WarnWave, 22050);
play(Audio);

```

**APPENDIX C: Plotted solar irradiance data for whole year in Malaysia**



**APPENDIX D: Hourly solar irradiance data for 30 days in Malaysia**

Time (Hour)	Irradiance (W/m <sup>2</sup> )	Time (Hour)	Irradiance (W/m <sup>2</sup> )	Time (Hour)	Irradiance (W/m <sup>2</sup> )
1	0	41	327	81	115
2	0	42	182	82	267
3	0	43	46	83	383
4	0	44	1	84	531
5	0	45	0	85	644
6	0	46	0	86	703
7	0	47	0	87	622
8	10	48	0	88	491
9	118	49	0	89	331
10	269	50	0	90	202
11	383	51	0	91	56
12	531	52	0	92	1
13	642	53	0	93	0
14	699	54	0	94	0
15	617	55	0	95	0
16	486	56	8	96	0
17	326	57	99	97	0
18	181	58	246	98	0
19	45	59	382	99	0
20	1	60	488	100	0
21	0	61	550	101	0
22	0	62	565	102	0
23	0	63	531	103	0
24	0	64	450	104	8
25	0	65	330	105	106
26	0	66	184	106	287
27	0	67	47	107	477
28	0	68	1	108	609
29	0	69	0	109	687
30	0	70	0	110	706
31	0	71	0	111	623
32	8	72	0	112	492
33	117	73	0	113	331
34	324	74	0	114	186
35	547	75	0	115	49
36	641	76	0	116	1
37	644	77	0	117	0
38	563	78	0	118	0
39	528	79	0	119	0
40	447	80	10	120	0

Time (Hour)	Irradiance (W/m <sup>2</sup> )	Time (Hour)	Irradiance (W/m <sup>2</sup> )	Time (Hour)	Irradiance (W/m <sup>2</sup> )
121	0	161	421	201	95
122	0	162	238	202	243
123	0	163	63	203	383
124	0	164	1	204	490
125	0	165	0	205	555
126	0	166	0	206	572
127	0	167	0	207	538
128	11	168	0	208	458
129	142	169	0	209	338
130	370	170	0	210	210
131	593	171	0	211	62
132	720	172	0	212	2
133	758	173	0	213	0
134	707	174	0	214	0
135	665	175	0	215	0
136	565	176	11	216	0
137	416	177	148	217	0
138	221	178	378	218	0
139	54	179	593	219	0
140	1	180	721	220	0
141	0	181	759	221	0
142	0	182	709	222	0
143	0	183	668	223	0
144	0	184	569	224	9
145	0	185	420	225	123
146	0	186	239	226	333
147	0	187	65	227	545
148	0	188	2	228	698
149	0	189	0	229	790
150	0	190	0	230	814
151	0	191	0	231	707
152	9	192	0	232	538
153	120	193	0	233	339
154	306	194	0	234	194
155	480	195	0	235	54
156	614	196	0	236	1
157	693	197	0	237	0
158	713	198	0	238	0
159	671	199	0	239	0
160	571	200	7	240	0

Time (Hour)	Irradiance (W/m <sup>2</sup> )	Time (Hour)	Irradiance (W/m <sup>2</sup> )	Time (Hour)	Irradiance (W/m <sup>2</sup> )
241	0	281	341	321	91
242	0	282	196	322	239
243	0	283	55	323	380
244	0	284	2	324	488
245	0	285	0	325	555
246	0	286	0	326	573
247	0	287	0	327	541
248	7	288	0	328	462
249	109	289	0	329	344
250	317	290	0	330	199
251	544	291	0	331	57
252	642	292	0	332	2
253	649	293	0	333	0
254	571	294	0	334	0
255	538	295	0	335	0
256	459	296	6	336	0
257	340	297	92	337	0
258	195	298	239	338	0
259	54	299	379	339	0
260	1	300	487	340	0
261	0	301	552	341	0
262	0	302	570	342	0
263	0	303	539	343	0
264	0	304	461	344	4
265	0	305	343	345	72
266	0	306	207	346	215
267	0	307	61	347	379
268	0	308	2	348	488
269	0	309	0	349	554
270	0	310	0	350	573
271	0	311	0	351	543
272	8	312	0	352	465
273	115	313	0	353	347
274	300	314	0	354	201
275	475	315	0	355	58
276	573	316	0	356	2
277	604	317	0	357	0
278	571	318	0	358	0
279	539	319	0	359	0
280	460	320	6	360	0

Time (Hour)	Irradiance (W/m <sup>2</sup> )	Time (Hour)	Irradiance (W/m <sup>2</sup> )	Time (Hour)	Irradiance (W/m <sup>2</sup> )
361	0	401	349	441	97
362	0	402	203	442	280
363	0	403	60	443	475
364	0	404	2	444	576
365	0	405	0	445	609
366	0	406	0	446	578
367	0	407	0	447	548
368	6	408	0	448	470
369	90	409	0	449	352
370	239	410	0	450	206
371	380	411	0	451	62
372	489	412	0	452	2
373	556	413	0	453	0
374	574	414	0	454	0
375	544	415	0	455	0
376	467	416	6	456	0
377	349	417	89	457	0
378	203	418	238	458	0
379	59	419	380	459	0
380	2	420	490	460	0
381	0	421	558	461	0
382	0	422	578	462	0
383	0	423	547	463	0
384	0	424	469	464	6
385	0	425	351	465	89
386	0	426	205	466	238
387	0	427	61	467	380
388	0	428	2	468	490
389	0	429	0	469	558
390	0	430	0	470	579
391	0	431	0	471	549
392	6	432	0	472	471
393	90	433	0	473	354
394	238	434	0	474	207
395	379	435	0	475	63
396	489	436	0	476	2
397	557	437	0	477	0
398	577	438	0	478	0
399	546	439	0	479	0
400	468	440	6	480	0

Time (Hour)	Irradiance (W/m <sup>2</sup> )	Time (Hour)	Irradiance (W/m <sup>2</sup> )	Time (Hour)	Irradiance (W/m <sup>2</sup> )
481	0	521	356	561	103
482	0	522	210	562	260
483	0	523	65	563	382
484	0	524	2	564	495
485	0	525	0	565	564
486	0	526	0	566	585
487	0	527	0	567	556
488	6	528	0	568	478
489	88	529	0	569	360
490	238	530	0	570	213
491	380	531	0	571	67
492	491	532	0	572	3
493	559	533	0	573	0
494	578	534	0	574	0
495	549	535	0	575	0
496	472	536	7	576	0
497	354	537	109	577	0
498	209	538	296	578	0
499	64	539	474	579	0
500	2	540	614	580	0
501	0	541	701	581	0
502	0	542	728	582	0
503	0	543	649	583	0
504	0	544	519	584	5
505	0	545	358	585	87
506	0	546	212	586	238
507	0	547	66	587	382
508	0	548	3	588	494
509	0	549	0	589	564
510	0	550	0	590	585
511	0	551	0	591	556
512	6	552	0	592	479
513	88	553	0	593	361
514	238	554	0	594	214
515	381	555	0	595	67
516	491	556	0	596	3
517	560	557	0	597	0
518	580	558	0	598	0
519	551	559	0	599	0
520	474	560	7	600	0

Time (Hour)	Irradiance (W/m <sup>2</sup> )	Time (Hour)	Irradiance (W/m <sup>2</sup> )	Time (Hour)	Irradiance (W/m <sup>2</sup> )
601	0	641	364	681	87
602	0	642	217	682	238
603	0	643	69	683	384
604	0	644	3	684	498
605	0	645	0	685	569
606	0	646	0	686	591
607	0	647	0	687	562
608	5	648	0	688	485
609	87	649	0	689	367
610	238	650	0	690	219
611	382	651	0	691	71
612	494	652	0	692	3
613	565	653	0	693	0
614	586	654	0	694	0
615	558	655	0	695	0
616	481	656	5	696	0
617	363	657	87	697	0
618	216	658	238	698	0
619	68	659	382	699	0
620	3	660	496	700	0
621	0	661	566	701	0
622	0	662	588	702	0
623	0	663	560	703	0
624	0	664	483	704	4
625	0	665	365	705	69
626	0	666	196	706	215
627	0	667	55	707	384
628	0	668	2	708	497
629	0	669	0	709	568
630	0	670	0	710	590
631	0	671	0	711	563
632	5	672	0	712	487
633	87	673	0	713	369
634	237	674	0	714	221
635	381	675	0	715	72
636	494	676	0	716	3
637	565	677	0	717	0
638	587	678	0	718	0
639	558	679	0	719	0
640	482	680	5	720	0

## APPENDIX E: Excel spreadsheet for COE calculation

	A	B	C	D	X	Y	Z	AA	AB	AC
1		0	1	2	22	23	24	25		
2	<b>Discount factor</b>	1	0.944465	0.892015	0.284507	0.268707	0.253785	0.239691		
3	<b>Nominal</b>									
4	<b>Converter</b>	30								
5	Capital	16500	\$0	\$0	\$0	\$0	\$0	\$0		
6	Fuel	\$0	\$0	\$0	\$0	\$0	\$0	\$0		
7	Operating	\$0	\$300	\$300	\$300	\$300	\$300	\$300		
8	Replacement	\$0	\$0	\$0	\$0	\$0	\$0	\$0		
9	Salvage	\$0	\$0	\$0	\$0	\$0	\$0	\$5,500		
10	<b>Converter Total</b>	16500	\$300	\$300	\$300	\$300	\$300	(\$5,200)		
11	<b>Diesel</b>	50								
12	Capital	25000	\$0	\$0	\$0	\$0	\$0	\$0		
13	Fuel	\$0	45336	45336	45336	45336	45336	45336		
14	Operating	\$0	184.225	184.225	184.225	184.225	184.225	184.225		
15	Replacement	\$0	0	0	0	25000	0	25000		
16	Salvage	\$0	\$0	\$0	\$0	\$0	\$0	\$17,958		
17	<b>Diesel Total</b>	25000	\$45,520	45520.225	45520.225	70520.225	45520.225	\$52,562		
19	<b>PV</b>	60								
20	Capital	120000	\$0	\$0	\$0	\$0	\$0	\$0		
21	Fuel	\$0	\$0	\$0	\$0	\$0	\$0	\$0		
22	Operating	\$0	\$600	\$600	\$600	\$600	\$600	\$600		
23	Replacement	\$0	\$0	\$0	\$0	\$0	\$0	\$0		
24	Salvage	\$0	\$0	\$0	\$0	\$0	\$0	\$0		
25	<b>PV Total</b>	120000	\$600	\$600	\$600	\$600	\$600	\$600		
26	<b>ES</b>	3								
27	Capital	\$26,400	\$0	\$0	\$0	\$0	\$0	\$0		
28	Fuel	\$0	\$0	\$0	\$0	\$0	\$0	\$0		
29	Operating	\$0	\$240	\$240	\$240	\$240	\$240	\$240		
30	Replacement	\$0	\$0	\$0	\$0	\$0	\$26,400	\$0		
31	Salvage	\$0	\$0	\$0	\$0	\$0	\$0	\$24,200		
32	<b>ES Total</b>	\$26,400	\$240	\$240	\$240	\$240	\$26,640	(\$23,960)		
33	<b>Nominal Total</b>	\$208,900	\$47,260	\$47,260	\$47,260	\$72,260	\$73,660	\$17,602	1726047.3	
34	<b>Discounted Total</b>	208900	44635.649	42156.827	13445.881	19416.854	18693.846	4219.0146	988354.21	NPC